Exploring the impact of heterogeneities on HIV dynamics within host

Ward, Zoe

Award date:
2011

Awarding institution:
University of Bath

Exploring the impact of heterogeneities on HIV dynamics within host

submitted by

Zoë Ward

for the degree of Doctor of Philosophy

of the

University of Bath

Department of Mathematical Sciences

December 2011

Acknowledgements

I would like to thank my supervisor Jane White for her guidance and advice throughout the course of my PhD, it has been invaluable. Many thanks to Ivana Gudelj, Ben Adams and George Van Voorn for mathematical discussions which have furthered my understanding.

To my husband Chris and son Samuel, without you by my side the ups and downs would have been much harder to negotiate and I am so thankful to have had you with me on this journey.

Completing my PhD would not have been possible without the support of my friends both within the university and without. Special thanks go to Vicki, my partner in crime in knitting capers and sounding board for mathematical ideas - remember "there is no spoon"! To Matt Dorey and Damien Harwin, many thanks for your support during the early stages of my time at Bath. Without your help it would have taken me much longer to find my feet! To Julie, Katharine, Lesley, Paula, Liz and Sarah, I would like to say thank you for keeping me sane whilst trying to finish my PhD and look after a toddler. It was not an easy task and you guys certainly made it more enjoyable.

And finally, for their encouragement and support anytime I needed someone to talk to, thanks go to my parents. It has taken a long time to get to this point and you have been of tremendous help every step of the way.

Summary

This thesis is concerned with exploring how cell heterogeneity and drug resistance can cause long term persistence of HIV. We examine models of multiple viral strains to assess the impact of drug resistance on viral persistence and extend our cell heterogeneity models to include multiple strains.

Chapter 1 summarises the nature of HIV infection within host. The key barriers to HIV eradication within host and the role of mathematical models to help understand these issues are discussed.

In Chapter 2 we analyse models that include cell heterogeneity. We find robust long term viral persistence is possible on therapy and differences in viral load between body compartments explained by cell heterogeneity. The inclusion of a drug sanctuary also allows low level viral load on treatment.

Competition and evolutionary models of wildtype and drug resistant strains of virus are described in Chapter 3. We analyse two models containing three strains of virus with different mutation mechanisms. We find that the proportion of the minority strains of virus is determined by the number of mutations away from the dominant strain.

In Chapter 4 we extend our cell heterogeneity models from Chapter 2 to include a drug resistant strain of virus. We find that when a drug sanctuary is present coexistence is possible in the absence of an evolutionary mechanism. The two compartment model also shows differential dominance whereby a different strain is dominant in each compartment.

Chapter 5 is concerned with the impact of latently infected cells on the viral strain distribution within the host. We find the latent cell reservoir acts as an archive for previously dominant viral strains when there is a mechanism for latent cell maintenance and that the balance between ongoing viral and latent cell replication determines the longevity of the archive.

Contents

1 Introduction **10**

1.1 Background 10

1.1.1 The Life Cycle of HIV 10

1.1.2 Treatment of HIV 11

1.1.3 Mathematical Modelling 13

1.2 Thesis Outline 17

2 Single Strain Models **18**

2.1 Chapter Outline 18

2.2 Background and Motivation 18

2.3 One Compartment Model with a constant input 20

2.3.1 Model Equations 20

2.3.2 Steady State Analysis 20

2.3.3 Numerical Results 21

2.3.4 Summary 23

2.4 Two Compartment Model 23

2.4.1 Model Equations 25

2.4.2 Null Neutral Model 26

2.4.3 Cell Heterogeneity Model 30

2.4.4 Drug Sanctuary Model 32

2.4.5 Combined Model 38

2.4.6 Summary 38

2.5 Model with two target cell populations 42

2.5.1 Steady State Analysis 43

2.5.2 Numerical Solutions 44

2.5.3 Summary 45

2.6 Conclusions 49

3 Multistrain Models **50**
3.1 Chapter Outline . . . 50
3.2 Background and Motivation . . . 50
3.2.1 Biological Background on Drug Resistance . . . 50
3.2.2 Mathematical Modelling of Drug Resistance . . . 53
3.3 Competition Models . . . 53
3.3.1 Two Strain Competition Model . . . 54
3.3.2 Three Strain Competition Model . . . 56
3.4 Evolutionary Models . . . 59
3.4.1 Two Strain Evolutionary Model . . . 59
3.4.2 Three Strain Evolutionary Models . . . 69
3.5 Conclusions . . . 76

4 Multistrain Models with Heterogeneity **80**
4.1 Chapter Outline . . . 80
4.2 Background and Motivation . . . 80
4.3 Two Target Cell Two Strain Model . . . 83
4.3.1 Model Equations . . . 83
4.3.2 Steady State Analysis . . . 84
4.3.3 Summary of Results . . . 93
4.4 Two Compartment Two Strain Model . . . 96
4.4.1 Model Equations . . . 96
4.4.2 Steady State Analysis . . . 98
4.4.3 Numerical Analysis . . . 103
4.4.4 Summary of Results . . . 107
4.5 Conclusions . . . 111

5 Modelling Latently Infected Cells **113**
5.1 Introduction . . . 113
5.1.1 Chapter Outline . . . 113
5.1.2 Motivation and Background . . . 114
5.2 Base Model with Latent Cells . . . 117
5.2.1 Model Equations . . . 117
5.2.2 Steady State Analysis . . . 119
5.2.3 Numerical Solutions . . . 122
5.2.4 Summary . . . 130
5.3 Two target cell model with latent cells . . . 133
5.3.1 Model Equations . . . 133

5.3.2 Steady state analysis 134
5.3.3 Numerical Solutions 139
5.3.4 Summary 145
5.4 Conclusions 145

6 Conclusions **149**

References **152**

Appendix **162**

List of Figures

1-1 Schematic of the HIV life cycle 12
1-2 Behaviour of the basic model (1.1) over time 16

2-1 Constant input model: possible steady states of v 23
2-2 Constant input model: Bifurcation diagrams 24
2-3 Schematic of Two Compartment Model 25
2-4 Two Compartment Model: Bifurcation Graph of v_1 in null neutral model 29
2-5 Two Compartment Model: Bifurcation Graph of v_1 in cell heterogeneity model 33
2-6 Two Compartment Model: Viral loads in cell heterogeneity model . . . 34
2-7 Two Compartment Model: Drug sanctuary and steady state viral load . 36
2-8 Two Compartment Model: Drug sanctuary compartment size and viral load 37
2-9 Two Compartment Model: Steady state viral load in cell heterogeneity model 40
2-10 Two Compartment Model: Interplay of drug penetrance, drug efficacy and infected cell death rates 41
2-11 Schematic of the Two Target Cell Model. 42
2-12 Two Target Cell Model: Bifurcation Diagram 47
2-13 Two Target Cell Model: Drug penetrance and steady state viral load . . 48
2-14 Two Target Cell Model: Interplay of drug penetrance and drug efficacy 48

3-1 Two strain evolutionary model: Steady state values of S and v_i 62
3-2 Two strain evolutionary model: Steady state diagram 64
3-3 Two strain evolutionary model: Steady state viral load 64
3-4 Two strain evolutionary model: Frequency of mutants prior to therapy . 66
3-5 Two strain evolutionary model: Time to emergence of mutant strain - $\beta_w = 0$ 68

3-6 Two strain evolutionary model: Time to emergence of mutant strain - $\beta_w > 0$ 68
3-7 Jump three strain evolutionary model: Steady state behaviour 73
3-8 Serial three strain evolutionary model: Steady state behaviour 74
3-9 Serial three strain evolutionary model: Time to emergence of dominant mutant strain 77

4-1 Schematic of Two target cell two strain model 85
4-2 Two target cell two strain model: Steady state viral loads 91
4-3 Two target cell two strain model: Stability of endemic steady states . . 92
4-4 Two target cell two strain model: Steady state viral loads in model with mutation 93
4-5 Two target cell two strain model: Low level viral load 94
4-6 Schematic of the Two Compartment Two Strain Model (4.7) which allows virus diffusion between two separate body compartments. The diffusion is along a concentration gradient. In compartment 1 the diffusion term for wildtype virus is $\frac{L}{1-u}(v_{2w} - v_{1w})$ and in compartment 2 we have $\frac{L}{u}(v_{1w} - v_{2w})$, where L is the transport coefficient and u is the scaled size of compartment 2. The diffusion terms for drug resistant virus are modelled in the same way. 97
4-7 Two compartment two strain model: steady state stability 104
4-8 Two compartment two strain model: Steady states/dominance for different drug and resistance scenarios 106
4-9 Two compartment two strain model: Steady state/dominance for different compartment sizes and cell heterogeneity parameters 108
4-10 Two compartment two strain model: Viral loads and compartment size 109
4-11 Two compartment two strain model: Viral loads and infected cell death rates 110

5-1 Schematic of the Basic Latent Cell model (5.1). 118
5-2 Base model with latent cells, model 1: Switch over in strain dominance 124
5-3 Base model with latent cells, model 1: Effects of latent cell parameters . 125
5-4 Base model of latent cells, model 2: Effects of latent cell parameters on archive time 127
5-5 Base model of latent cells, model 2: Effect of resistance factor on archive time 128
5-6 Base model of latent cells, model 3: Graph comparing switching and average activation rate α. 130

5-7 Base model of latent cells, model 3: Switchover in strain dominance . . 131
5-8 Base model with latent cells, model 3: Effects of activation rate and resistance factor on archive time 132
5-9 Schematic of two target cell two strain model with latent cells 135
5-10 Two target cell two strain model with latent cells, model 1: Switchover in strain dominance 141
5-11 Two target cell two strain model with latent cells, model 1: Effect of activation rate, α 142
5-12 Two target cell two strain model with latent cells, model 2: Effects of model parameters on archive time 143
5-13 Two target cell two strain model with latent cells, model 3: Switchover in strain dominance 144
5-14 Two target cell two strain model with latent cells, model 3: Effects of model parameters on archive time 146

List of Tables

2.1 Antiretroviral drug concentrations in male genital tract 19
2.2 Constant Input Model parameter descriptions and values. 22
2.3 Two target cell model parameter descriptions and values. 46

4.1 Two compartment two strain model parameter descriptions and values. 98

5.1 Base model with Latent cells parameter descriptions and values. 118
5.2 Latent cell models: definitions of P and Q 119
5.3 Two target cell two strain model with latent cells parameter descriptions and values 134

Chapter 1

Introduction

1.1 Background

HIV was first identified in 1983 as the causative agent of acquired immunodeficiency syndrome (AIDS) [Levy, 1995]. Since then it has been studied extensively in order to produce effective treatments. The prevalence of HIV is growing globally. In 2006 there were an estimated 39.5 million people living with HIV or AIDS of which 2.3 million were children and in the same year an estimated 4.3 million people became infected with HIV [UNAIDS, 2006].

1.1.1 The Life Cycle of HIV

HIV is present in the body fluids of an infected individual (blood, semen, vaginal fluid, breast milk) and can be contracted intravenously, by sexual contact, during birth or from breast feeding. Once in the body HIV particles infect host cells by binding to a specific protein (CD4) on the cell surface to promote cell fusion. The ribonucleic acid (RNA) genome and other proteins present in the core of the HIV particle are taken into the cell. One of these proteins is reverse transcriptase which reverse transcribes the RNA genome into deoxyribonucleic acid (DNA). The DNA genome is then inserted into the host cell genome by another viral protein called integrase. The virus uses the host cell machinery to transcribe the DNA genome into RNA in order to produce proteins and copies of the viral RNA genome. Another important viral protein, protease, cleaves the long polyproteins produced into the required proteins. New virus particles are assembled in the cell, which then bud from the cell surface incorporating the viral envelope glycoproteins which have migrated there. These new virus particles are then free to infect new host cells [Lever, 1996]. A schematic of the life cycle of HIV can be seen in Figure 1-1.

Many different cell types can be infected by HIV, including CD4+ T cells, CD8+ T cells, macrophages and dendritic cells [Levy, 1995]. The characteristics of these cells mean that there are differences in the death rate of infected cells and the production rate of new virions. Some cells can even be latently infected whereby the viral DNA lies dormant and no viral protein production takes place [Levy, 1995]. This allows the cells to escape detection and is thought to be a reservoir which is not affected by drug therapy [Lever, 1996].

1.1.2 Treatment of HIV

Treatment is initiated when a patient has a CD4+ cell count between 200 and 350 cells/μl [Gazzard, 2006]. First-line therapy is based on virus phenotyping which should be carried out as soon as the infection is diagnosed [Gazzard, 2006]. Viral phenotyping finds all of the wild type and drug resistant strains of virus which are present above the level of 20% of the total population. In order to treat HIV the viral load in the blood needs to be decreased, meaning drugs need to inhibit steps in the virus life cycle.

Drugs inhibit either reverse transcriptase, protease or integrase, all of which are viral proteins encoded on the virus genome. There are three different classes of reverse transcriptase inhibitor (RTI) : nucleoside (NRTI), non-nucleoside (NNRTI) and nucleotide inhibitors. These inhibitors generally have a low genetic barrier to resistance, meaning that only a few mutations are needed to confer resistance to a specific drug [Pillay et al., 2000]. Cross resistance, where a mutation confers resistance to more than one drug in the same class is a problem with reverse transcriptase inhibitors. This is due to the sites of action for the drugs being too similar.

Protease inhibitors (PIs) act against the enzyme responsible for cleaving the viral polypeptide into separate viral proteins. Protease inhibitors work better if they are boosted by a drug called Ritonavir which helps reduce degradation of the drug and so maintain an effective concentration. Mutations conferring resistance to these inhibitors have also been seen but it takes longer for mutations to occur if the drug is boosted with Ritonavir [Reeves and Pifer, 2005].

There is currently only one integrase inhibitor, called Raltegravir, that is licensed for use in the UK. This acts to stop integration of the converted viral DNA into the host cell genome [Reeves and Pifer, 2005].

Inhibitors of maturation are another class of drugs being developed. These inhibit the maturation of viral particles by targeting the polypeptide substrate of the protease enzyme [Reeves and Pifer, 2005].

The final class of drugs in development are entry inhibitors which prevent HIV envelope proteins from binding to and fusing with target cells [Reeves and Pifer, 2005].

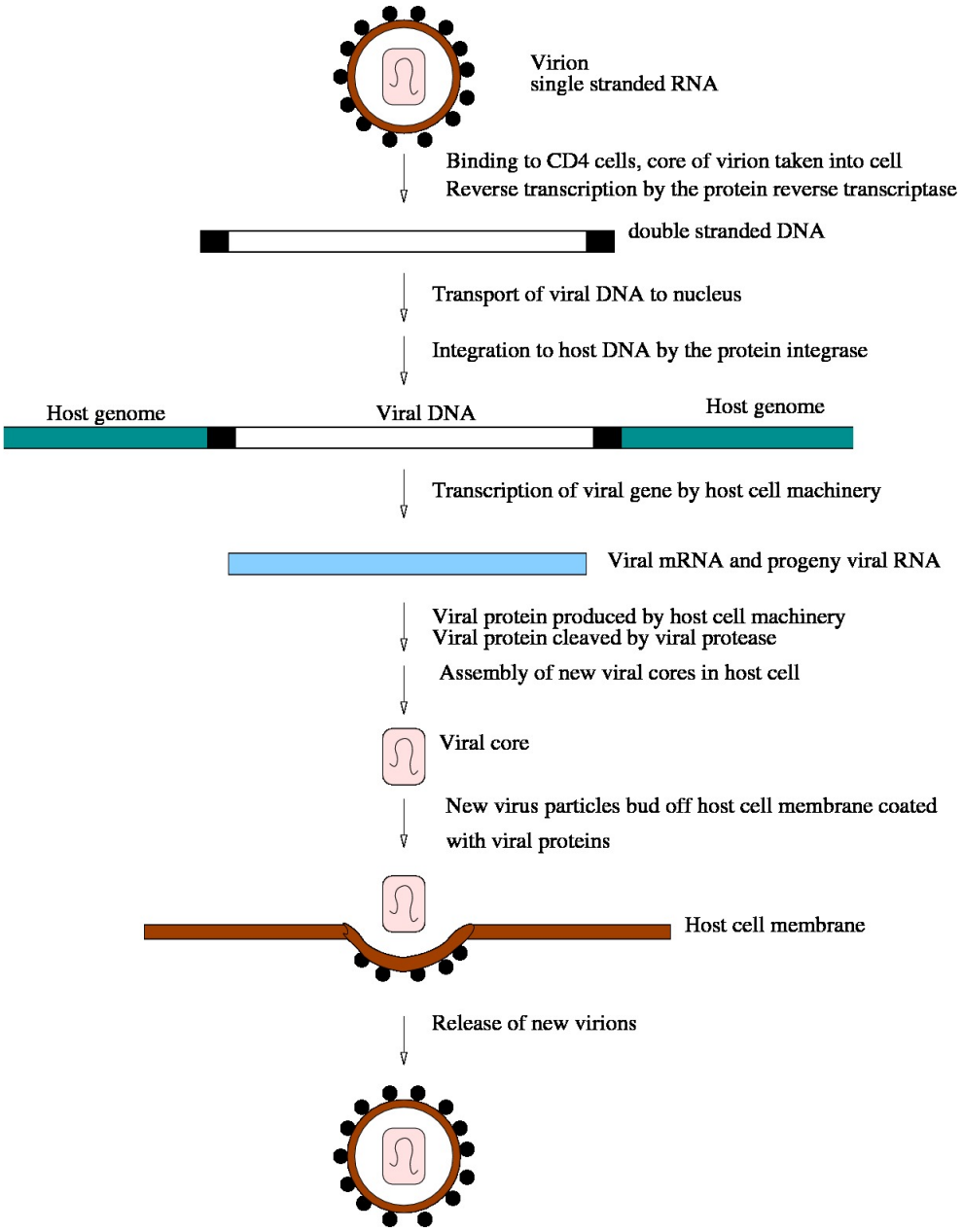

Figure 1-1: Schematic of the HIV life cycle in host adapted from Brock [1997]

There are a number of entry inhibitors in clinical trials at the moment. However most are large protein molecules that need to be administered by intravenous infusion and therefore will remain options for salvage cases only (where a patient has no other treatment options available). One exception to this is the co-receptor (CCR5) binding inhibitor Maraviroc; however it is also likely to be reserved for salvage patients.

Both single drug therapies and dual drug therapies were tried when drugs against HIV first became available; drug resistance quickly developed in these cases [Larder et al., 1989, Miller et al., 1998, Pillay et al., 2000]. Highly active antiretroviral therapy (HAART) comprising of three drugs was introduced in the late nineties and has a much better record against the development of resistance mutations; viral reproduction is suppressed to a very low level with viral loads typically below 100 copies/ml. A triple drug regimen based on NNRTI's is generally used for initial therapy with boosted PI regimens reserved for when the patient fails initial therapy due to accumulation of mutations. A change in regimen is typically considered if the viral load increases from less than 50 copies/ml to persistently above 400 copies/ml. Treatment experienced patients, who have no options left in terms of available drug classes, are supported by a maintaining regimen until a novel drug class is made available [Gazzard, 2006].

1.1.3 Mathematical Modelling

The first mathematical modelling of within host HIV aimed to describe what happened to the viral load after initial infection and once treatment was initiated [McLean et al., 1991]. Nearly all contemporary models used to describe viral load are constructed from the original model which is outlined below.

The Basic Model

The simplest structure to explore virus production within the body comprises of three components; the concentration of uninfected and infected target cells and cell free virions per ml, given by S, I and v respectively. Uninfected cells are produced at a constant rate λ cells per day and die at a rate d per day. The uninfected cells and virions interact to produce infected cells at rate β per virion per day (using a mass action assumption). Infected cells produce new virions at a burst rate of k per day and die at a rate a per day. Virions die at a rate c per day. Combining these elements gives the basic model form:

$$\begin{aligned} \dot{S} &= \lambda - dS - \beta Sv, \\ \dot{I} &= \beta Sv - aI, \\ \dot{v} &= kI - cv \end{aligned} \tag{1.1}$$

[McLean et al., 1991, Nowak and May, 2000, Perelson et al., 1996, Britton, 2002]. Model behaviours are determined through the calculation of R_0, the basic reproductive ratio, and steady state analysis (an overview of the methods involved can be found in [Edelstein-Keshet, 1988]). The basic reproductive ratio, R_0, is the expected number of virions that one virion gives rise to in an uninfected cell population, where $S = \frac{\lambda}{d}$. One virion gives rise to βS infected cells in a time $\frac{1}{c}$. Each of these infected cells gives rise to k virions in a time $\frac{1}{a}$. This gives the reproductive ratio to be

$$R_0 = \frac{\beta \lambda k}{acd}.$$

If $R_0 > 1$ the virus spreads throughout the population of target cells, otherwise the virus becomes extinct.

Setting the left hand sides of the model equations (1.1) to zero and solving for each variable gives the steady states of the system: the disease free steady state $(S, I, v) = (\lambda/d, 0, 0)$ and the endemic steady state $(S, I, v) = (S^*, I^*, v^*)$ where

$$\begin{aligned} S^* &= \frac{\lambda}{dR_0} := \frac{S_0}{R_0}, \\ I^* &= \frac{dc}{\beta k}(R_0 - 1), \\ v^* &= \frac{d}{\beta}(R_0 - 1), \end{aligned}$$

where $S_0 = \frac{\lambda}{d}$ is the value of S in the disease free steady state ($I = v = 0$).

The stability of the steady states is determined by the Jacobian of the system:

$$J = \begin{pmatrix} -d - \beta v & 0 & -\beta S \\ \beta v & -a & \beta S \\ 0 & k & -c \end{pmatrix}.$$

evaluated at the steady state. The characteristic polynomial is the determinant of $(xI - J)\mathbf{v} = 0$, the roots of which are the eigenvalues of the system (1.1). If the real parts of each eigenvalue are negative the steady state is stable, otherwise it is unstable. This can be determined using Descartes rule of signs which states that if the terms of a single-variable polynomial with real coefficients are ordered by descending variable exponent, then the number of positive roots of the polynomial is either equal to the number of sign differences between consecutive nonzero coefficients, or is less than it by a multiple of 2. Therefore there are no positive roots if all of the coefficients are either all positive or all negative, meaning the steady state is stable.

The characteristic polynomial of the disease free steady state is

$$(x+d)((x+a)(x+c)+ac-\frac{\beta\lambda k}{d})=0.$$

This has negative roots, which means the disease free steady state is stable, if and only if $R_0<1$.

The characteristic polynomial of the endemic steady state is

$$x^3+(a+c+dR_0)x^2+(a+c)dR_0x+acd(R_0-1)=0.$$

This has negative roots, which means the endemic steady state is stable, if and only if $R_0>1$.

The behaviour of the system (1.1) over time when $R_0>1$ is shown in Figure 1-2.

The basic model (1.1), gives a good comparison with data for the first few months of infection, however in real life the behaviour of the viral load and CD4+ cell count in the long term does not remain static. For some reason after a period of time (months or years) in undiagnosed and untreated patients, the CD4+ cell count goes down and the viral load goes up. Patients become susceptible to opportunistic infections and develop full blown AIDS. One hypothesis to explain this observation is that another population of immune cells called CD8 cells control the infection but over time HIV mutates and evolves to escape the immune response [Nowak et al., 1991].

Including drug treatment into this model is simple. In order to model reverse transcriptase inhibitors the infection rate β is premultiplied by a factor $(1-e)$, where e is the drug efficacy. This changes the results of the long term analysis and it becomes theoretically possible to eradicate the disease if

$$R_0^e=\frac{(1-e)\beta\lambda k}{acd}<1$$

giving a critical level of drug efficacy

$$e_c=1-1/R_0.$$

Protease inhibitors can be included in the same way by premultiplying the burst size k.

If the efficacy of the drug is assumed to be 100% the basic system (1.1) is reduced to a linear system. The viral load decays away to zero and the CD4+ cell count rises to its pre-infection level. This assumption allows the estimation of the infected cell death rate a and the virus death rate c. In reality on treatment viral loads are maintained

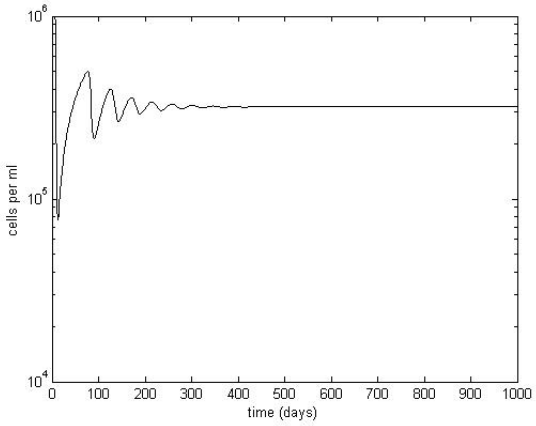

(a) susceptible cells, S

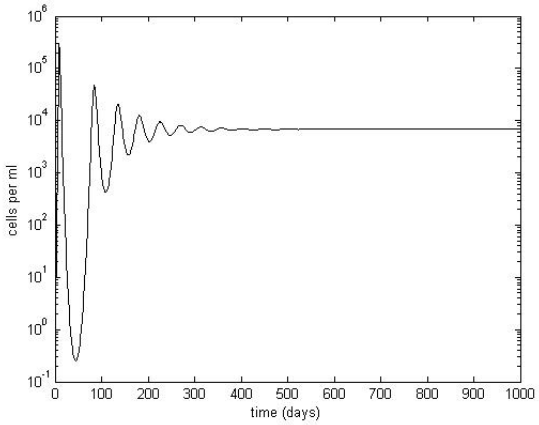

(b) infected cells, I

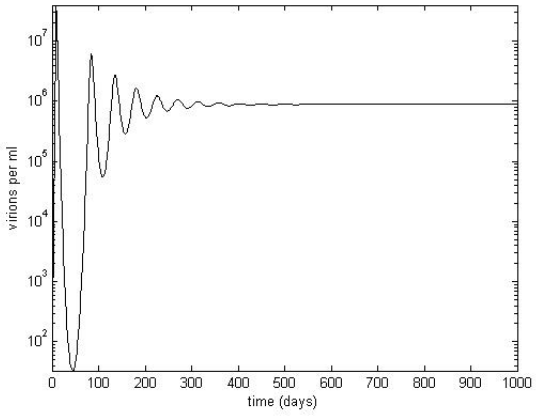

(c) virus, v

Figure 1-2: Graph showing the behaviour of the basic model for HIV (1.1) over time when $R_0 > 1$. Parameter values: $\lambda = 10^4$ cells ml^{-1}, $d = 0.01$ day^{-1},$\beta = 2.4 \times 10^{-8}$ virions^{-1} day^{-1},$a = 1$ day^{-1}, $k = 3000$ virions cell^{-1} day^{-1}, $c = 23$ day^{-1}.

at a very low, in most cases undetectable levels, for some period of time before viral rebound occurs due to the accumulation of drug resistant mutations. If the drug is not considered to be 100% effective the system settles to another steady state with higher CD4+ cell concentrations and lower viral load (than the system with no treatment), as long as the R_0 value for the system incorporating drug is above 1. However the steady state viral load is very sensitive to drug efficacy, either being unreasonably high on treatment or zero. This means that the low level viral loads (< 100 virions per ml) seen in patients on treatment cannot be adequately modelled with this simple system.

1.2 Thesis Outline

This thesis seeks to investigate some of the reasons why drug therapy is not a cure for HIV using biologically realistic models. Particular attention is given to the problem of drug resistance. It is important when attributing a result to a particular feature of a model, that the neutral null model is studied also [Lipsitch et al., 2009]. The neutral null model is one where the mechanism in question is not included in order to check that the behaviour you are interested in comes from the mechanism you are studying, not the underlying model. Throughout this thesis we analyse baseline model behaviours in order to be sure of the cause of interesting results.

Chapter 2 presents models which allow low level viral load on treatment through the examination and improvement of models by Callaway and Perelson [2002]. Drug resistance models are the focus of Chapter 3, which describes models that include either two or three strains of virus as well as a mutation mechanism. The results from this work and that in Chapter 2 are combined in Chapter 4 to analyse systems that allow low level viral load with two strains of virus. Chapter 5 investigates a different reason for the failure of drug therapy, namely the presence of latently infected cells. We analyse models including two strains of virus to find the cause of persistent viral archives. The discussion is contained in Chapter 6.

Parts of the work from chapters 2,3 and 4 have been published in Ward et al. [2009] and sections of Chapter 5 have been submitted for publication.

Chapter 2

Single Strain Models

2.1 Chapter Outline

This chapter is concerned with modelling the low level viral loads seen in patients on treatment. To this end we will begin with an overview of the relevant biology and the mathematical modelling by Callaway and Perelson [2002] which investigates a range of biological scenarios. The presence of a drug sanctuary allows the most robust low level viral load on therapy and we extend this work by considering what other facets of the models can bring about the same behaviour. In addition we include host cell heterogeneity in the models in order to make them more biologically realistic.

In order to understand the behaviour of a two compartment system we first consider a single compartment system with a constant external input. Following on from that we consider a two compartment system (the blood and genital tract) in which one compartment can act as a drug sanctuary. Finally we discuss a two target cell model (blood compartment only) which allows one of the target cells to be a drug sanctuary.

2.2 Background and Motivation

It is well known that viral loads go undetectable in patients on highly active antiretroviral therapy (HAART) but the virus is not eradicated [Wong et al., 1997, Chun et al., 1997a,b]. One likely reason is the presence of drug sanctuaries [Cohen et al., 2007]. A drug sanctuary is a place, either an infected cell or a body compartment, that does not absorb the drug to the same extent as CD4+ T cells in the blood allowing the virus a possible mechanism for evading the effect of the drug.

The viral load and quasispecies complement seem to differ between the semen and the blood [Kalichman et al., 2008, Zhang et al., 1998, Craigo et al., 2004]. This has im-

	PI	**NNRTI**	**nucleotide RTI**
Above 100%	indinavir (100%)		lamivudine (600%) tenofovir (500%) zidovudine (200%) abacavir (150%)
Below 100%	amprenavir (20%) lopinavir (5%) nelfinavir(5%) ritonavir (3%) saquinavir (3%)	nevirapine (70%) efavirenz (3%)	stavudine (2%)

Table 2.1: Antiretroviral drug concentrations in the male genital tract relative to blood plasma concentrations adapted from Cohen et al. [2007]

plications in the transmission of HIV to other individuals. For example if blood plasma viral load is negligible, semen viral load could still be high enough that transmission could occur. Moreover, the infecting virus could be of a different genotype to that seen in the blood [Tirado et al., 2004, Zhu et al., 1996, Liuzzi et al., 2004].

There is evidence that the genital tract of males and females is a reservoir for HIV [Tirado et al., 2004, Byrn et al., 1997], both in terms of drug escape and separate evolution of drug resistant strains. Lowe et al. [2004] argued against the male genital tract (MGT) being a drug sanctuary site saying that some drugs have good penetrance in the male genital tract and therefore it is not a sanctuary site for HIV during drug treatment. However, there are more drugs where this is not the case. Protease inhibitors are well known to be found at lower concentrations in semen. Table 2.1 shows the relative concentrations of some common drugs in the semen compared with the blood.

Similar differences in drug efficacies have been noted between CD4+ T cells and monocyte derived macrophages. In particular protease inhibitors seem to be less effective in macrophages. This could also be a possible source of ongoing viral replication on treatment [Perno et al., 1998, Puddu et al., 1999, Kim et al., 1998].

The basic model (1.1) predicts the virus will be eradicated once critical drug efficacy is surpassed. The problem with the basic model in this context is that the behaviour of the steady state viral load is very sensitive to the efficacy of the drug. The steady state viral load remains high near the critical value of drug efficacy then drops dramatically to zero once the critical value is reached. Callaway and Perelson [2002] modelled possible biological reasons the virus is not eradicated and some viral replication remains. A number of different modifications to the basic model have been analyzed including latently infected cells, different drug treatments (reverse transcriptase and protease

inhibitors) and using density dependent infected cell death rates. With the latter model the rationale is that infected cells should be cleared by the immune system at a rate dependent on the number of infected cells present. Although the density dependent cell death model gave low level viral loads at steady state it also showed an unrealistically low level of infected cells and a high level of CD4+ target cells. Also investigated were two models that allowed target cells with different responses to antiretroviral drugs creating a drug sanctuary: a two compartment model with identical target cells similar to that in Kepler and Perelson [1998] and a model with two distinct populations of target cells in one compartment. Both of these models were capable of having low level steady state viral load for a range of drug efficacies. The possibility that the differences in target cell life cycle parameters might also allow low level viral loads to occur was not considered, in Sections 2.4 and 2.5 we rectify this.

2.3 One Compartment Model with a constant input

Our first model is based on the single strain blood plasma model of Perelson et al. [1996] that was analysed in Chapter 1. The only addition is of a constant input/output into the virus differential equation which represents an input from, or output into, a separate body compartment which replicates viral particles independently. Including this extra parameter allows us to understand the implications of the presence of compartments in the body that harbour HIV infection as well as the blood.

2.3.1 Model Equations

A one compartment model adapted from the basic model (1.1) is given by

$$\begin{aligned} \dot{S} &= \lambda - dS - \beta Sv, \\ \dot{I} &= \beta Sv - aI, \\ \dot{v} &= kI - cv + \delta, \end{aligned} \tag{2.1}$$

where δ is a constant parameter which when positive denotes an input of virions and when negative denotes loss of virions. All other parameters have the same definitions as the basic model (1.1).

2.3.2 Steady State Analysis

When $\delta = 0$ the steady states and stability criteria are the same as the basic model given in 1.1.3. That is the disease free steady is stable for $R_0 < 1$ and the endemic

steady state is stable for $R_0 > 1$. When $\delta \neq 0$ the situation is more complicated; the steady state level for v is given by the root of the following quadratic equation

$$\begin{aligned} &v^2 + x_1 v + x_0 = 0, \\ &\text{where} \\ &x_1 = \frac{d}{\beta}\left(1 - R_0 - \frac{\beta\delta}{dc}\right), \\ &x_0 = -\frac{\delta d}{\beta c}, \end{aligned} \tag{2.2}$$

and $R_0 = \frac{\lambda\beta k}{acd}$. The steady state expressions for susceptible cells, S and infected cells, I can be written as the following functions of the steady state value of v,

$$\begin{aligned} S =& \frac{\lambda}{d + \beta v}, \\ I =& \frac{cv + \delta}{k}. \end{aligned}$$

The behaviour of the solutions of the quadratic for steady state virus are explored in Figure 2-1 using the parameter values found in Table 2.2. We can see that solutions of (2.2) can be positive, negative or complex depending on the parameter values used. When $R_0 > 1 - \frac{\beta\delta}{dc} + 2\sqrt{\frac{\beta\delta}{dc}}$ we obtain two positive viral steady states even when $\delta < 0$, corresponding to an output of viral particles from the blood compartment. When $\delta > 0$ there is only one possible positive steady state value for v. There is also a range of values of δ for which there are no real values of v, corresponding to negative values of the discriminant. We are only interested in the biologically realistic steady state solutions where all of the variables are positive or zero. The stability of the steady states was analysed numerically.

2.3.3 Numerical Results

From Figure 2-2a we see that when $R_0 > 1$, it is possible to have two positive steady states, however for large negative values of δ there are no stable positive steady states. Indeed when δ takes large negative values which give a negative discriminant or no stable positive steady states the system goes to negative infinity. It is possible to have a stable positive steady state for small negative values of δ, the extent of this range depends on the size of R_0. When R_0 is larger the viral population can withstand a larger constant output δ from the system. When $\delta > 0$ there is only one positive solution of the quadratic for steady state virus which is stable. The negative root is unstable. When $R_0 < 1$ and $\delta > 0$ as seen in Figure 2-2b there is one positive root of

Parameter Description	**Value**	**Source**
λ, Birth rate of primary target cells	10^4 cells ml^{-1} day^{-1}	Callaway and Perelson [2002]
β, Infection rate	2.4×10^{-8} virion^{-1} day^{-1}	Perelson et al. [1993]
d, Death rate of target cells	0.01 day^{-1}	Mohri et al. [1998]
a, Death rate of infected cells	1 day^{-1}	Markowitz et al. [2003]
c, Death rate of virions	23 day^{-1}	Ramratnam et al. [1999]
k, Production rate of virions	3000 virions cell^{-1} day^{-1}	Hockett et al. [1999]
δ, Input/output rate of virions	varies virions ml^{-1} day^{-1}	see text

Table 2.2: Constant Input Model parameter descriptions and values.

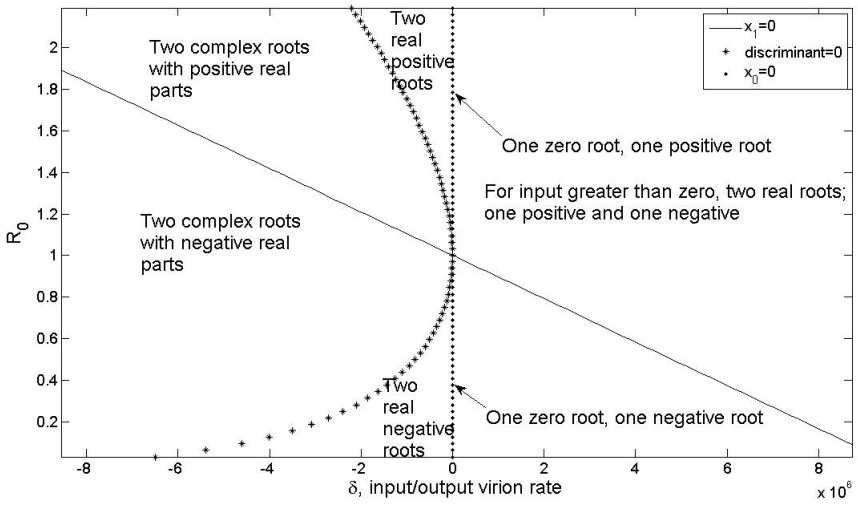

Figure 2-1: Graph showing the possible steady states of v for varying values of R_0 and the input/output rate δ. R_0 was varied by changing the value of the burst size k; other parameter values used are given in Table 2.2.

the quadratic for steady state viral load which is stable.

2.3.4 Summary

This model gives us an idea of what would happen if there were two compartments in which the virus could proliferate and migrate between. If you imagine two connected compartments which allow virus migration you would expect, from the results of the constant input model, that if $R_0 < 1$ in both compartments the virus will become extinct as neither compartment will produce viral particles to sustain either compartment. You would also expect that if one of the compartments has an $R_0 < 1$ and the other an $R_0 > 1$ the virus population will be maintained in both compartments at some level. The next step is to model two linked compartments that allow virus migration between them.

2.4 Two Compartment Model

We now wish to consider a model with two separate body compartments with virus migration between the two compartments. This will allow us to look at the effect of a drug sanctuary on viral load as well as investigating the effects of different types of target cells on steady state viral load both before and after therapy. Callaway and Perelson [2002] used a two compartment model that had identical target cells to

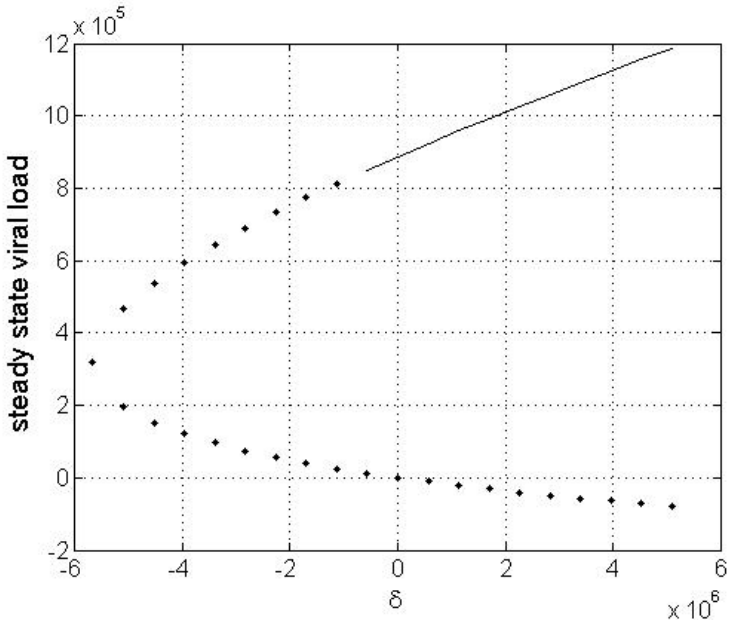

(a) $R_0 > 1$

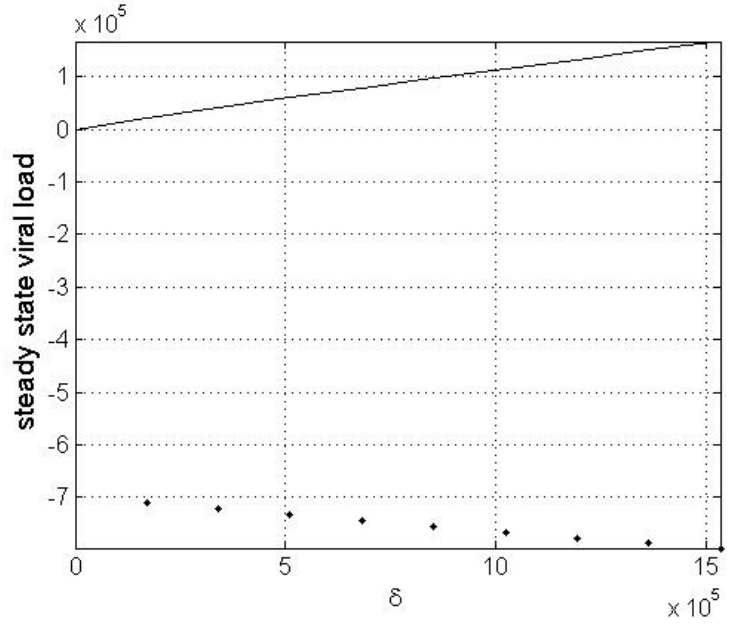

(b) $R_0 < 1$

Figure 2-2: Bifurcation diagrams for virus steady state and the parameter δ. Solid lines denote stable steady states. Dotted lines denote unstable steady states. Parameter values as in Table 2.2.

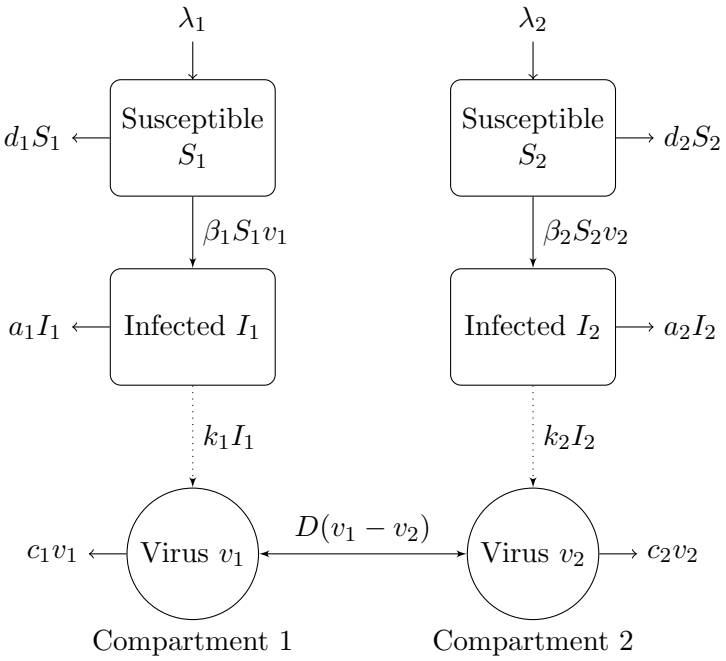

Figure 2-3: Schematic of the Two Compartment Model which allows virus diffusion between two separate body compartments. The diffusion between compartments is along a concentration gradient. In compartment 1 the diffusion term is $\frac{L}{1-u}(v_2 - v_1)$ and in compartment 2 we have $\frac{L}{u}(v_1 - v_2)$, where L is the transport coefficient and u is the scaled size of compartment 2.

investigate the role of a drug sanctuary in maintaining low level viral loads on therapy. By identical target cells we mean that both the susceptible and infected target cell parameters had the same values in each compartment. Here we relax that assumption in order to investigate the effects of target cell heterogeneity between compartments.

2.4.1 Model Equations

We assume that only viral particles can move between the body compartments and that we have distinct target cell types in each compartment. A diagram of the model is given in Figure 2-3. The ordinary differential equations for the system are:

$$\begin{aligned} \dot{S}_i &= \lambda_i - d_i S_i - \beta_i v_i S_i, \\ \dot{I}_i &= \beta_i v_i S_i - a_i I_i, \\ \dot{v}_i &= k_i I_i - c_i v_i + D_i(v_{\hat{i}} - v_i), \end{aligned} \tag{2.3}$$

where $i = 1, 2$ and $\hat{i}$ means "the other one", for example $v_{\hat{1}} = v_2$. We model diffusion of viral particles between compartments using a discrete derivation of Fick's Law

[Macheras and Iliadis, 2006] which gives

$$D_1 = \frac{L}{1-u}, D_2 = \frac{L}{u}$$

where L is the transport coefficient day^{-1}; the total volume of the two compartments is scaled to 1 and u is the proportion of that volume occupied by compartment 2. With this choice of diffusion coefficients, the system exhibits symmetry between compartments. This method of modelling the diffusion of viral particles between compartments is different from that in Kepler and Perelson [1998] in order to obtain symmetry in the model. The meanings of the parameters are the same as for all previous models.

There are a number of different cases that we could look at for this model depending on the component we wish to study in detail:

1. Null neutral model; the cell parameters are the same between compartments allowing us to establish baseline behaviour.

2. Cell heterogeneity model; target cell and infected cell parameters are allowed to vary between compartments in order to model different cell types and immune responses respectively.

3. Drug sanctuary model; the infection rate parameter β is allowed to differ between compartments in order to model a drug sanctuary.

We consider each case in turn, investigating the steady state behaviours analytically where possible and numerically otherwise.

2.4.2 Null Neutral Model

The simplest case of the two compartment model has all the parameters the same between compartments so that $\lambda_i = \lambda, d_i = d, \beta_i = \beta, a_i = a, k_i = k$ and $c_i = c$ and (2.3) becomes

$$\begin{aligned} \dot{S}_i &= \lambda - dS_i - \beta v_i S_i, \\ \dot{I}_i &= \beta v_i S_i - aI_i, \\ \dot{v}_i &= kI_i - cv_i + D_i(v_{\bar{i}} - v_i). \end{aligned} \tag{2.4}$$

Steady State analysis

There are four possible steady states:

1. The disease free steady state

$$(S_1, S_2, I_1, I_2, v_1, v_2) = \left(\frac{\lambda}{d}, \frac{\lambda}{d}, 0, 0, 0, 0\right).$$

2. The endemic steady state

$$(S_1, S_2, I_1, I_2, v_1, v_2) = \left(\frac{S_0}{R_0}, \frac{S_0}{R_0}, \frac{cd}{\beta k}(R_0 - 1), \frac{cd}{\beta k}(R_0 - 1), \frac{d}{\beta}(R_0 - 1), \frac{d}{\beta}(R_0 - 1)\right),$$

where $S_0 = \lambda/d$ and $R_0 = \frac{\lambda\beta k}{acd}$. This is the same as that of the basic one compartment model (1.1) regardless of the value of u. If $R_0 > 1$ then all variables in the endemic steady state will be positive.

3. Two further steady states are possible; they are determined from the roots of the quadratic equation in v_1,

$$x_2 v_1^2 + x_1 v_1 + x_0 = 0, \tag{2.5}$$

where

$$\begin{aligned} x_2 =& a\beta^2(c + D_1)(c + D_1 + D_2), \\ x_1 =& \beta(c + D_1 + D_2)(ad(c + D_1) - \lambda\beta k), \\ x_0 =& dD_1(ad(c + D_1 + D_2) - \lambda\beta k). \end{aligned}$$

Expressions for the other variables given in terms of v_1 and v_2:

$$\begin{aligned} S_1 =& \frac{\lambda}{d + \beta v_1}, \\ I_1 =& \frac{\lambda\beta v_1}{a(d + \beta v_1)}, \\ v_2 =& \frac{v_1(a(c + D_1)(d + \beta v_1) - \lambda\beta k)}{aD_1(d + \beta v_1)}, \\ S_2 =& \frac{\lambda}{d + \beta v_2}, \\ I_2 =& \frac{\lambda\beta v_2}{a(d + \beta v_2)}. \end{aligned}$$

The quadratic in v_1 (2.5) has at least one solution with a positive real part when $x_1 < 0$, the condition for which is $\frac{\lambda\beta k}{ad(c+D_1)} > 1$. Conditions on x_0 then determine the number of solutions with a positive real part. If $x_0 > 0$ there could be two solutions with positive real parts, however if $x_0 < 0$, meaning $\frac{\lambda\beta k}{ad(c+D_1+D_2)} > 1$

there is only one positive real solution. The other variables are positive if and only if $v_1 > \max\{0, \frac{d}{\beta}\left(\frac{\lambda\beta k}{ad(c+D_1)} - 1\right)\}$.

The Jacobian matrix for this system is

$$J = \begin{pmatrix} -d-\beta v_1 & 0 & -\beta S_1 & 0 & 0 & 0 \\ \beta v_1 & -a & \beta S_1 & 0 & 0 & 0 \\ 0 & k & -c-D_1 & 0 & 0 & D_1 \\ 0 & 0 & 0 & -d-\beta v_2 & 0 & -\beta S_2 \\ 0 & 0 & 0 & \beta v_2 & -a & \beta S_2 \\ 0 & 0 & D_2 & 0 & k & -c-D_2 \end{pmatrix}.$$

1. The characteristic polynomial for the disease free steady state can be factorized and the polynomial factors are

$$\begin{aligned} &(\Lambda + d)^2 = 0, \\ &\Lambda^2 + (a+c)\Lambda + ac - \frac{\lambda\beta k}{d} = 0, \\ &\Lambda^2 + (a+c+D_1+D_2)\Lambda + a(c+D_1+D_2) - \frac{\lambda\beta k}{d} = 0. \end{aligned}$$

   The coefficients of these polynomials are all positive and therefore the disease free steady state stable if $R_0 < 1$.

2. The characteristic polynomial for the disease steady state can be factorized into the two cubic equations:

$$\begin{aligned} &\Lambda^3 + (dR_0 + c + a)\Lambda^2 + R_0 d(a+c)\Lambda + adc(R_0 - 1) = 0, \\ &\Lambda^3 + (a+c+dR_0+D_1+D_2)\Lambda^2 + (a(R_0 d + D_1 + D_2) + dR_0(c+D_1+D_2))\Lambda + \\ &\quad + acd(R_0(1 + \frac{D_1+D_2}{c}) - 1) = 0. \end{aligned}$$

   The coefficients of these cubic equations are positive if $R_0 > 1$. Therefore the disease steady state is stable if $R_0 > 1$.

3. The stability of the further two steady states was explored numerically and were found to be locally unstable. The existence and stability of the steady state values for v_1 are shown in Figure 2-4. The bifurcation diagram shows that when $R_0 > 1$ the only stable steady state is the endemic steady state.

These results show that the viral load in two compartments will be the same if the target cell parameters and viral parameters are the same prior to treatment. However

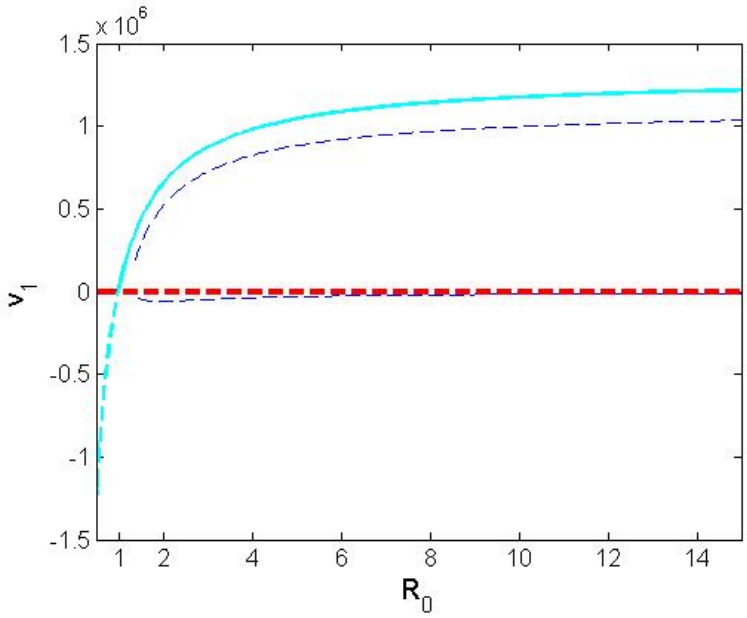

Figure 2-4: Bifurcation Graph of steady state v_1 against R_0 for the null neutral two compartment model. The solid lines denote a stable steady state, the dotted lines unstable steady states. The thick red lines are the disease free steady state, the light blue line is the endemic steady state and the remaining thin dark blue lines are the steady states that are solutions of the quadratic in v_1 given by (2.5). Parameter values used as given in Table 2.2 with $u = 0.5$ and $L = 2$ and varying β.

in reality the viral load in two compartments is rarely the same. A good example of this is in the male genital tract where the viral load is different to that in the blood [Craigo and Gupta, 2006]. There are a number of possible explanations why the two compartment model with identical target cells is not a good one in this case. One possible reason is that the model does not contain latently infected cells, that is cells that have been infected but are not actively producing virus. It has been shown that in the male genital tract there is a higher concentration of latently infected cells than in the blood [Craigo and Gupta, 2006]. Another possible reason could be that the target cells in the second compartment are different and therefore should have different values for parameters relating to cell growth and death. For example viral particles in semen originate from both the prostate and seminal cells in the epididymis [Craigo and Gupta, 2006].

This model is sufficient for drugs that act equally in both compartments. It predicts that the viral load would be the same in both compartments after treatment, although at a lower level than prior to treatment, in the same way as the basic model (1.1).

2.4.3 Cell Heterogeneity Model

In order to study the effects of cell heterogeneity on viral load we need to allow the parameter values to differ between the two compartments. The two compartment model with different parameters (2.3) is a more complicated system. In order to analyse the system we allow only the infection rate β and the infected cell death rate a to vary between compartments. In this section we will consider numerical solutions where $\beta_1 = \beta_2$ in order to concentrate on the effects of cell heterogeneity.

Steady State Analysis

There are four possible steady states:

1. The disease free steady state

$$(S_1, I_1, v_1, S_2, I_2, v_2) = \left(\frac{\lambda}{d}, 0, 0, \frac{\lambda}{d}, 0, 0\right).$$

2. The endemic steady state and two further steady states are solutions of a cubic in v_1

$$y_3 v_1^3 + y_2 v_1^2 + y_1 v_1 + y_0 = 0$$

where

$$\begin{aligned}
y_3 =&\beta_1^2\beta_2 c a_2 a_1^2(c+D_1)(c+D_2+D_1),\\
y_2 =&\beta_1 a_1(a_1 a_2 cd(2\beta_2(c+D_1)(c+D_1+D_2)+\beta_1 D_1(c+D_1+D_2))\\
&-\lambda\beta_1\beta_2 k(a_1 D_1(c+D_1)+a_2(2c(c+D_1+D_2)+D_1D_2))),\\
y_1 =&a_1^2 a_2 d^2 c((c+D_1)(2\beta_1(D_1+D_2)+\beta_2 D_2)+\beta_2(c^2+D_1^2))\\
&-\lambda k d a_1 a_2(2c\beta_1\beta_2(c+D_1+D_2)+\beta_1 D_1(\beta_1(c+D_2)+\beta_2 D_2)))\\
&-\lambda k d a_1^2\beta_1\beta_2 2D_1(c+D_1)+\lambda^2 k^2\beta_1^2\beta_2(a_2(c+D_2)+a_1 D_1),\\
y_0 =&\lambda^2 k^2\beta_1\beta_2 a_1 d D_1 + a_1^2 a_2 c d^3 D_1(c+D_1+D_2)\\
&-\lambda k d^2 a_1 D_1(a_2\beta_1(c+D_2)+a_1\beta_2(c+D_1)).
\end{aligned}$$

Expressions for other variables given in terms of v_1 and v_2 are

$$\begin{aligned}
S_1 =&\frac{\lambda}{d+\beta_1 v_1},\\
I_1 =&\frac{\lambda\beta_1 v_1}{a_1(d+\beta_1 v_1)},\\
v_2 =&\frac{v_1(a_1(c+D_1)(d+\beta_1 v_1)-\lambda\beta_1 k)}{a_1 D_1(d+\beta v_1)},\\
S_2 =&\frac{\lambda}{d+\beta_2 v_2},\\
I_2 =&\frac{\lambda\beta_2 v_2}{a_2(d+\beta_1 v_2)}.
\end{aligned}$$

The Jacobian matrix for this system is given by

$$J=\begin{pmatrix}
-d-\beta_1 v_1 & 0 & -\beta_1 S_1 & 0 & 0 & 0\\
\beta_1 v_1 & -a_1 & \beta_1 S_1 & 0 & 0 & 0\\
0 & k & -c-D_1 & 0 & 0 & D_1\\
0 & 0 & 0 & -d-\beta_2 v_2 & 0 & -\beta_2 S_2\\
0 & 0 & 0 & \beta_2 v_2 & -a_2 & \beta_2 S_2\\
0 & 0 & D_2 & 0 & k & -c-D_2
\end{pmatrix}.$$

1. The characteristic polynomial for the disease free steady state is

$$(\Lambda+d_1)(\Lambda+d_2)(\Lambda^4+x_3\Lambda^3+x_2\Lambda^2+x_1\Lambda+x_0),$$

where

$$
\begin{aligned}
x_0 =& a_1 a_2 c_1 c_2 \left(\left(1 + \frac{D_1}{c_1} - R_{01} \right) \left(1 + \frac{D_2}{c_2} - R_{02} \right) - \frac{D_1 D_2}{c_1 c_2} \right), \\
x_1 =& a_1 c_1 \left(\left(1 + \frac{D_1}{c_1} - R_{01} \right) (D_2 + a_2 + c_2) - \frac{D_1 D_2}{c_1} \right) + \\
& + a_2 c_2 \left(\left(1 + \frac{D_2}{c_2} - R_{02} \right) (D_1 + a_1 + c_1) - \frac{D_1 D_2}{c_2} \right), \\
x_2 =& a_1 c_1 \left(1 + \frac{D_1}{c_1} - R_{01} \right) + a_2 c_2 \left(1 + \frac{D_2}{c_2} - R_{02} \right) + \\
& + (a_1 + c_1 + D_1)(a_2 + c_2 + D_2) - D_1 D_2, \\
x_3 =& a_1 + c_1 + D_1 + a_2 + c_2 + D_2,
\end{aligned}
$$

and

$$
R_{0i} = \frac{\lambda_i \beta_i k_i}{a_i c_i d_i}.
$$

The disease free steady state is stable if all of the coefficients x_i are positive. The coefficient x_3 is always positive and if x_0 and x_1 are positive then so is x_2. The R_0 for this system as calculated using the next generation method [Heffernan et al., 2005] (see the appendix for a worked example) is the positive root of the following quadratic equation

$$
R_0^2 - \left(\frac{\lambda k (a_1 \beta_2 (c + D_1) + a_2 \beta_1 (c + D_2))}{a_1 a_2 d c (c + D_1 + D_1)} \right) R_0 + \frac{\beta_1 \beta_2 \lambda^2 k^2}{a_1 a_2 c d^2 (c + D_1 + D_2)} = 0.
$$

The bifurcation diagram for this system is shown in Figure 2-5. We can see that the disease free steady state is stable if and only if $R_0 < 1$.

2. It is not possible to derive a characteristic polynomial for the other steady states. Figure 2-5 shows that when the disease free steady state is unstable the endemic steady state is stable. As with the null neutral two compartment model there are two other steady states which are unstable.

In contrast to the null neutral model we find the viral load differs between the two compartments. From Figure 2-6 we can see that when the infected cell death rate differs between the compartments the viral load differs also. By changing the parameter values between compartments we can model a drug sanctuary or cell heterogeneity.

2.4.4 Drug Sanctuary Model

If we set $u < 0.5$ then the second compartment will be the smaller of the two compartments. We can then investigate whether the presence of a small compartment that is

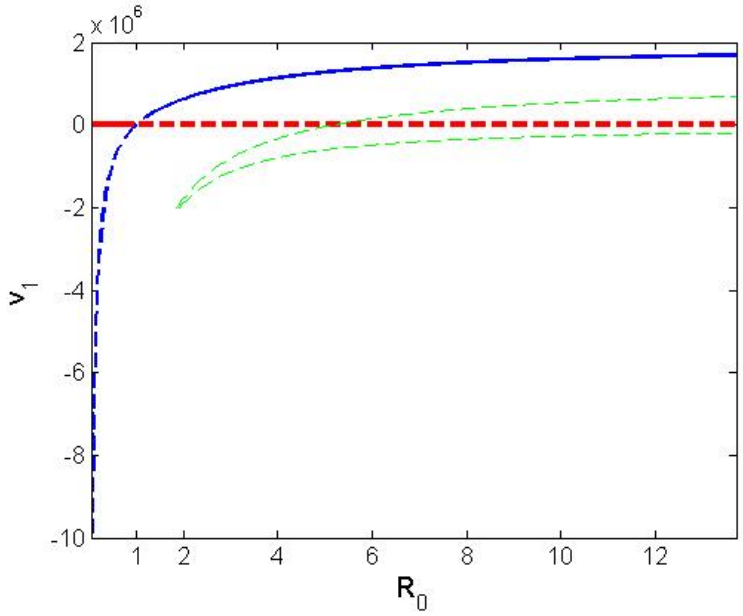

Figure 2-5: Bifurcation Graph of steady state v_1 against R_0 for the cell heterogeneity model. The solid lines denote a stable steady state, the dotted lines unstable steady states. The thick red lines are the disease free steady state, the dark blue line is the endemic steady state and the thin green lines are the steady states that the remaining solutions of the cubic in v_1. Parameter values used as given in Table 2.2 with $u = 0.5, a_2 = 0.2$ and $L = 2$ and varying $\beta_1 = \beta_2$.

more difficult for drugs to reach has an effect on the dynamics of the HIV infection. Both reverse transcriptase inhibitors and protease inhibitors can be modelled easily in HIV infection by lowering the values of the infection rate β and the burst size k respectively. We can model the effect of the drug differently in each compartment to see what effect a lower drug concentration in the smaller compartment has on the dynamics of the system. We can model the effect of a reverse transcriptase inhibitor by changing the value of β in the presence of the drug as given below.

$$\beta_1 = (1 - e)\beta,$$
$$\beta_2 = (1 - eh)\beta,$$

where β_1 is for compartment 1 and β_2 is for compartment 2, with the drug efficacy, e and drug penetrance, h, varying between zero and one. Figure 2-7a shows the viral steady state of the large compartment in the two compartment model compared with a one compartment model when the drug efficacy is varied. The presence of the second smaller compartment (with a lower drug efficacy) allows the virus to persist in the system even

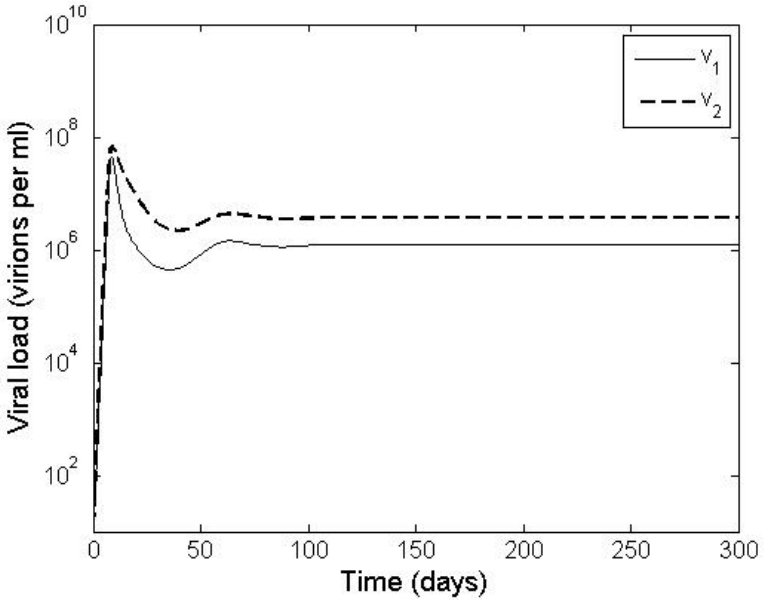

Figure 2-6: Graph showing the viral load when the infected cell death rates differ between compartments. Parameters are the same as those in Table 2.2 with $a_2 = 0.2, a_1 = 1, u = 0.05, L = 2$.

if the drug is 100% effective in the main compartment. This agrees with work by Callaway and Perelson [2002] which also included a subset of chronically infected cells. These were found to dampen the oscillations to the disease steady state making it less likely that the viral population would become extinct due to stochasticity. Low steady state viral loads can also be obtained when modelling a protease inhibitor, which acts on k in the model, as shown in Figure 2-7b. Notice that the relationship between viral load and drug efficacy is now linear up until a critical value of drug efficacy. This can be explained by looking at the steady state expression for viral load in the one compartment model which is given by

$$v^* = \frac{d}{\beta}\left(\frac{\lambda\beta k}{acd} - 1\right).$$

The viral load is a linear function of k and inverse linear function of β, hence explaining the behaviour of the steady state value up to a critical value of drug efficacy. Protease inhibitors lower the steady state viral load over a large range of drug efficacies whereas reverse transcriptase inhibitors have a much smaller effective range. This could have an impact on the emergence of drug resistance. The lower the viral load the less likely a resistant mutant will arise in the population.

The size of the smaller sanctuary compartment also influences the steady state viral

load as can be seen in Figure 2-8. The larger the sanctuary compartment is compared to the main compartment the higher the steady state viral load in the main compartment for all drug efficacies.

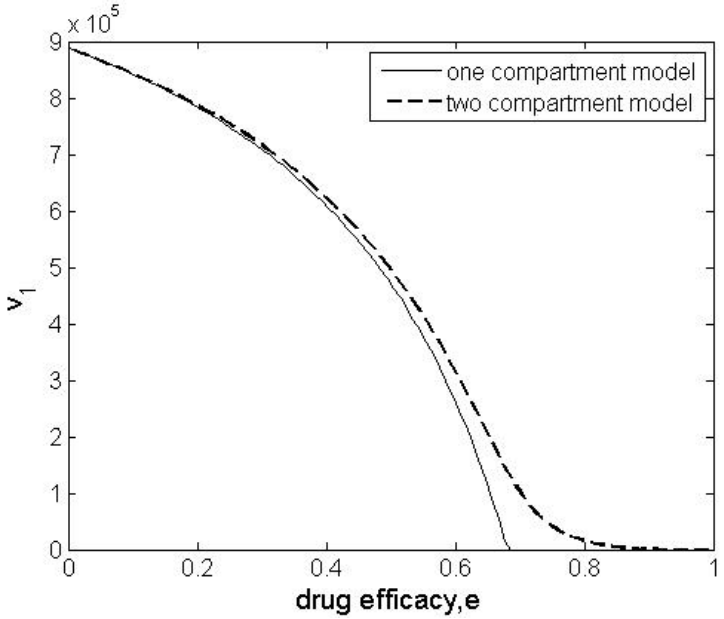

(a) Reverse transcriptase inhibitor acting on β

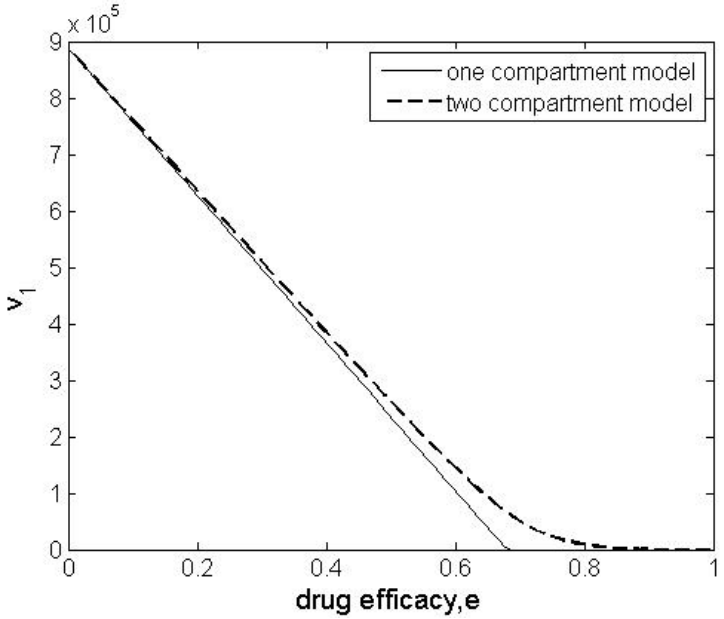

(b) Protease inhibitor acting on k

Figure 2-7: Graphs showing how drug efficacy changes the steady state viral load in the large compartment of a 2 compartment model compared with a one compartment model for (a) reverse transcriptase inhibitors and (b) protease inhibitors. The parameter values used are the same as those in Table 2.2 with $u = 0.1, h = 0.5, L = 2$.

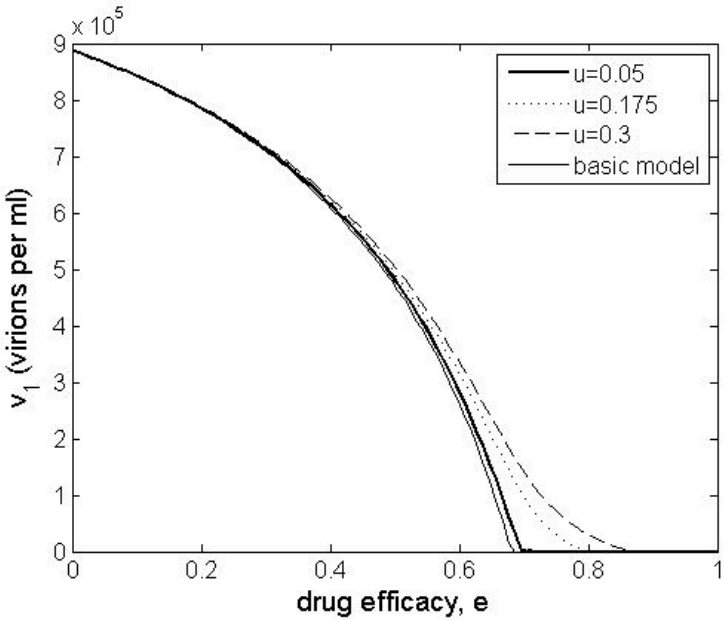

Figure 2-8: Graph comparing the steady state viral load for different drug efficacies and values of u. Drug acts in both compartments with compartment 2 acting as a drug sanctuary, giving $\beta_1 = (1-e)\beta$ and $\beta_2 = (1-eh)\beta$. Parameter values used are the same as those in Table 2.2 with $h = 0.7, L = 2$.

2.4.5 Combined Model

It has been suggested that cell-free virions in semen originate from the prostate whereas cell-associated virions in semen originates from the testis [Craigo and Gupta, 2006]. However the cellular origin of the virions in semen is as yet unknown. There are some data that suggest that viral clearance in the semen is at a slower rate than the blood during antiretroviral therapy suggesting that infected cell death rates may be lower in the semen compartment [Craigo and Gupta, 2006]. The two compartment model can also be used to look at the possibility that the smaller compartment is not a drug sanctuary but instead has different target cell types or that the target cells have different behavours in different compartments.

Considering different target cell types in a two compartment model (and hence using different parameter values for cell growth and death) can produce behaviour similar to that observed in the previous section provided that $R_{02} = \frac{\lambda_2\beta_2 k_2}{a_2 c_2 d_2} > R_{01} = \frac{\lambda_1\beta_1 k_1}{a_1 c_1 d_1}$. This is shown in Figure 2-9 where the target cells vary between compartments. Increasing the value of λ_2 or decreasing the value of d_2 or a_2 produce the same qualitative results: low level viral load at a wider range of drug efficacies than in the one compartment model. These results suggest that even if drug penetrance is good it is still possible to get persistent, low-level steady state viral loads if there are small compartments with a higher viral replicative capacity than the main blood compartment.

The interplay of the main parameters we are interested in here, drug penetrance, drug efficacy and infected cell death, is explored in Figure 2-10. The parameter space between the $R_0^e = 1$ lines for the one compartment model (1.1) and the two compartment model (2.3) in Figures 2-10a and 2-10b is where low level viral load occurs. In Figure 2-10c the $R_0^e = 0$ for the one compartment model (1.1) as the drug is completely effective, i.e. $e = 1$. Low level viral load is seen for a wide range of values of infected cell death, a_2, and drug penetrance, h. The presence of cell heterogeneity widens the range of values of drug penetrance for which low level viral load can be observed and vice versa.

2.4.6 Summary

The two compartment model is capable of allowing low level viral in a number of situations: firstly when there is a drug sanctuary in the smaller compartment in agreement with the work of Callaway and Perelson [2002] and secondly when there is a difference between the cell parameters in the two compartments that means that the small compartment has a higher replicative capacity even before treatment is initiated. When there is both cell heterogeneity and a drug sanctuary present low level viral load can be

seen for a wider range of drug efficacies up to and including the drug being completely effective in the large compartment, $e = 1$.

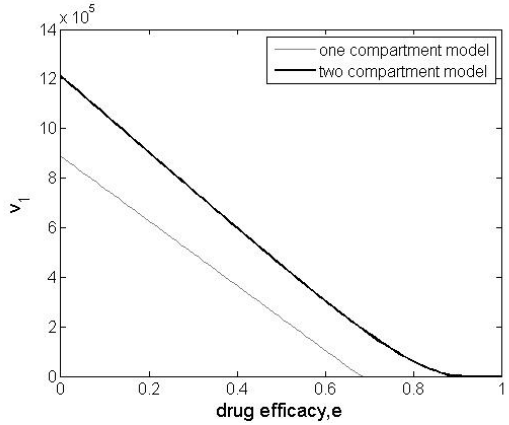

(a) $a_2 = 0.2$

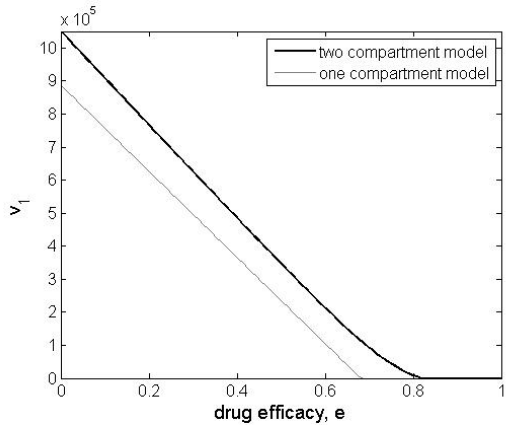

(b) $\lambda_2 = 3 \times 10^4$

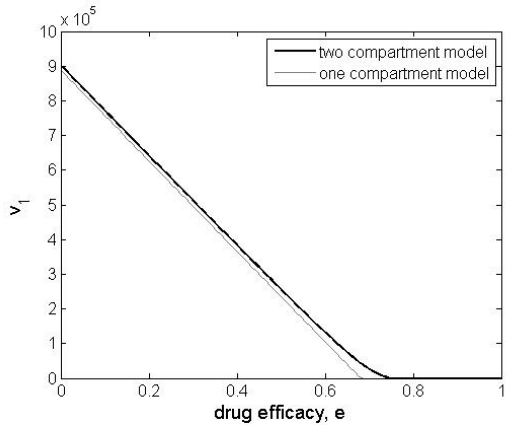

(c) $d_2 = 0.005$

Figure 2-9: Graph comparing the steady state viral load in the large compartment for different drug efficacies (protease inhibitor) when there is cell heterogeneity. Other parameters are the same as in Table 2.2 with $u = 0.1, h = 1$ and $L = 2$.

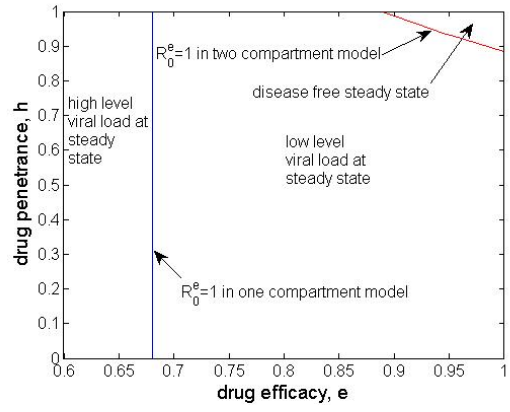

(a)

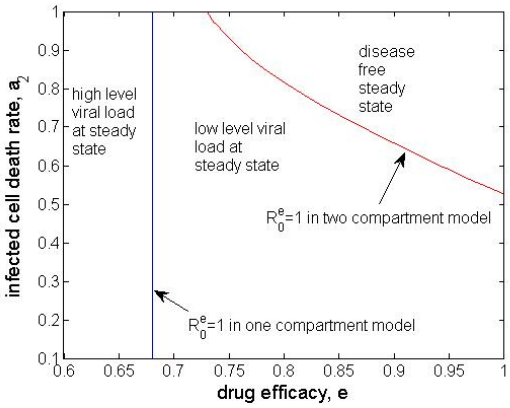

(b)

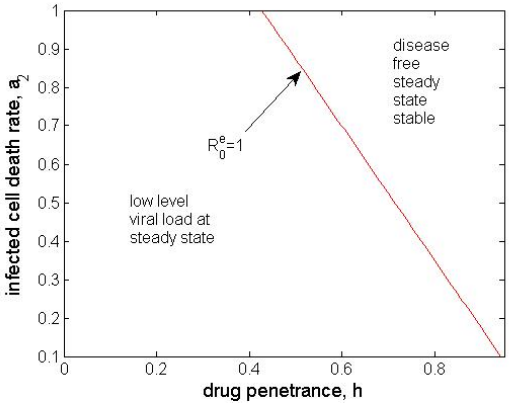

(c)

Figure 2-10: Graphs showing how drug penetrance, drug efficacy and infected cell death rates affect the steady state behaviour of the two compartment model. a) $a_2 = 0.2$, b) $h = 0.9$, c) $e = 1$. In all of the graphs the parameters are as given in Table 2.2 with $L = 2$ and $u = 0.1$.

2.5 Model with two target cell populations

Callaway and Perelson [2002] also considered a model with two co-circulating distinct target cell populations with chronic infection. We follow their work and present a similar model (which does not include chronically infected cells), a schematic of which is shown in Figure 2-11, to ascertain whether low level viral load can be seen without the presence of a drug sanctuary. The primary target cells are assumed to be the ones most commonly associated with HIV, CD4+ T cells. The secondary target cells are assumed to be macrophages with a much lower concentration in the blood but a higher infection rate compared with primary target cells. This is due to lack of activation needed for infection of macrophages to occur [Stevenson and Gendelman, 1994].

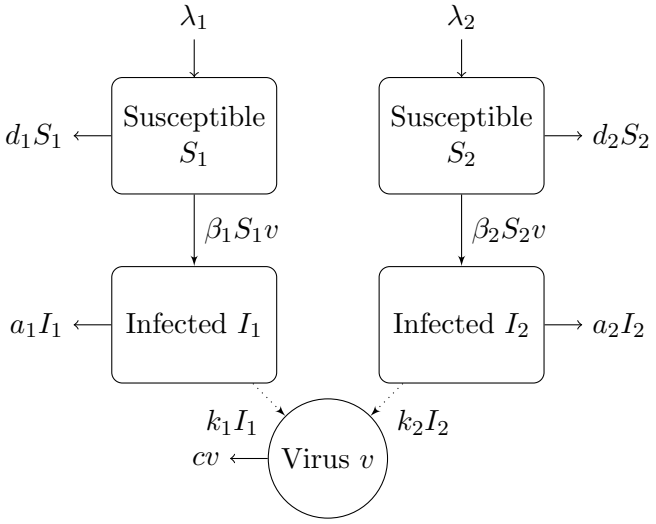

Figure 2-11: Schematic of the Two Target Cell Model.

The equations are given as:

$$\begin{aligned}
\dot{S}_1 &= \lambda_1 - d_1S_1 - \beta_1S_1v, \\
\dot{S}_2 &= \lambda_2 - d_2S_2 - \beta_2S_2v, \\
\dot{I}_1 &= \beta_1S_1v - a_1I_1, \\
\dot{I}_2 &= \beta_2S_2v - a_2I_2, \\
\dot{v} &= k_1I_1 + k_2I_2 - cv,
\end{aligned} \tag{2.6}$$

where parameters are as defined in the basic model (1.1) and Table 2.3.

2.5.1 Steady State Analysis

Setting the left hand side of the ordinary differential equations (2.6) to zero we can find the steady states of the system.

1. The disease free steady state of this system is $(S_1, S_2, I_1, I_2, v) = (\frac{\lambda_1}{d_1}, \frac{\lambda_2}{d_2}, 0, 0, 0)$.

2. The endemic steady state is found by solving the following quadratic in v

$$v^2 + x_1 v + x_0 = 0, \tag{2.7}$$

where

$$x_1 = \frac{d_1}{\beta_1}(1 - R_{01}) + \frac{d_2}{\beta_2}(1 - R_{02}),$$
$$x_0 = \frac{d_1 d_2}{\beta_1 \beta_2}(1 - R_{01} - R_{02}),$$

and $R_{0i} = \frac{\lambda_i \beta_i k_i}{a_i c d_i}$ for $i = 1, 2$. Provided that $R_{01} + R_{02} \geq 1$, we obtain a single positive solution for v; in particular when $R_{01} + R_{02} = 1$,

$$v = \frac{d_1}{\beta_1}(R_{01} - 1) + \frac{d_2}{\beta_2}(R_{02} - 1).$$

This is the minimum value of the steady state viral load as x_0 becomes negative when $R_0 = R_{01} + R_{02} > 1$. The expressions for the other variables are

$$S_1 = \frac{\lambda_1}{d_1 + \beta_1 v},$$
$$S_2 = \frac{\lambda_2}{d_2 + \beta_2 v},$$
$$I_1 = \frac{\beta_1 v \lambda_1}{a_1(d_1 + \beta_1 v)},$$
$$I_2 = \frac{\beta_2 v \lambda_2}{a_2(d_2 + \beta_2 v)}.$$

The Jacobian matrix for this system is

$$J = \begin{pmatrix} -d_1 - \beta_1 v & 0 & 0 & 0 & -\beta_1 S_1 \\ 0 & -d_2 - \beta_2 v & 0 & 0 & -\beta_2 S_2 \\ \beta_1 v & 0 & -a_1 & 0 & \beta_1 S_1 \\ 0 & \beta_2 v & 0 & -a_2 & \beta_2 S_2 \\ 0 & 0 & k_1 & k_2 & -c \end{pmatrix}.$$

1. The characteristic polynomial for the disease free steady state is given by

$$(\Lambda + d_1)(\Lambda + d_2)(\Lambda^3 + y_2\Lambda^2 + y_1\Lambda + y_0) = 0,$$

where

$$\begin{aligned} y_2 &= c + a_1 + a_2, \\ y_1 &= c(a_1 + a_2) + a_1a_2 - \frac{k_1\beta_1\lambda_1}{d_1} - \frac{k_2\beta_2\lambda_2}{d_2}, \\ y_0 &= ca_1a_2 - \frac{k_1\beta_1\lambda_1a_2}{d_1} - \frac{k_2\beta_2\lambda_2a_1}{d_2}. \end{aligned}$$

The condition for which all the eigenvalues are negative and the steady state stable is

$$R_{01} + R_{02} < 1.$$

2. The stability of the endemic steady state was investigated numerically and the bifurcation diagram is shown in Figure 2-12. The endemic steady state becomes positive and stable when $R_0 > 1$, corresponding to when the disease free steady state becomes unstable.

2.5.2 Numerical Solutions

Parameter values used for numerical solutions of the two target cell model can be found in Table 2.3. In order to investigate the behaviour of the steady state viral load when drug was present we replace β_1 and β_2 with $\hat{\beta}_1 = (1-e)\beta_1$ and $\hat{\beta}_2 = (1-eh)\beta_2$ respectively in (2.6). Values for the cell production rate, λ_2, and the infection rate, β_2, for the secondary target cells were calculated using the following constraints [Callaway and Perelson, 2002]. Constraint 1: given $e = 1$ and $h = 0$ (drug 100% effective in main target cell and completely ineffective in second target cell) the viral load should be 100 virions per ml. Constraint 2: given $e = 1$ and $h = 0.5$ (drug half as effective in second target cell) the viral load should be 0 . Assuming $e = 1$ and all the other parameters are the same between target cells gives

$$v_w = \frac{\lambda_2 k}{ac} - \frac{d}{\beta_2(1-h)}.$$

Using the two constraints and parameter values from Table 2.3 we find $\lambda_2 = 1.533$ and $\beta_2 = 10^{-4}$.

The behaviour of the model when the susceptibility of the two populations of cells

was the same ($h = 1$) or different($h < 1$) was investigated. The results can be seen in Figure 2-13. The parameter values used in this example give $R_{02} > 1$, meaning that if the second population of cells was the only population of target cells they would allow the disease to be maintained. If a different set of parameter values is used which gives $R_{02} < 1$ the same concave behaviour can be obtained, but the critical value of drug efficacy e, at which the disease free steady state becomes stable is much closer to that of the basic model (1.1). Decreasing values of drug penetrance, h, allow low level viral load at steady state for a larger range of values of drug efficacy, e, which can be seen in Figure 2-14.

2.5.3 Summary

The two target cell model is capable of allowing low level viral load in a number of situations: firstly when the secondary target cells act as a drug sanctuary in agreement with the work of Callaway and Perelson [2002] and secondly when there is a difference between the cell parameters in the two types of target cell. This is an important result as it means that low level viral load can happen in the absence of external input.

Parameter Description	**Value**	**Source**
λ_1, Birth rate of primary target cells	10^4 cells ml^{-1} day^{-1}	Callaway and Perelson [2002]
λ_2, Birth rate of secondary target cells	1.53 cells ml^{-1} day^{-1}	Callaway and Perelson [2002]
β_1, Infection rate	2.4×10^{-8} virion^{-1} day^{-1}	Perelson et al. [1993]
β_2, Infection rate	10^{-4} virion^{-1} day^{-1}	Callaway and Perelson [2002]
d_1, Death rate of target cells	0.01 day^{-1}	Mohri et al. [1998]
d_2, Death rate of secondary target cells	0.01 day−1	text
a_1, Death rate of infected cells	1 day^{-1}	Markowitz et al. [2003]
a_2, Death rate of infected cells	1 day^{-1}	text
c, Death rate of virions	23 day^{-1}	Ramratnam et al. [1999]
k_1, Production rate of virions	3000 virions cell^{-1} day^{-1}	Hockett et al. [1999]
k_2, Production rate of virions	3000 virions cell^{-1} day^{-1}	text
e, Drug efficacy	0.9	text
h, Drug penetrance	0.7	text

Table 2.3: Two target cell model parameter descriptions and values.

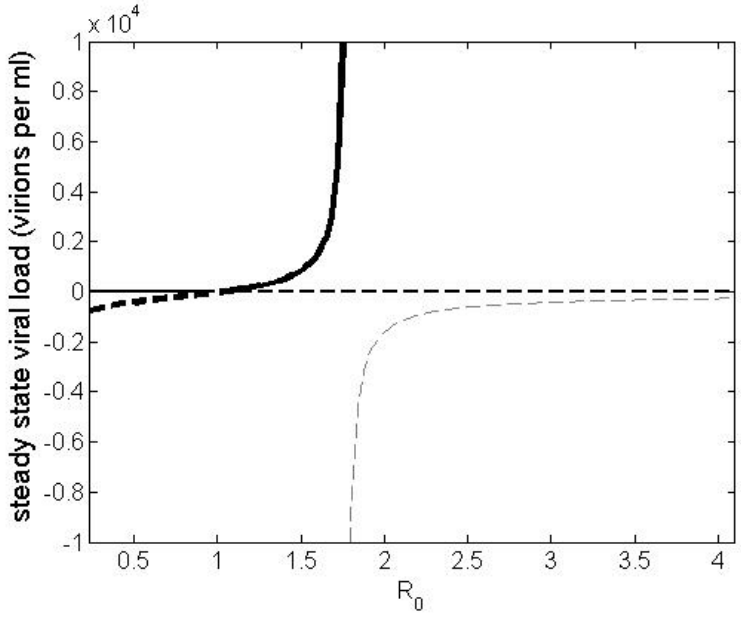

(a)

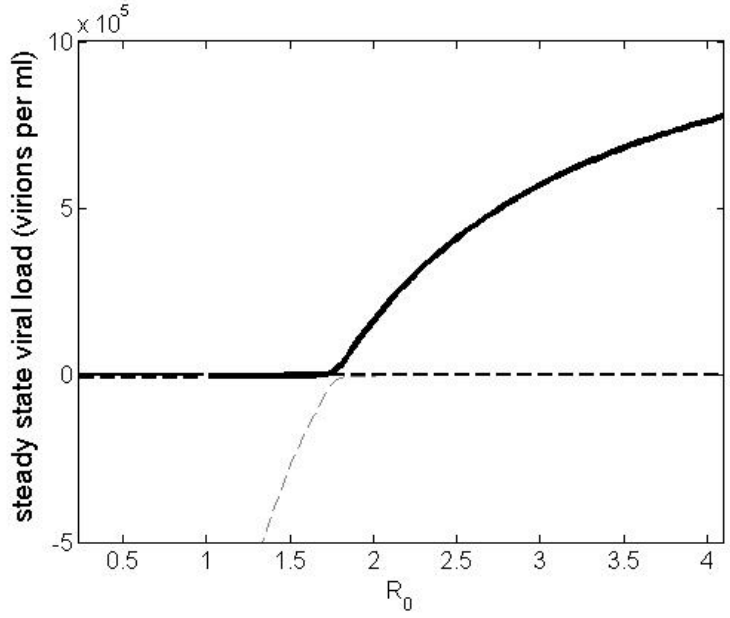

(b)

Figure 2-12: Bifurcation Diagram for the Two Target Cell Model (2.6). Solid lines denote stable steady states and dashed lines unstable ones. The thick black line and thin grey lines are the roots of the quadratic in v (2.7) and the thin black line is the disease free steady state. Graph a is a close up of the region around $R_0 = 1$ of graph b. Parameter values used are given in Table 2.3 and varying drug efficacy e.

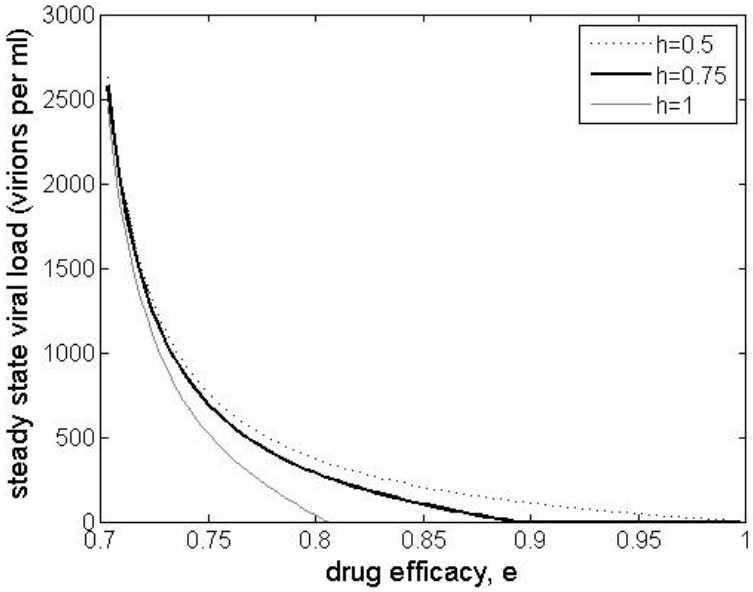

Figure 2-13: Graph showing the effect of drug susceptibility of two different populations of cells, h, on the steady state viral load for different drug efficacies. For the range of drug efficacies shown here the disease free steady state would be stable in the basic HIV model (1.1). Parameter values use are as given in Table 2.3.

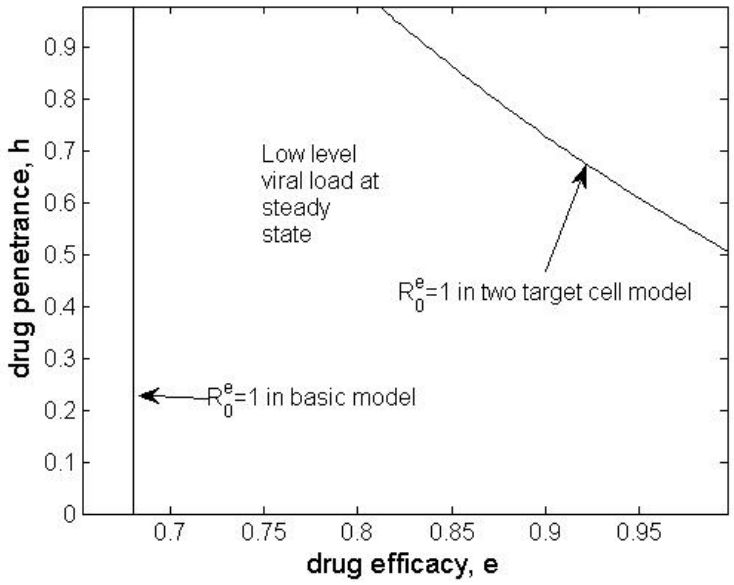

Figure 2-14: Graph showing how two parameters, drug penetrance,h, and drug efficacy, e, affect the behaviour of the model at steady state. Parameter values used are as given in Table 2.3.

2.6 Conclusions

From our investigation of robust models of low lovel steady state viral loads we have a number of new results. Firstly that the two compartment model with identical parameters (2.4), does not describe the differences in viral loads seen in the blood and male genital tract before therapy and is therefore not necessarily a good model for these body compartments during therapy. Secondly the two compartment model with identical cell parameters can be used to model a drug sanctuary and that the steady state viral load profile for protease inhibitor therapy shows that this drug is more effective than reverse transcriptase therapy over a larger range of drug efficacies. Thirdly a two compartment model with distinct target cell parameters (2.3), can be used to model blood and male genital tract compartments before therapy as it gives different viral loads in each compartment. This model also allows a low level steady state viral load in the blood under drug therapy even if drug penetrance into the smaller compartment is the same as the blood. Finally a model with co-circulating distinct target cells in one compartment (2.6), where one of the populations of target cells is at a lower concentration, can also show low level steady state viral loads when the drug is equally effective in both populations as it allows viral replication for a wider range of drug efficacies.

Chapter 3

Multistrain Models

3.1 Chapter Outline

This chapter is concerned with modelling drug resistance in HIV patients and is important as background for the rest of the thesis. It is mainly a review of previous work adapted to fit in with the other models described in this thesis, with novel work on models containing three strains of virus.

We begin with a summary of the relevant biology.

We then describe both competition and evolutionary models to investigate the effect of drug resistance on the viral load of a HIV patient. Competition models have no mechanism of mutation from one strain to another and are therefore useful for comparison with the more complicated evolutionary models. Two and three strain competition models are described in Section 3.3.

The next step on from competition models are evolutionary models which are described in Section 3.4. Here we include mutation in two and three strain models in turn. We consider two different ways of modelling mutation in the three strain models: linear mutation, whereby a strain can mutate only to a neighbouring strain, and jump mutation, whereby a strain can mutate into either of the other two strains.

3.2 Background and Motivation

3.2.1 Biological Background on Drug Resistance

A great deal of research has been carried out to look at HIV drug resistance and how and when it arises [Craigo and Gupta, 2006, Tirado et al., 2004, Lowe et al., 2004, Mansky, 2002, Pillay et al., 2000, Tang and Pillay, 2004].

HIV has an average mutation rate of one mutation per newly synthesized virion

[Mansky, 2002]. This means that mutations arise frequently in the life cycle of HIV. Some of these mutations will confer advantages and some disadvantages. The wild type virus is assumed to have the highest fitness in the absence of drug selective pressure. There will be a number of closely related viral strains within the whole population termed quasispecies. Mutations which confer resistance to antiretroviral drugs arise at the same rate as any other mutation but the likelihood of these mutants becoming dominant in the quasispecies depends on the magnitude of the relative fitness of the mutant. A primary resistance mutation is defined as one which is sufficient to cause drug resistance. A secondary resistance mutation is defined as one which compensates for the reduced fitness caused by a primary resistance mutation [Tang and Pillay, 2004].

Due to the high mutation rate it is likely that drug resistance mutations are present in the viral quasispecies even in the absence of therapy [Bonhoeffer et al., 1997]. Once antiretroviral therapy starts it is likely that resistance will emerge and current practice is to suppress viral replication as much as possible [Gazzard, 2006]. Anything which lowers drug efficacy - differences in potency, pharmacological effects, compartmentalization, adherence and drug resistance - can cause a drug regimen to fail. These factors differ according to the specific drug regimen and the behaviour of individual patients [Pillay et al., 2000].

Drug resistance mutations have been found for all of the common antiretroviral drugs. Unsurprisingly the mutations seen in individual cases will depend on the regimen history of the patient, where different resistance pathways can be seen according to the order and length of time which the patient was exposed to different drugs [Pillay et al., 2000]. If a patient has been on the same therapy for a long time, primary and secondary resistance mutations may have emerged so that the resistant strain is dominant. In some cases these resistant strains can be as fit as the wild type strain in *in vitro* experiments [Pillay et al., 2000].

Transmission and Persistence of Drug Resistance

The transmission of drug resistant strains has been documented for most methods of transmission including sexual transmission, intravenous transmission (blood donors, needlestick injury and drug users) and vertical transmission from mother to baby. Resistance has major implications for the treatment options available to the newly infected individual [Grant et al., 2002, Weinstock et al., 2004, Little et al., 2002]. The prevalence of transmitted drug resistance is currently around 8% of all new diagnoses in the United Kingdom [Resistance et al., 2007] which has dropped from 14% in 2001. The persistence of drug resistant strains depends on whether the infection is from a mix of wild type and drug resistant strains or from drug resistant strains only. In the

former case the wild type strain would be expected to re-emerge as the dominant strain as the patient would not be receiving therapy. In the latter case, back mutation to wild type would need to occur. This would seem unlikely for resistant strains of high fitness that are separated from wild type by a number of mutations. A good example of this is the T215Y 3-azido 3-deoxythymidine (AZT) drug resistant mutation. This differs from wild type by two mutations and the intermediate mutations (there are a number of different possible intermediates) although resistant to drug are as fit as wild type [Tang and Pillay, 2004].

Reversion to wild type has been seen in some case studies [Gandhi et al., 2003, Brenner et al., 2002]. In Gandhi et al. [2003] a patient infected with multiple drug resistant virus was followed for a year with regular monitoring of the mutations present in the viral quasispecies. Phenotypic assays for drug resistance and fitness assays compared with a laboratory wild type strain were also carried out. Over the course of the year, five of the twelve resistance mutations reverted to wild type and an increase in overall fitness was seen. This patient was not on any drug therapy meaning that replicative fitness was the overiding selective pressure. In contrast a study by Brenner et al. [2002], which included the source partners of infection, showed that although in the source partners wild type outgrowth was seen once therapy was interrupted, the recipient partners showed the presence of resistant mutations for long periods from 6 weeks to 5 years. This suggests a role for latent infection of compartments of cells by wild type in the source partners allowing rapid outgrowth of wild type. It also suggests that the recipient partners were infected by the dominant resistant strain in the source partners.

When resistance mutations to a certain drug are present, treatment with that drug is unlikely to be successful so it is important that newly diagnosed individuals are screened for mutations before commencing therapy. However, routine tests are not able to detect minority mutants below 20% prevalence in the viral quasispecies [Palmer et al., 2005]. This could mean that transmitted drug resistance is not always picked up and that in some cases drug resistance is present and treatment will fail. New techniques are being developed to detect prevalence at a lower level. One such technique is allele specific polymerase chain reaction (PCR). An interesting study using this method followed mothers who took single dose Nevaripine to prevent mother to baby transmission of HIV [Palmer et al., 2006]. Allele specific PCR was used to detect the presence of mutants down to 0.1% in the quasispecies. It was found that mutants persisted for over one year at levels undetectable by standard methods after 2 months.

In summary, drug resistance mutations can arise before treatment and are present in the quasispecies. Once therapy starts resistant strains can emerge and become

dominant if the viral load is not suppressed sufficiently. Transmission of drug resistant strains between partners is of concern and screening needs to occur in order to start the patient on the best therapy. The long term presence of resistant strains is determined by their fitness both on and off therapy.

3.2.2 Mathematical Modelling of Drug Resistance

There have been many models that investigate the effect of drug resistance on HIV infection and an excellent review of the body of work up until 2000 can be found in Nowak and May [2000]. Here we will pick out the models relevant to the thesis from the last two decades since the research into this area began. The first multistrain models of HIV infection were interested in the effect of drug resistance on viral load after treatment commenced and the time to emergence of the resistant strain [McLean and Nowak, 1992, McLean and Frost, 1995, Frost and McLean, 1994]. Later models were concerned with the frequency of virus before treatment commenced [Bonhoeffer et al., 1997, Ribeiro et al., 1998]. More recent models investigate how other important biological aspects of HIV infection affect the emergence of drug resistance such as how drug concentration and adherence to therapy affects the emergence of drug resistance [Smith and Wahl, 2005, Smith, 2006, Rong et al., 2007a]. Rong et al. [2007b] include a non-productive eclipse phase to investigate how drug resistance develops during HIV infection. In later chapters we will consider the impact of cell heterogeneity and the presence of latently infected cells on drug resistance. For now we will describe the simplest versions of competition and evolutionary models of HIV infection with reference to the relevant papers as necessary background to the later chapeters.

We will obtain the steady states and stability criteria for each model as well as investigate the frequency of mutants before therapy is commenced in addition to the time to emergence of mutants after therapy is initiated. In the case of two strain models this has been shown before by others [Ribeiro et al., 1998, Nowak et al., 1997, Nowak and May, 2000], whereas the three strain model work is novel.

3.3 Competition Models

Competition models such as those in Nowak and May [2000] aim to investigate the effect that a strain of virus resistant to drug treatment has on viral load and CD4+ T cell levels. They contain no mechanism for the mutation of one strain of virus to another. Competition models almost always show competitive exclusion, a phenomenon whereby the strain with the largest replicative capacity outcompetes the other strain and drives it to extinction. First we present and analyse a two strain model of drug resistance

and then go on to describe a three strain model.

3.3.1 Two Strain Competition Model

This model has two strains of virus present, which are assumed to differ only in the value of the infection rate β. This is to model the difference between RTI sensitive and RTI resistant strains. The value of β for the sensitive strain will be assumed to be greater than that of the resistant strain when there is no drug present. A similar model looking at PI resistance could be modelled by allowing the value of the burst size, k, to be different for each strain. It should be pointed out that in models without mutation you cannot get a steady state of a particular strain if that strain wasn't present to start with.

Model Equations

A system with two viral strains (differing in their β values only), adapted from the basic model (1.1) is given below:

$$\begin{aligned} \dot{S} =& \lambda - dS - \beta_w S v_w - \beta_m S v_m, \\ \dot{I}_i =& \beta_i S v_i - a I_i, \\ \dot{v}_i =& k I_i - c v_i, \end{aligned} \tag{3.1}$$

for $i = w, m$ and where $i = w$ for the wildtype drug sensitive strain and $i = m$ for the resistant strain.

Using the next generation matrix method (see appendix for details) to find the R_0 for this system gives $R_0 = max_i\{R_{0i}\}$ where $R_{0i} = \frac{\lambda \beta_i k}{acd}$ for $i = w, m$.

Steady State Analysis

There are three steady states for this system (3.1).

1. The disease free steady state is

$$\left(S = \frac{\lambda}{d} = S_0, I_w = 0, I_m = 0, v_w = 0, v_m = 0 \right).$$

2. The wildtype strain only endemic steady state is

$$\begin{aligned} S =& \frac{S_0}{R_{0w}}, \\ I_w =& \frac{cd}{k\beta_w}(R_{0w} - 1), \\ v_w =& \frac{d}{\beta_w}(R_{0w} - 1), \\ I_m =& 0, \\ v_m =& 0, \end{aligned}$$

   which is biologically realistic when $R_{0w} > 1$.

3. The mutant strain only endemic steady state is

$$\begin{aligned} S =& \frac{S_0}{R_{0m}}, \\ I_m =& \frac{cd}{k\beta_m}(R_{0m} - 1), \\ v_m =& \frac{d}{\beta_m}(R_{0m} - 1), \\ I_w =& 0, \\ v_w =& 0, \end{aligned}$$

   which is biologically realistic when $R_{0m} > 1$.

The Jacobian matrix for this system is

$$\begin{pmatrix} -d - \beta_w v_w - \beta_m v_m & 0 & 0 & -\beta_w S & -\beta_m S \\ \beta_w v_w & -a & 0 & \beta_w S & 0 \\ \beta_m v_m & 0 & -a & 0 & \beta_m S \\ 0 & k & 0 & -c & 0 \\ 0 & 0 & k & 0 & -c \end{pmatrix},$$

with corresponding eigenvalues Λ.

1. The disease free steady state characteristic polynomial can be factorised into

smaller polynomials:

$$\Lambda + d = 0,$$
$$\Lambda^2 + (a+c)\Lambda + ca - \frac{\lambda\beta_w k}{d} = 0,$$
$$\Lambda^2 + (a+c)\Lambda + ca - \frac{\lambda\beta_m k}{d} = 0.$$

Therefore the disease free steady state is stable if $R_{0w} < 1$ and $R_{0m} < 1$ as this gives positive coefficients. Combining these results for each polynomial we find the disease free steady state is stable when R_0 is less than unity.

2. The wildtype strain only endemic steady state characteristic polynomial can be factorised into a quadratic and a cubic:

$$\Lambda^2 + (a+c)\Lambda + ca\left(1 - \frac{\beta_m}{\beta_w}\right) = 0,$$
$$\Lambda^3 + \left(a + c + \frac{\lambda\beta_w k}{d}\right)\Lambda^2 + \left(\frac{\lambda\beta_w k}{c} + \frac{\lambda\beta_w k}{a}\right)\Lambda + \lambda\beta_w k - acd = 0.$$

Through consideration of the behaviour of these polynomials, we see that the wildtype strain only endemic steady state is stable if $\beta_w > \beta_m$ and $R_{0w} > 1$.

3. Similarly the mutant strain only endemic steady state is stable if $\beta_m > \beta_w$ and $R_{0m} > 1$.

This model shows competitive exclusion which means that one viral strain, the one with the highest R_0 value, will always outcompete the other so that at steady state only the fittest viral strain is present. Before treatment we would expect the wildtype strain to be the fittest, with $\beta_w > \beta_m$ and once treatment has started the drug resistant strain may or may not be fitter than the wildtype strain. If we assume that treatment is modelled in the same way as the previous chapter with $\beta_w^e = (1-e)\beta_w$ and β_m unaffected by treatment then the wildtype strain will outcompete the mutant strain when drug efficacy $e < 1 - \frac{\beta_m}{\beta_w}$, otherwise the mutant strain will win as long as $R_{0m} > 1$.

3.3.2 Three Strain Competition Model

Modelling three strains is also very straightforward. The assumption is made that one strain is sensitive to RTI's and two are resistant.

Model Equations

The model equations can be written in the same form as the two strain equations.

$$\begin{aligned}\dot{S} =&\lambda - dS - \beta_w S v_w - \beta_{m1} S v_{m1} - \beta_{m2} S v_{m2},\\ \dot{I}_i =&\beta_i S v_i - a I_i,\\ \dot{v}_i =&k I_i - c v_i,\end{aligned} \tag{3.2}$$

for $i = w, m1, m2$. Here strain w is the wildtype drug sensitive strain and strains $m1$ and $m2$ are drug resistant.

The next generation matrix method gives three possible values of R_0 depending on which strain $R_{0i} = \frac{\lambda \beta_i k}{acd}$ is the largest. Therefore $R_0 = max_i\{R_{0i}\}$.

Steady State Analysis

There are 4 different steady states, one disease free and three with disease (one for each strain of virus) which can be written in exactly the same form as for the two strain system (3.1).

1. The disease free steady state is

$$\left(S = \frac{\lambda}{d} = S_0, I_w = 0, I_{m1} = 0, I_{m2} = 0, v_w = 0, v_{m1} = 0, v_{m2} = 0\right).$$

2. The endemic steady states are given by

$$\begin{aligned}S =&\frac{S_0}{R_{0i}},\\ I_i =&\frac{cd}{k\beta_i}(R_{0i} - 1),\\ I_{\hat{i}} =&I_{\check{i}} = 0,\\ v_i =&\frac{d}{\beta_i}(R_{0i} - 1),\\ v_{\hat{i}} =&v_{\check{i}} = 0,\end{aligned}$$

where $i = w, m1, m2$ and $\hat{i}$ and $\check{i}$ are the two other strains, so if $i = w$ then $\hat{w} = m1$ and $\check{w} = m2$.

The Jacobian matrix for this system is

$$\begin{pmatrix} -d-\beta_w v_w-\beta_{m1}v_{m1}-\beta_{m2}v_{m2} & 0 & 0 & 0 & -\beta_w S & -\beta_{m1}S & -\beta_{m2}S \\ \beta_w v_w & -a & 0 & 0 & \beta_w S & 0 & 0 \\ \beta_{m1}v_{m1} & 0 & -a & 0 & 0 & \beta_{m1}S & 0 \\ \beta_{m2}v_{m2} & 0 & 0 & -a & 0 & 0 & \beta_{m2}S \\ 0 & k & 0 & 0 & -c & 0 & 0 \\ 0 & 0 & k & 0 & 0 & -c & 0 \\ 0 & 0 & 0 & k & 0 & 0 & -c \end{pmatrix},$$

with corresponding eigenvalues Λ.

1. The disease free steady state characteristic polynomial can be factorised into smaller polynomials:

$$\begin{aligned} &\Lambda + d = 0, \\ &\Lambda^2 + (a+c)\Lambda + ca - \frac{\lambda\beta_w k}{d} = 0, \\ &\Lambda^2 + (a+c)\Lambda + ca - \frac{\lambda\beta_{m1} k}{d} = 0, \\ &\Lambda^2 + (a+c)\Lambda + ca - \frac{\lambda\beta_{m2} k}{d} = 0. \end{aligned}$$

   Therefore the disease free steady state is stable if $R_0 < 1$ as this gives positive coefficients.

2. The characteristic polynomial for the all the endemic steady states can be written generally and factorised into two quadratics and a cubic:

$$\begin{aligned} &\Lambda^2 + (a+c)\Lambda + ca\left(1 - \frac{\beta_{\hat{i}}}{\beta_i}\right) = 0, \\ &\Lambda^2 + (a+c)\Lambda + ca\left(1 - \frac{\beta_{\tilde{i}}}{\beta_i}\right) = 0, \\ &\Lambda^3 + \left(a + c + \frac{\lambda\beta_i k}{d}\right)\Lambda^2 + \left(\frac{\lambda\beta_i k}{c} + \frac{\lambda\beta_i k}{a}\right)\Lambda + \lambda\beta_i k - acd = 0, \end{aligned}$$

   for $i = w, m1, m2$. Therefore each one strain only endemic steady state i is stable if $\beta_i > \beta_{\hat{i}}$ and $\beta_i > \beta_{\tilde{i}}$ and $R_{0i} > 1$.

Drug treatment can be modelled in the same way as for the two strain system (3.1) and gives the same results. In order to model drug resistance we can assume that the drug resistant strains have larger β values than the drug sensitive strain and that one

of the R_{0i} for strains $m1$ and $m2$ is greater than unity. Whichever strain is fittest outcompetes the rest showing competitive exclusion as in the two strain model (3.1).

3.4 Evolutionary Models

In order to model the situation more realistically a number of features should be included in the model. Firstly, new mutants should arise at the reverse transcription stage, as this is where errors causing mutations occur, giving rise to a cell that is infected with a mutant virus. Secondly, mutations should only occur at a high rate; HIV mutates at a high rate equivalent to one base pair per round of replication. Thirdly, mutations are assumed to cause a change in efficiency of the protein encoded by the mutated gene. This can be modelled by each viral strain either having a different value for β or k depending on whether the protein affected is reverse transcriptase or protease (as in the competition models).

A number of different models will be considered in this section. The first is a two strain model with mutation detailed in Section 3.4.1. The final two models given in Section 3.4.2 describe two different ways of modelling mutation with three strains, along a linear genotype or by assuming all mutants differ by one mutation.

Analytical Techniques

Evolutionary models are more complicated to analyse than competition models and the results obtained are harder to relate to the biology, due to the inclusion of mutation. As the mutation rate is very small we can use this parameter to carry out a perturbation analysis on the exact solutions of each model to obtain an approximate solution. These approximate solutions are more easily related to the underlying biology than the exact solutions. We show both the exact and approximate solutions for the two strain model where it is possible to obtain the solutions analytically and the approximate solutions for the three strain models.

3.4.1 Two Strain Evolutionary Model

Modelling mutation at the reverse transcription stage and assuming that there is an equal probability of mutating from wild type to the resistant or from resistant to wildtype gives a symmetric two strain model. With only two viral strains there is no difference between mutation modelled as a linear genotype or as a difference of only one mutation. This model can be used to look at the emergence of a resistant strain on treatment and the factors which affect this happening. It can also be compared with the two strain competition model to see whether modelling mutation changes the behaviour of the model.

Model Equations

A system with two viral strains and mutation adapted from Bonhoeffer et al. [1997] is given below:

$$\begin{aligned}\dot{S} =&\lambda - dS - \beta_w S v_w - \beta_m S v_m,\\ \dot{I}_i =&(1-\epsilon)\beta_i S v_i + \epsilon\beta_{\hat{i}} S v_{\hat{i}} - aI_i,\\ \dot{v}_i =&kI_i - cv_i,\end{aligned} \tag{3.3}$$

for $i = w, m$. The symbol $\hat{i}$ means the other strain of virus and ϵ is the mutation rate.

Using the next generation matrix method there are two possible eigenvalues which could be the R_0 for this system. Using perturbation theory and assuming $\epsilon \ll 1$ the expressions can be simplified to give $R_{0w} \simeq \frac{\lambda\beta_w k(1-\epsilon)}{acd}$ and $R_{0m} \simeq \frac{\lambda\beta_m k(1-\epsilon)}{acd}$. Therefore $R_0 = max_i\{R_{0i}\}$. These expressions are not valid very near $\beta_w = \beta_m$ as the system collapses to a one strain model.

Steady State Analysis

There are three steady states for this system (3.3): disease free and two endemic steady states.

1. The disease free steady state is

$$\left(S = \frac{\lambda}{d}, I_1 = 0, I_2 = 0, v_1 = 0, v_2 = 0\right).$$

2. The endemic steady states can be found be solving the quadratic for S,

$$(2\epsilon - 1)\beta_w\beta_m S^2 + (1-\epsilon)(\beta_w + \beta_m)\frac{ac}{k}S - \frac{a^2c^2}{k^2} = 0, \tag{3.4}$$

and substituting the solutions for S into the following expressions for the other variables

$$\begin{aligned}v_w =&\frac{k\epsilon(\lambda - dS)}{k\beta_w(2\epsilon-1)S + ac},\\ v_m =&\frac{v_w}{\epsilon\beta_m S}\left(\frac{ac}{k} - (1-\epsilon)\beta_w S\right),\\ I_w =&\frac{acv_w}{k},\\ I_m =&\frac{acv_m}{k}.\end{aligned}$$

Figure 3-1 shows how the roots of the quadratic in S, (3.4), change with the

value of β_w. Similar results can be seen when β_m is varied. The values of the other variables obtained from substituting in the roots of (3.4) showed that root 1 (calculated by adding the discriminant), though positive, never gives biologically realistic (non-negative) values for the other steady state variables: it is associated with the unstable endemic steady state. This can be seen in Figure 3-1 where root 1 of the quadratic in S gives $v_m < 0$ then $v_w < 0$ as the infection rate β_w increases. Root 2 (calculated by subtracting the discriminant) is associated with the prevailing stable endemic steady state. When $\beta_w = \beta_m$ the above expressions are not valid as root 2 of the quadratic in S, gives a zero denominator in the expression for v_w at steady state. When the infection rates are equal ($\beta_w = \beta_m = \beta$) we obtain the same steady state expressions as the one strain system (1.1.3) with $v_m = v_w = v$ and $I_w = I_m = I$ at steady state.

In order to obtain more useful steady state expressions for S a pertubation analysis was performed assuming that S could be represented as a polynomial function of the small parameter ϵ

$$S = S_0 + \epsilon S_1 + \epsilon^2 S_2 + O(\epsilon^3),$$

which was then substituted into the quadratic (3.4) and the coefficients of ϵ equated. This gave the solutions to $O(\epsilon)$

$$S = \frac{ac(1+\epsilon)}{k\beta_i}, \tag{3.5}$$

for $i = w, m$. Figure 3-1 shows how these values compare with the roots of the quadratic obtained in the normal way. Here the perturbation root containing β_w corresponds to first root 1 then root 2 of (3.4) as β_w becomes greater than β_m. The approximation is not valid when $\beta_w = \beta_m$ as the system has a simpler solution not involving the mutation rate.

Substituting in these approximations for the value of S, (3.5), gives the following approximate solutions for v_w and v_m to $O(\epsilon)$,

$$\begin{aligned}
S &\simeq \frac{ac(1+\epsilon)}{\beta_w k}, & S &\simeq \frac{ac(1+\epsilon)}{\beta_m k},\\
v_w &\simeq \frac{d}{\beta_w}\left(R_{0w} - (1+\epsilon)\right), & v_w &\simeq \epsilon\frac{d}{\beta_w}\left(R_{0m} - 1\right),\\
v_m &\simeq \epsilon\frac{d}{\beta_m}\left(R_{0w} - 1\right), & v_m &\simeq \frac{d}{\beta_m}\left(R_{0m} - (1+\epsilon)\right),
\end{aligned}$$

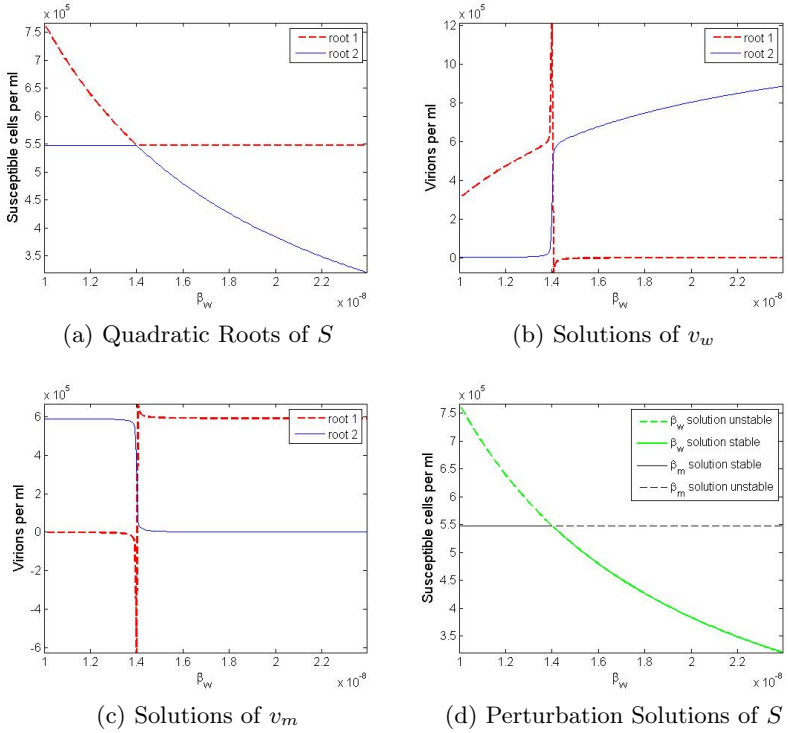

Figure 3-1: Graphs showing roots of quadratic in S calculated numerically and from approximations using perturbation theory (dashed lined indicate unstable steady states and solid lines stable steady states): a) Solutions of the quadratic in S, b) v_w steady state solutions calculated using each root of the quadratic in S, c) v_m steady state solutions calculated using each root of the quadratic in S, d) Steady state perturbation solutions of S. Other parameter values were $\beta_m = 1.4^{-8}$ and $\epsilon = 0.0005$, and values given in Table 2.2.

where R_{0i} are defined as in the two strain competition model (3.1). A number of interesting things can be seen from these approximations. Firstly, the disease steady states are only positive if the corresponding $R_{0i} > 1 + \epsilon$ (or alternatively with R_{0i} defined as including ϵ, $R_{0i} > 1$). Secondly, for each of the two disease steady states one viral strain is of $O(\epsilon)$ and is therefore much smaller than the other one. This means that as long as one of the strains has an $R_{0i} > 1 + \epsilon$ both strains will coexist albeit with one strain dominant over the other.

The Jacobian matrix for this system is

$$\begin{pmatrix} -d-\beta_w v_w-\beta_m v_m & 0 & 0 & -\beta_w S & -\beta_m S \\ (1-\epsilon)\beta_w v_w+\epsilon\beta_m v_m & -a & 0 & (1-\epsilon)\beta_w S & \epsilon\beta_m S \\ (1-\epsilon)\beta_m v_m+\epsilon\beta_w v_w & 0 & -a & \epsilon\beta_w S & (1-\epsilon)\beta_m S \\ 0 & k & 0 & -c & 0 \\ 0 & 0 & k & 0 & -c \end{pmatrix}.$$

1. The disease free steady state characteristic polynomial can be factorised

$$(\Lambda+d)(x_4\Lambda^4+x_3\Lambda^3+x_2\Lambda^2+x_1\Lambda+x_0)=0,$$

where

$$\begin{aligned} x_4 =& 1, \\ x_3 =& 2a+2c, \\ x_2 =& (a+c)^2+2ac-\frac{\lambda k}{d}(1-\epsilon)(\beta_w+\beta_m), \\ x_1 =& (a+c)\left(2ac-\frac{\lambda k}{d}(1-\epsilon)(\beta_w+\beta_m)\right), \\ x_0 =& a^2c^2\left(1-\frac{\lambda k}{acd}(1-\epsilon)(\beta_w+\beta_m)+\frac{\lambda^2k^2\beta_w\beta_m}{a^2c^2d^2}(1-2\epsilon)\right). \end{aligned}$$

For the coefficients of the characteristic polynomial to be positive

$$(R_{0w}+R_{0m})(1-\epsilon)<2 \text{ and } (1-R_{0w}(1-\epsilon))(1-R_{0m}(1-\epsilon))>R_{0w}R_{0m}\epsilon^2,$$

where R_{0i} is defined in the usual way. When ϵ is zero these criteria reduce to both $R_{0i}<1$ as in the corresponding system without mutation (3.1). When $\epsilon << 1$ then $R_{0i}<1+\epsilon$ for $i=w,m$ are necessary conditions for the disease free steady state to be stable.

2. The stability of the two endemic steady states was checked numerically by experimenting with different values of β_w and β_m to obtain a picture of when the various steady states for this system were stable. Figure 3-2 gives the results in diagrammatic form. The endemic steady state with strain w dominant is stable when $\beta_w>\beta_m$ and $R_{0w}>1+\epsilon$, whereas the strain m dominant steady state is stable when $\beta_m>\beta_w$ and $R_{0m}>1+\epsilon$. This can be seen in Figure 3-3. The disease free steady state is stable when both $R_{0i}<1+\epsilon$.

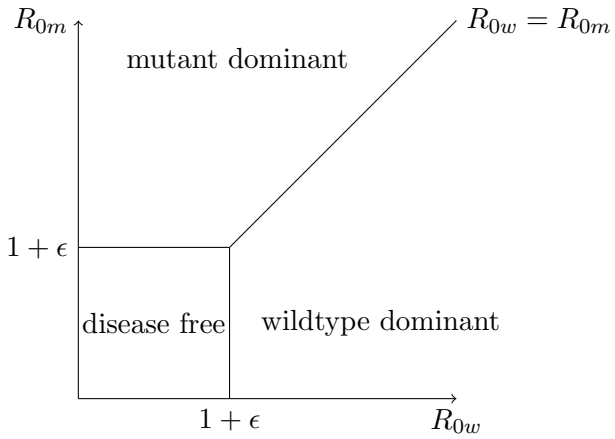

Figure 3-2: Diagram showing the regions where each of the three steady states of the two strain evolution model are stable. These conditions were checked numerically.

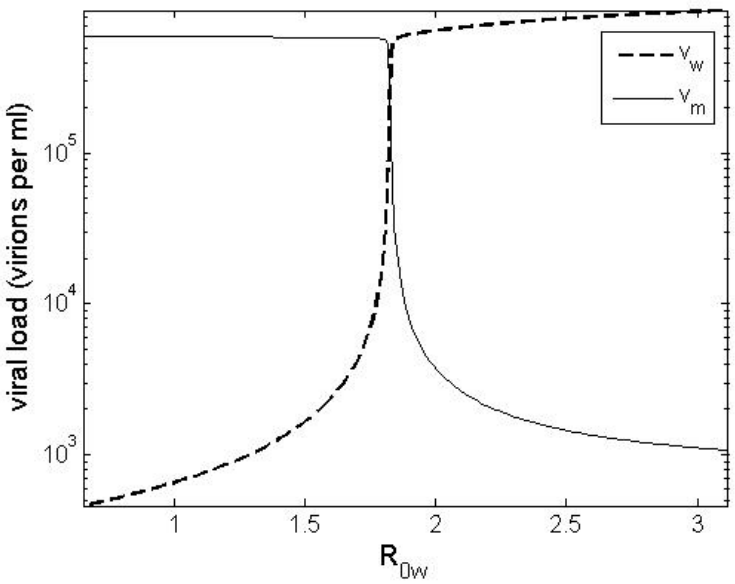

Figure 3-3: Graph showing the steady state values of both strains of virus for different values of R_{0w}. R_{0w} was varied by changing the value of β_w with $\beta_m = 1.4 \times 10^{-8}$, $\epsilon = 0.0005$ and other variables the same as in Table 2.2 ($R_{0m} = 1.8261$). Here R_{0w} is defined as in the competition model (3.1).

Frequency of the Mutant Prior to Therapy

It is possible to obtain an analytical expression for the frequency of a resistant mutant prior to the commencement of therapy. This is achieved by assuming that the system is in dynamic equilibrium, that the mutant does not back mutate and that there is a cost for the mutant of resistance. Here we present a summary of the work by Ribeiro et al. [1998] for single mutation resistant mutants changing variable names to be consistent with the body of our work. Ignoring back mutations gives a simplified system:

$$\begin{aligned}
\dot{S} =& \lambda - dS - \beta_w S v_w - \beta_m S v_m, \\
\dot{I}_w =& (1-\epsilon)\beta_w S v_w - a I_w, \\
\dot{I}_m =& \beta_m S v_m + \epsilon \beta_w S v_w - a I_m, \\
\dot{v}_w =& k I_w - c v_w, \\
\dot{v}_m =& k I_m - c v_m.
\end{aligned}$$

Setting the left hand sides of the simplified system to zero and solving for S using $\dot{I}_w = 0$ and $\dot{v}_w = 0$ gives $S = \frac{ac(1+\epsilon)}{\beta_w k}$. Rearranging the equation $\dot{I}_m = 0$ and substituting in the solution for S gives

$$\frac{v_m}{v_w} = \frac{\epsilon v_m}{1 - \frac{\beta_m}{\beta_w}}.$$

If we assume that $\beta_m = r\beta_w$ where r is a resistance factor between 0 and 1 then we can write

$$\frac{v_m}{v_w} = \frac{\epsilon}{1 - r - \epsilon} \simeq \frac{\epsilon}{1 - r}, \tag{3.6}$$

as $\epsilon << 1$. This means that the frequency of the mutant prior to therapy depends on the mutation rate and the cost of being resistant to therapy. Figure 3-4 shows that the mutation rate has a much greater affect on the proportion of the mutant prior to therapy than the resistance factor. However when the resistance factor is close to 1, meaning that the mutant is almost as fit as the wildtype prior to therapy, the proportion of mutant rises dramatically. The numerical result using the full system is almost identical to the analytical approach and is therefore not plotted on Figure 3-4. This suggests that the assumption of no back mutations is valid prior to therapy.

Time to Emergence of the Resistant Strain

Here we are concerned with finding an expression for the time taken for the drug resistant strain to become dominant in the viral population, in order to find out which of the parameters governing viral dynamics is important in the timing of emergence of the resistant strain. This section is a summary of the work by Nowak et al. [1997] with

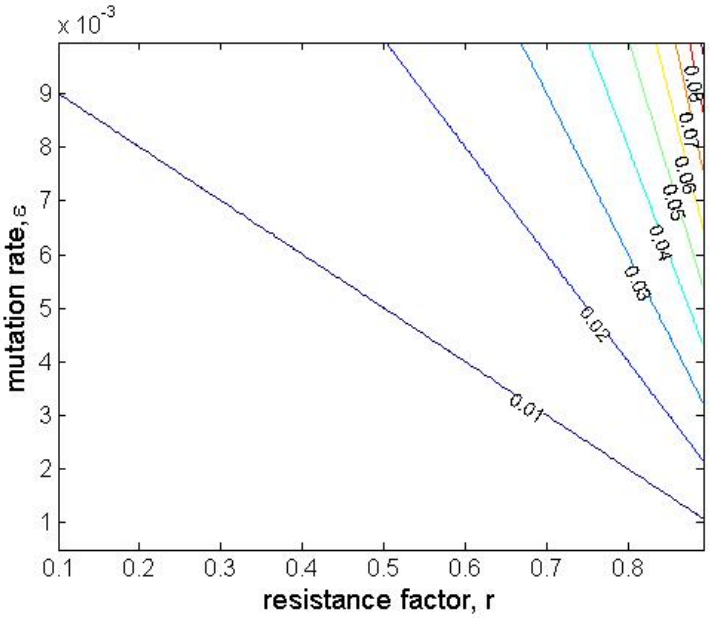

Figure 3-4: Contour plot showing the behaviour of the frequency of mutants, v_m/v_w, before therapy with varying resistance factor, r ($\epsilon = 0.0005$)and mutation rate, ϵ ($r = 0.58$). Parameter values are as given in Table 2.2.

variable name changes to fit with our nomenclature.

To make any progress analytically it is necessary to make some assumptions with the model. We consider the two strain evolutionary model with the following assumptions:

- As $c >> a$ we can assume that the concentration of each viral strain can be approximated by the expression $\frac{kI_i}{c}$.
- The mutation rate $\epsilon = 0$ once drug treatment is initiated.
- Drug treatment is 100% effective therefore $\beta_w = 0$
- As the initial value of I_m at the start of drug therapy is of the order ϵ the infection term in $\dot{S}$ can be ignored.

These assumptions taken at the disease steady state before drug treatment is initiated give us the following revised system:

$$\begin{aligned}\dot{S} =& \lambda - dS,\\ \dot{I}_w =& -aI_w,\\ \dot{I}_m =& \frac{\beta_m k I_m S}{c} - aI_m.\end{aligned}$$

Solving for I_w gives

$$I_w(t) = I_w(0)e^{-at}.$$

Non-dimensionalising by substituting $S = \frac{\lambda}{d}\hat{S}$ and $I_m = \frac{dc}{\beta_m}\hat{I}_m$ gives

$$\begin{aligned}\dot{\hat{S}} =& d(1-\hat{S}),\\ \dot{\hat{I}}_m =& (\frac{\lambda\beta_m k}{cd}\hat{S} - a)\hat{I}_m.\end{aligned}$$

Therefore

$$\hat{S}(t) = 1 - (1 - \frac{1}{R_{0w}})e^{-dt},$$

where $R_{0w} = \frac{\lambda\beta_w k}{acd}$. Substituting this into the ODE for $\hat{I}_m$ gives the following solution

$$\hat{I}_m(t) = \hat{I}_m(0)\exp\left[a\left\{(R_{0m}-1)\,t - \frac{R_{0m}}{d}(1-\frac{1}{R_{0w}})(1-e^{-dt})\right\}\right],$$

where $R_{0m} = \frac{\lambda\beta_m k}{acd}$.

In order to find out when the switch over happens we need to calculate when the number of wildtype infected cells equals the number of mutant infected cells. Therefore we take

$$\frac{I_m}{I_w} = \frac{I_m(0)}{I_w(0)}\exp\left[a\left\{R_{0m}t - \frac{R_{0m}}{d}(1-\frac{1}{R_{0w}})(1-e^{-dt})\right\}\right].$$

Using the taylor expansion of $(1-e^{-dt}) = (dt - d^2t^2/2\ldots)$ we obtain

$$\frac{I_m}{I_w} \approx \frac{I_m(0)}{I_w(0)}\exp\left[a\left\{\frac{1}{R_{0w}}t + \frac{R_{0m}}{2}(1-\frac{1}{R_{0w}})dt^2\ldots\right\}\right].$$

When this ratio is 1 we can solve the following quadratic to get the time t_I when each type of infected cell is present at 50%.

$$\frac{R_{0m}(1-\frac{1}{R_{0w}})}{2}adt_I^2 + a\frac{R_{0m}}{R_{0w}}t_I - \ln\left[\frac{I_w(0)}{I_m(0)}\right] = 0.$$

From Figure 3-5 we can see that the analytical solution and numerical solutions agree closely for a range of values of R_{0m}. The time it takes for the mutant to emerge is very small, less than 20 days for the parameter values chosen here. When the drug is not 100% effective ($e < 1, \beta_w > 0$), the time to emergence will increase as shown in Figure 3-6 (calculated numerically), showing the closer the two R_{0i} values, the longer the time to emergence.

This system, whereby the wild type strain and a single mutant strain are considered, is sufficient to model examples of where a single nucleotide polymorphism is all that is

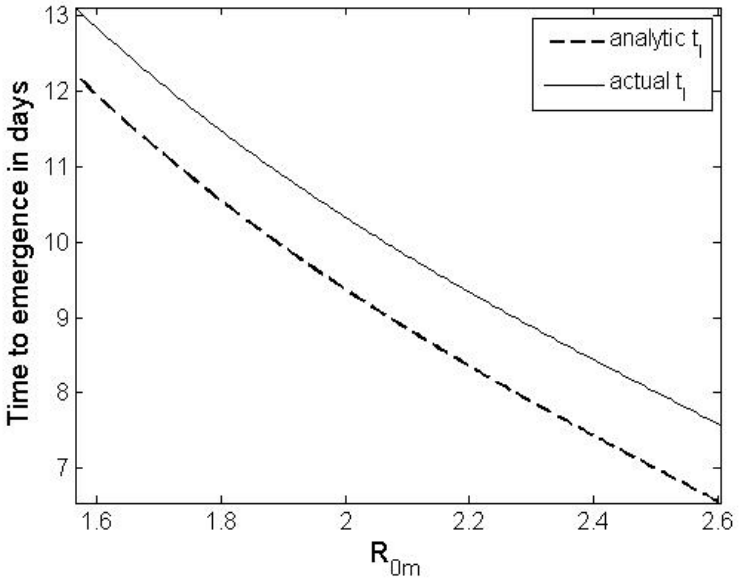

Figure 3-5: Graph showing how time to emergence of the mutant strain is affected by the value of R_{0m}. R_{0m} is varied using β_m, with $\beta_w = 2.4 \times 10^{-8}$ prior to therapy and $\beta_w = 0$ on therapy. Other parameter values are as given in Table 2.2.

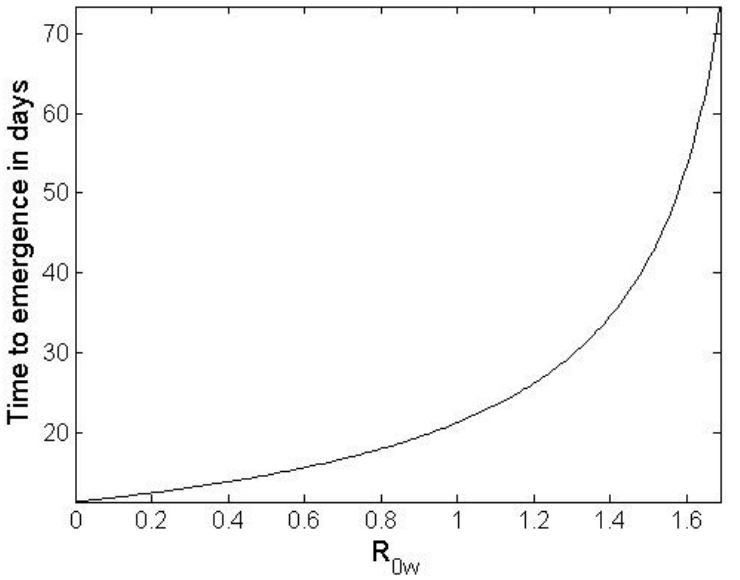

Figure 3-6: Graph showing how time to emergence of the mutant strain is affected by the value of R_{0w}. R_{0w} is varied using β_w, with $\beta_m = 1.4 \times 10^{-8}$ ($R_{0m} = 1.8261$). Other parameter values are as given in Table 2.2.

necessary for drug resistance to occur. However in cases where two or more mutations are necessary for resistance or where compensatory mutations develop, a model with more mutants present is needed.

3.4.2 Three Strain Evolutionary Models

There are two models analysed in this section differing in the way in which mutation is modelled. In the first, mutation is modelled so that it is equally likely that a mutation can occur to change one strain to any other strain. This model will be referred to as the 'jump model'. The assumption here is that all of the strains differ by only one mutation from the wild type strain. There is redundancy in the mechanism encoding for most amino acids; for example, histidine is encoded by the nucleotide sequences CAT and CAC [Brock, 1997]. Therefore we allow a strain to mutate to itself. This approach was used by Ball et al. [2007] to model the evolution of virulence in HIV.

In the second model we assume that evolution can only occur along a linear genotype so that only mutation to a neighbouring strain is possible. Mutants will be conserved by using zero flux boundary conditions similar to that found in Gudelj et al. [2007], which modelled evolution in microbes. This model will be referred to as the 'serial model'.

The total probability of a useful mutation occuring is taken to be ϵ. Therefore in the jump model the probability that a mutation occurs to change from one strain to another is $\frac{\epsilon}{3}$. In the serial model mutation can only occur linearly and so the probability that mutation occurs from one strain to the neighbouring strain is $\frac{\epsilon}{2}$.

Model Equations

The jump model is given by

$$\begin{aligned}
\dot{S} =& \lambda - dS - \beta_w S v_w - \beta_{m1} S v_{m1} - \beta_{m2} S v_{m2}, \\
\dot{I}_i =& \frac{\epsilon}{3} \sum_{i=1}^{3} \beta_i S v_i + (1-\epsilon)\beta_i S v_i - a I_i, \\
\dot{v}_i =& k I_i - c v_i,
\end{aligned} \tag{3.7}$$

where $i = w, m1, m2$.

The serial model is given by

$$\begin{aligned}
\dot{S} =&\lambda - dS - \beta_w S v_w - \beta_{m1} S v_{m1} - \beta_{m2} S v_{m2},\\
\dot{I}_w =&(1-\frac{\epsilon}{2})\beta_w S v_w + \frac{\epsilon}{2}\beta_{m1} S v_{m1} - aI_w,\\
\dot{I}_{m1} =&\frac{\epsilon}{2}\beta_w S v_w + (1-\epsilon)\beta_{m1} S v_{m1} + \frac{\epsilon}{2}\beta_{m2} S v_{m2} - aI_{m1},\\
\dot{I}_{m2} =&\frac{\epsilon}{2}\beta_{m1} S v_{m1} + (1-\frac{\epsilon}{2})\beta_{m2} S v_{m2} - aI_{m2},\\
\dot{v}_i =&kI_i - cv_i,
\end{aligned} \tag{3.8}$$

where $i = w, m1, m2$.

Steady State Analysis

1. The disease free steady state for both the jump model and the serial model are the same

$$\left(S = \frac{\lambda}{d}, I_w = 0, I_{m1} = 0, I_{m2} = 0, v_w = 0, v_{m1} = 0, v_{m2} = 0\right).$$

2. The disease steady states in both models depend on cubics in S similar to the quadratic in S, (3.4), for the two strain system with mutation. For the sake of clarity this will be omitted and the simplified expressions obtained using perturbation analysis using ϵ as the small parameter will be presented.

   Due to the symmetry in the system it is possible to write the three endemic steady states generally for the jump model:

$$\begin{aligned}
S \simeq&\frac{ac}{k\beta_i}\left(1-\frac{2\epsilon}{3}\right),\\
v_i \simeq&\frac{d}{\beta_i}(R_{0i}-1)\left(1+\frac{\epsilon}{3}\left(\frac{\beta_w^2-\beta_{m1}\beta_{m2}}{(\beta_w-\beta_{m1})(\beta_w-\beta_{m2})}-1\right)\right)+\frac{\epsilon}{3}\frac{2\lambda k\beta_w^2}{ac(\beta_w-\beta_{m1})(\beta_w-\beta_{m2})},\\
v_{\hat{i}} \simeq&\frac{\epsilon}{3}\frac{d}{\beta_i-\beta_{\hat{i}}}(R_{0i}-1),\\
v_{\check{i}} \simeq&\frac{\epsilon}{3}\frac{d}{\beta_i-\beta_{\check{i}}}(R_{0i}-1),
\end{aligned}$$

   where $i = w, m1, m2$ and $\hat{i}$ and $\check{i}$ are the other two strains of virus. R_{0i} is taken to be $\frac{\lambda\beta_i k}{acd}$ in this section. From the expressions it is easy to see that as ϵ is small the dominant strain is i and the other two strains are present at $O(\epsilon)$.

   The serial model has two different types of endemic steady state: one for each of the two end point strains being dominant and one for the midde strain being

dominant. The endemic steady state for the wildtype or $m2$ strain being dominant can be generalised and is given as

$$\begin{aligned} S \simeq & \frac{ac}{k\beta_i}\left(1+\frac{\epsilon}{2}\right), \\ v_i \simeq & \frac{d}{\beta_i}(R_{0i}-1)(1+\frac{\epsilon}{2}), \\ v_{m1} \simeq & \frac{\epsilon}{2}\frac{d}{\beta_{m1}}(R_{0i}-1), \\ v_{\hat{i}} \simeq & \frac{\epsilon^2}{4}\frac{d}{\beta_i-\beta_{\hat{i}}}(R_{0i}-1), \end{aligned}$$

where $i = w$ or $i = m2$, and $\hat{i}$ is the strain at the other end of the linear genotype. Here it should be noted that the strain that is two mutations away, $\hat{i}$, is present at $O(\epsilon^2)$ whereas the strain that is only one mutation away is present at $O(\epsilon)$.

The endemic steady state for the middle strain, $m1$, is

$$\begin{aligned} S \simeq & \frac{ac}{k\beta_{m1}}(1+\epsilon), \\ v_w \simeq & \frac{\epsilon}{2}\frac{(R_{0m1}-1)}{\beta_{m1}-\beta_w}, \\ v_{m1} \simeq & \frac{d}{\beta_{m1}}(R_{0m1}-1)\left(1+\frac{\epsilon}{2}\frac{\beta_w\beta_{m2}}{(\beta_{m1}-\beta_w)(\beta_{m1}-\beta_{m2})}\right) \\ & -\frac{\epsilon}{2}\left(\frac{d}{\beta_{m1}}(R_{0m1}+1)-\frac{\beta_{m1}}{(\beta_{m1}-\beta_w)(\beta_{m1}-\beta_{m2})}\right), \\ v_{m2} \simeq & \frac{\epsilon}{2}\frac{(R_{0m1}-1)}{\beta_{m1}-\beta_{m2}}. \end{aligned}$$

In this steady state expression the two end strains are only one mutation away from the middle strain and are therefore found at $O(\epsilon)$.

1. The Jacobian matrix for the disease free steady state of the jump model is

$$\begin{pmatrix} -d & 0 & 0 & 0 & -\beta_w S & -\beta_{m1} S & -\beta_{m2} S \\ 0 & -a & 0 & 0 & (1-\frac{2\epsilon}{3})\beta_w S & \frac{\epsilon}{3}\beta_{m1} S & \frac{\epsilon}{3}\beta_{m2} S \\ 0 & 0 & -a & 0 & \frac{\epsilon}{3}\beta_w S & (1-\frac{2\epsilon}{3})\beta_{m1} S & \frac{\epsilon}{3}\beta_{m2} S \\ 0 & 0 & 0 & -a & \frac{\epsilon}{3}\beta_w S & \frac{\epsilon}{3}\beta_{m1} S & (1-\frac{2\epsilon}{3})\beta_{m2} S \\ 0 & k & 0 & 0 & -c & 0 & 0 \\ 0 & 0 & k & 0 & 0 & -c & 0 \\ 0 & 0 & 0 & k & 0 & 0 & -c \end{pmatrix}.$$

When $\epsilon = 0$ the Jacobian has the same form as for the disease free steady state of

the three strain competition model (3.2). This means that the stability criteria will be a perturbation of those for the three strain competition model, namely $R_{0i} < 1$ for the disease free steady state to be stable.

2. Given the complicated nature of this system it is not possible to obtain stability criteria analytically. However, it would seem likely that the criteria will be a perturbation of the three strain competition model (3.2), namely the strain with the largest $R_{0i} > 1$ will be the stable dominant strain endemic steady state. This has been verified numerically as shown in Figure 3-7. In Figure 3-7a $\beta_{m1} > \beta_{m2}$ meaning that as β_w increases first v_{m1}, then v_w is the dominant strain with v_{m2} at $O(\epsilon)$. In figure 3-7b $\beta_{m2} > \beta_{m1}$ therefore as β_w increases v_{m2} is the first dominant strain, then v_w.

1. The Jacobian matrix for the disease free steady state of the serial model is

$$\begin{pmatrix} -d & 0 & 0 & 0 & -\beta_w S & -\beta_{m1} S & -\beta_{m2} S \\ 0 & -a & 0 & 0 & (1-\frac{\epsilon}{2})\beta_w S & \frac{\epsilon}{2}\beta_{m1} S & 0 \\ 0 & 0 & -a & 0 & \frac{\epsilon}{2}\beta_w S & (1-\epsilon)\beta_{m1} S & \frac{\epsilon}{2}\beta_{m2} S \\ 0 & 0 & 0 & -a & 0 & \frac{\epsilon}{2}\beta_{m1} & (1-\epsilon)\beta_{m2} S \\ 0 & k & 0 & 0 & -c & 0 & 0 \\ 0 & 0 & k & 0 & 0 & -c & 0 \\ 0 & 0 & 0 & k & 0 & 0 & -c \end{pmatrix}.$$

When $\epsilon = 0$ the Jacobian has the same form as for the disease free steady state of the three strain competition model (3.2). Therefore the stability criteria will be a perturbation of those for the disease free steady state for the three strain competition model, namely if $R_{0i} < 1$ for $i = w, m1, m2$ then the disease free steady state will be stable.

2. It is not possible to obtain the endemic steady state criteria analytically. However, numerical solutions show that the strain with the largest $R_{0i} > 1$ has the stable endemic steady state as seen in Figure 3-8. In Figure 3-8a $\beta_{m1} > \beta_{m2}$, therefore as β_w increases, first v_{m1}, then v_w is the dominant strain. When v_{m1} is the dominant strain both the losing strains are at $O(\epsilon)$ as they are both one mutation away from the v_{m1}. However when v_w is dominant the strain two mutations away, v_{m2} is at $O(\epsilon^2)$. In Figure 3-8b where $\beta_{m2} > \beta_{m1}$ this behaviour can also be seen: when $\beta_{m2} > \beta_w$ the wildtype strain is at $O(\epsilon^2)$ and when $\beta_w > \beta_{m2}$ the $m2$ strain is at $O(\epsilon^2)$. The $m1$ strain remains at $O(\epsilon)$ as it is always one strain away from the dominant strain.

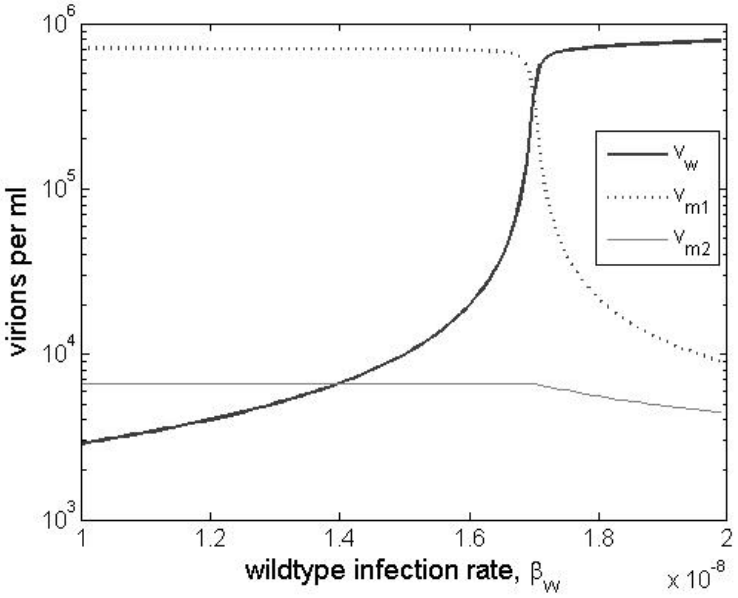

(a)

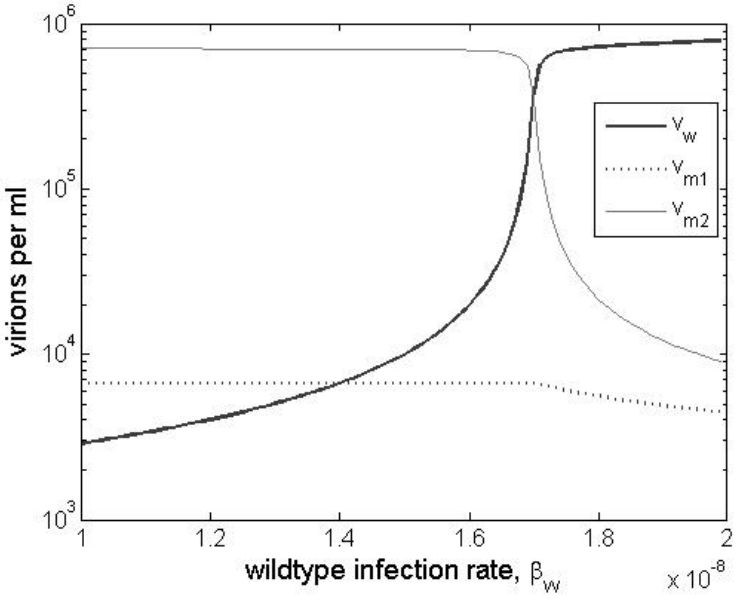

(b)

Figure 3-7: Graphs showing the steady state behaviour of the jump mutation model for two cases a)Infection rate of strain m_1, $\beta_{m1} = 1.7 \times 10^{-8}$ and infection rate of strain $m2$, $\beta_{m2} = 1.4 \times 10^{-8}$, with β_w varying, b)Infection rates of strain $m1$ and $m2$ reversed with β_w varying. All other parameters are as given in Table 2.2.

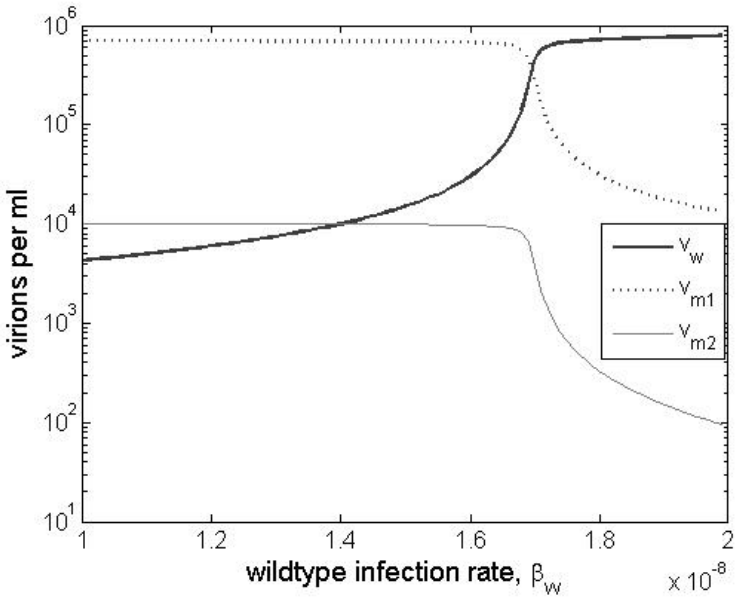

(a)

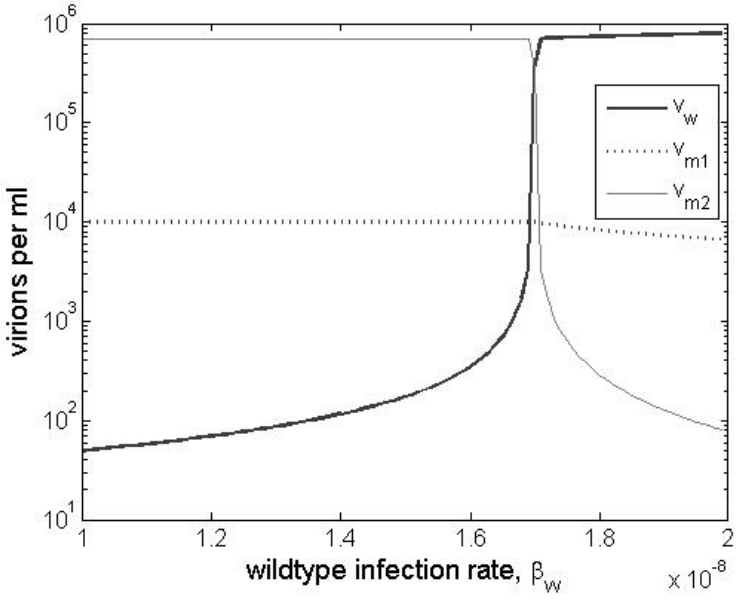

(b)

Figure 3-8: Graphs showing the steady state behaviour of the serial mutation model for two cases a)Infection rate of strain m_1, $\beta_{m1} = 1.7 \times 10^{-8}$ and infection rate of strain $m2$, $\beta_{m2} = 1.4 \times 10^{-8}$, with β_w varying, b)Infection rates of strain $m1$ and $m2$ reversed with β_w varying. All other parameters are as given in Table 2.2.

Frequency of the mutants before therapy

Using the same method [Ribeiro et al., 1998] as for the two strain model (3.3), neglecting back mutations from the mutants, we obtain for the jump model:

$$\frac{v_{m1}}{v_w} = \frac{\epsilon}{3(1-\frac{2\epsilon}{3}-r_1)} \simeq \frac{\epsilon}{3(1-r_1)}$$

and

$$\frac{v_{m2}}{v_w} = \frac{\epsilon}{3(1-\frac{2\epsilon}{3}-r_2)} \simeq \frac{\epsilon}{3(1-r_2)},$$

where r_1 and r_2 are the resistance factors for strains $m1$ and $m2$ respectively. This shows that the frequency of the two mutants will be of $O(\epsilon)$, with the mutant with the highest resistance factor being at a higher frequency.

The serial model gives different results:

$$\frac{v_{m1}}{v_w} = \frac{\epsilon}{2(1-\frac{\epsilon}{2}-r_1)} \simeq \frac{\epsilon}{2(1-r_1)}$$

and

$$\frac{v_{m2}}{v_w} = \frac{\epsilon^2 r_1}{(1-\frac{\epsilon}{2}-r_1)(1-\frac{\epsilon}{2}-r_2)} \simeq \frac{\epsilon^2 r_1}{(1-r_1)(1-r_2)}.$$

Here the closest strain to the wildtype, $m1$, will be at a higher frequency than strain $m2$ unless $r_2 > 1 - \frac{\epsilon r_1}{2}$. As this condition would give a number very close to 1, this is unlikely to be the case.

After treatment has commenced the same method could be used to calculate the proportion of the minority strains among the population. In the jump model we would see both of the minority strains at $O(\epsilon)$, with the fitter of the two at a higher proportion as in Figure 3-7. In the serial model we would see the nearest neighbouring strain at a higher frequency than the one further away, unless the strain $m1$ was the dominant strain, in which case the minority strains would both be present at $O(\epsilon)$ with the fitter of the two at a higher frequency. Both these cases can be seen in Figure 3-8.

Time to Emergence of the Dominant Mutant

There are a number of questions about emergence of new strains that a model with three strains can answer such as does the number of mutations between the wildtype strain and the new dominant strain on treatment affect the time until that new strain emerges? Also does the fitness of the intermediate strain affect the time to emergence? The three strain system is too complicated to obtain an analytical expression for the time to emergence of the dominant mutant so numerical experiments have been carried

out using the serial model of mutation. Figure 3-9a shows that it takes longer for a strain that is two mutations away from the wildtype to emerge than a strain that is only one mutation away; the other resistant strain had the same fitness in both cases. Figure 3-9b shows that although a fitter intermediate strain of virus means the time to emergence of the new dominant strain is less, the effect is minimal.

3.5 Conclusions

The competition models show competitive exclusion behaviour. In order to model drug resistance initial conditions for all viral strains need to be non-zero. The fittest viral strain, which is the one with the largest R_0 value, is the one that outcompetes all the others.

Competition models are useful for modelling the premise that drug resistant strains are already present at very low prevalences in the viral quasispecies before treatment, in which case initial conditions need to be the drug sensitive strain disease steady state, perturbed slightly with the presence of resistant strains. However the modelling of evolution before, during and after treatment is not possible with competition models. Instead they are useful as a reference base case for evolutionary models where the minority strains are always present at very low levels of $O(\epsilon)$ or smaller. However given that the long term behaviour of the models is the same, an argument can be made for using the simpler competition models, which can be analysed more easily, in some cases. A good example of this would be when drug treatment commences. In contrast, evolutionary models will be needed in order to model ongoing evolution of HIV strains where the selection pressure changes over time, for example when a patient changes their drug regimen.

Both methods of modelling mutation discussed in this chapter (jump mutations and serial mutations) give the same qualitative results; the fittest strain (measured by R_0 value) dominates the other strains. In a model with only two strains the method by which mutation is modelled is the same, however when there are three or more strains the way in which you model mutation becomes important. The same qualitative outcome occurs for both models of mutation, the fittest strain dominates, however the amounts of the less fit strains differ: the jump model of mutation allows one strain to dominate and all other strains to be present at the same order of magnitude $O(\epsilon)$, however the serial model of mutation shows different orders of magnitude for the losing strain depending on how many mutations away the losing strain is from the fittest strain. In practice this means that if a strain differs by more than one or two mutations from the fittest one it is unlikely to be seen in the quasispecies.

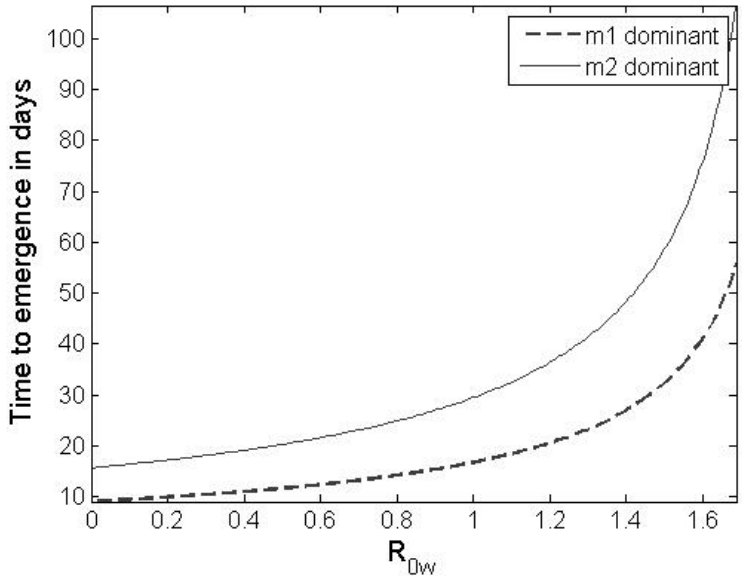

(a)

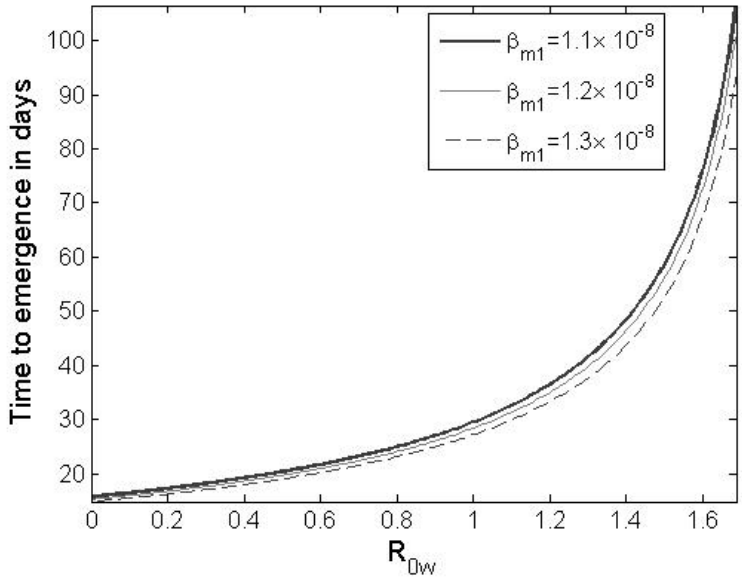

(b)

Figure 3-9: Graphs showing the time to emergence of the dominant mutant strain on therapy in different cases of the serial model a) $m1$ strain ($\beta_{m1} = 1.4 \times 10^{-8}, \beta_{m2} = 1.1 \times 10^{-8}$) or $m2$ strain dominant ($\beta_{m1} = 1.1 \times 10^{-8}, \beta_{m2} = 1.4 \times 10^{-8}$) on therapy, b) $m2$ strain dominant with different fitnesses of $m1$ ($\beta_{m2} = 1.4 \times 10^{-8}$). Other parameters as given in Table 2.2.

The serial model of mutation also showed that the time to emergence is increased when the number of mutations required to get to the new dominant strain is larger. Increasing the fitness of the intermediate strain only marginally decreased the time to emergence but this effect may be more pronounced when a larger number of mutations is needed.

Neither the jump or serial models of mutation are particularly useful for different reasons. The jump model doesn't give anymore insight into drug resistance than the two strain model of evolution, with the added negative of a strain mutating to itself. As mentioned earlier there is some redundancy in amino acid encoding, however some amino acids only have one codon, for instance methionine and tryptophan [Brock, 1997]. Also we don't allow mutating to the same strain in the two strain model of evolution. The serial model does not consider that there are two ways to get a double mutant: mutation 1, then mutation 2 or the other way around. This would neccesitate a four strain model such as that used by Ribeiro et al. [1998]. The mutation rates in their model differed between strains so that it was possible to go from wildtype to double mutant in one round of replication, at a very low rate. This model makes better biological sense. Ribeiro et al. [1998] also calculated the frequency of the mutants before therapy, obtaining identical results for the two strain and jump models when taking the difference in modelling the mutation rate into account. The frequency of the double mutant before therapy using the four strain model was

$$\frac{v_{m3}}{v_w} = \frac{\epsilon_1\epsilon_2}{1-r_{m3}}\left(\frac{1}{1-r_{m1}} + \frac{1}{1-r_{m2}} - 1\right),$$

where $m3$ is the double mutant, and $m1$ and $m2$ are the two single mutants with the respective r_i resistance factors. The mutation rates to produce single mutants are ϵ_i for $i = 1, 2$ for the m_1 and m_2 strains respectively. The two expressions for double mutant frequency are both of $O(\epsilon^2)$, however the four strain model gives a more realistic result, with the frequency depending on both of the intermediate single mutants.

As both of the three strain models described in this chapter are either not biologically sensible or more enlightening for the extra complexity, and the four strain model [Ribeiro et al., 1998] is too cumbersome, we will only include two strains of virus in our models from now on.

Clinicians currently cannot routinely detect members of the quasispecies that are below 20% prevalence in the population of viruses [Palmer et al., 2005]. Using one compartment models of mutation would suggest that minority mutants would never be seen in test results as the mutation rate ϵ is not big enough to give greater than 20% prevalence. It is likely that the presence of some minority mutants found in samples

is due to the proliferation of a new fitter mutant strain before "fixation" has occurred. However, it could also be that these minority mutants in patient samples could be coexisting at higher levels with the fitter strains. This is not explained by these one compartment models of evolution and may be due to some other mechanism acting on the system. Extensions to the two strain competition and evolution models will be considered in the following chapters.

Chapter 4

Multistrain Models with Heterogeneity

4.1 Chapter Outline

This chapter is concerned with models that include two strains of virus as well as cell heterogeneity and a drug sanctuary to see what effect each component has on drug resistance.

We begin by discussing previous work that models other interesting biological phenomena thought to have an effect on drug resistance.

We then describe two different models that include cell heterogeneity and a drug sanctuary with two strains of virus: a two target cell two strain model in Section 4.3 and a two compartment two strain model in Section 4.4. Both models are extensions of those seen in Chapter 2. For each model we employ both analytical and numerical techniques to investigate steady state, long term, behaviour.

4.2 Background and Motivation

A number of groups have investigated the impact of biological phenomena on drug resistance [Smith and Wahl, 2005, Smith, 2006, Kepler and Perelson, 1998, Rong et al., 2007a,b]. Most involve modelling some aspect of drug treatment more realistically, either by including drug concentration [Smith and Wahl, 2005], non-compliance with treatment [Smith, 2006, Rong et al., 2007a] or a drug sanctuary [Kepler and Perelson, 1998] into the model.

By modelling drug concentration impulsively, Smith and Wahl [2005] investigated the effect of different levels of drug on the emergence of a drug resistant strain. They

allowed target cells to be saturated with drug at different levels: low, intermediate or high, depending on the drug concentration, with susceptibility to infection governed by the level of drug saturation. The wildtype and resistant strains were sensitive to either intermediate and high or high levels of drug respectively. Steady state analysis was carried out for the three levels of drug saturation and drug resistance was found to emerge at both intermediate and high drug levels. At intermediate drug levels coexistence of the two strains occured whereas at high drug levels either the resistant strain emerged or both strains were driven extinct. At low levels of drug the wildtype only steady state was stable. One of the limitations of this model was that it assumed the drug effects were instantaneous and therefore there is no peaking of drug concentration. This has the biggest impact when dosing intervals are short. This model assumes that the mutant is already in the total population of free virus. It does not model the actual emergence of the mutant. The model also assumes that each dose is taken and does not include the effects of non-compliance. A further paper by this group [Smith, 2006], investigated how non-compliance with drug regimen affected the emergence of drug resistance using patient data and a model similar to their previous one. They calculated both the length of drug holiday (time not taking the drug) and the length of 100% adherence after the drug holiday in order for resistant mutants not to emerge. This paper looked specifically at non-protease inhibitor regimens and showed that for some drugs missing more than one dose was enough for resistance, whereas for others missing up to 40 doses would not result in resistance emerging as long as adherence after this was 100%. One possible extension to this work may be to look at whether sporadic adherence, missing an occasional dose, has an effect on resistance emerging for different drugs. It would also be interesting to look at what new threshold level dose arises for protease inhibitors.

Kepler and Perelson [1998] analysed a two compartment model for HIV dynamics to investigate the effect of a drug sanctuary on the emergence of resistant mutants in a similar model to that described in Chapter 2. The physiological and virological parameters in each compartment were taken to be the same in both compartments and the aim was to find the mean time for a resistant mutant to arise. It was found that the drug concentration range that allows mutants to arise and take over widens with inclusion of a drug sanctuary where drug concentration is lower than the main compartment. These results were obtained by using probabilities from the model which contained only one strain of virus, rather than looking at steady states and the behaviour of the model itself. As already noted in Chapter 2, this model is not symmetrical between compartments, a flaw corrected in our model. We analyse an explicit two strain model with the inclusion of a drug sanctuary in this chapter.

Rong et al. [2007a] analysed a basic model with 2 strains of virus, wild type and drug resistant, whereby new drug resistant mutants are produced when there is a mutation at the reverse transcription stage of the life cycle. The reproductive ratios, R_s and R_r, for wild type and drug resistant strains respectively, were calculated and used to infer results for the system. A disease free steady state is only stable if both reproductive ratios are less than unity. A resistant strain only steady state is found if $R_r > 1$ and a co-existence steady state is also possible for a range of values of R_s and R_r. The resistant strain only steady state is not possible if back mutation to the wild type is allowed to occur, giving a two strain evolution model identical to the one described in Chapter 3. A pharmacokinetic model of drug treatment is then used by Rong et al. [2007a] to describe drug concentration in blood and cell compartments taking processing necessary for activation of the drugs into account. This model is used in conjunction with the viral life cycle model to look at the effect of adherence on the proportion of wildtype to resistant strain present in the body. Their model suggests that perfect adherence will suppress wildtype virus but allow drug resistant virus to replicate very slowly. When adherence is not perfect the proportion of drug resistant strain rises more rapidly. These results closely mirror those of Smith and Wahl [2005], which analyses a competition model to a similar end. There are a number of assumptions made in this model. As previously mentioned back mutation is not considered which means that the model is more of a competition model than one looking at evolution. The model also assumes that the resistant strain is resistant to reverse transcriptase inhibitors and protease inhibitors to some degree. This is not a likely scenario in reality as more than one mutation would be necessary for this to occur. This model also shows that at high drug efficacy the viral population dies out. This is not the case in reality [Furtado et al., 1999].

Rong et al. [2007b] analysed a competition model of HIV dynamics that included a non-productive eclipse phase to investigate how drug resistance developes during HIV infection. The eclipse phase separates out entry into the cell from later stages of the life cycle including reverse transcription and integration into the host cell genome. The eclipse phase consisted of infected cells that are yet to have proviral DNA incorporated into the genome of the cell and can revert back to susceptible cells. Due to the inclusion of another variable (cells in eclipse phase of infection) the model has a slightly different reproductive ratio. One strain of virus was taken to be wildtype whilst the other strain was resistant to both reverse transcriptase inhibitors and protease inhibitors. The reproductive ratios of the two strains (when drug is present) were calculated and found to be functions of RTI drug efficacy and PI drug efficacy. The effects of the different types of drug were separated out and the effects on the fitness of the strains

was assessed. It was found that an optimal progression rate (from eclipse phase to productively infected) and optimal production rate of virions maximizes the fitness of a drug resistant strain in the presence of drugs. It was also shown that higher levels of drug efficacy allow a wider range of drug resistant strains to invade provided that level is not high enough to eradicate both strains.

What seems clear from these models is that regardless of how drug concentration is modelled, the likelihood of drug resistance emerging is greatly increased for high levels of drug efficacy where the wildtype strain is less fit than the resistant strain. Coexistence is seen when mutation is included in the model whereby one strain is dominant and the other is found at very low levels ($O(\epsilon)$). In this chapter we analyse two models which include both a wildtype and resistant strain and a drug sanctuary to examine the effect of heterogeneity on drug resistance. The two target cell model is considered first as it has a more tractable form. We then extend the two compartment model to see the effect of a drug sanctuary in a more heterogeneous environment. Analysis is carried out in the absence of mutation in order to understand the underlying behaviour of the models.

4.3 Two Target Cell Two Strain Model

In order to assess the effect of cell heterogeneity on the presence of drug resistant strains of virus we extend the two target cell model from Chapter 2 to include two strains of virus. This is done in the same manner as the evolutionary two strain model, (3.3), from Chapter 3.

4.3.1 Model Equations

We consider two strains of virus in the model: a wild-type and a drug resistant strain taken to be strain w and m respectively. The concentration of susceptible cells, infected cells and free virions for each type of target cell are given by S_i, I_{ij} , and v_j respectively, where $i = 1, 2$ indicates the target cell type and $j = w, m$ denotes the viral strain. We keep the assumptions of a primary target cell, S_1, which is wholly susceptible to drug (CD4+ T cells) and a secondary target cell, S_2, which acts as a drug sanctuary (macrophages) and model drug treatment in the same manner as before with the addition that the resistant strain is not affected by the drug, but that there is a cost to this resistance represented by the resistance factor, $0 < r < 1$. These elements

combine to give us the model equations:

$$\begin{aligned}
\dot{S}_1 =&\lambda_1 - dS_1 - S_1((1-e)\beta_1 v_w + r\beta_1 v_m),\\
\dot{S}_2 =&\lambda_2 - dS_2 - S_2((1-eh)\beta_2 v_w + r\beta_2 v_m),\\
\dot{I}_{1w} =&S_1((1-\epsilon)(1-e)\beta_1 v_w + \epsilon r\beta_1 v_m) - aI_{1w},\\
\dot{I}_{1m} =&S_1(\epsilon(1-e)\beta_1 v_w + (1-\epsilon)r\beta_1 v_m) - aI_{1m},\\
\dot{I}_{2w} =&S_2((1-\epsilon)(1-eh)\beta_2 v_w + \epsilon r\beta_2 v_m) - aI_{2w},\\
\dot{I}_{2m} =&S_2(\epsilon(1-eh)\beta_2 v_w + (1-\epsilon)r\beta_2 v_m) - aI_{2m},\\
\dot{v}_w =&k(I_{1w} + I_{2w}) - cv_w,\\
\dot{v}_m =&k(I_{1m} + I_{2m}) - cv_m.
\end{aligned} \tag{4.1}$$

A diagrammatic representation is shown in Figure 4-1.

4.3.2 Steady State Analysis

It is not possible to obtain explicit expressions for steady states when $\epsilon > 0$. However we can find series solutions of the form $T = \sum_{i=0}^{\infty} \epsilon^i T_i$, where $T = S, I, v$ is a given state variable. Below we give the O(1) solutions which are equivalent to finding the steady states of the corresponding competition model ($\epsilon = 0$). We obtain the following four steady states: disease free, dominant wild type, dominant resistant and 'coexistence'.

Steady State Levels

1. The disease free steady state is $S_1 = \frac{\lambda_1}{d}, S_2 = \frac{\lambda_2}{d}$ with all other state variables equal to zero.

2. The wild type dominant steady state depends on the roots of the quadratic:

$$\begin{aligned}
&v_w^2 + x_1 v_w + x_0 = 0,\\
&x_1 = \frac{d}{(1-e)\beta_1}(1 - R_{01w}) + \frac{d}{(1-eh)\beta_2}(1 - R_{02w}),\\
&x_0 = \frac{d^2}{(1-e)\beta_1(1-eh)\beta_2}(1 - R_{0w}),
\end{aligned} \tag{4.2}$$

   where the basic reproductive ratios are $R_{01w} = \frac{\lambda_1(1-e)\beta_1 k}{acd}$, $R_{02w} = \frac{\lambda_2(1-eh)\beta_2 k}{acd}$

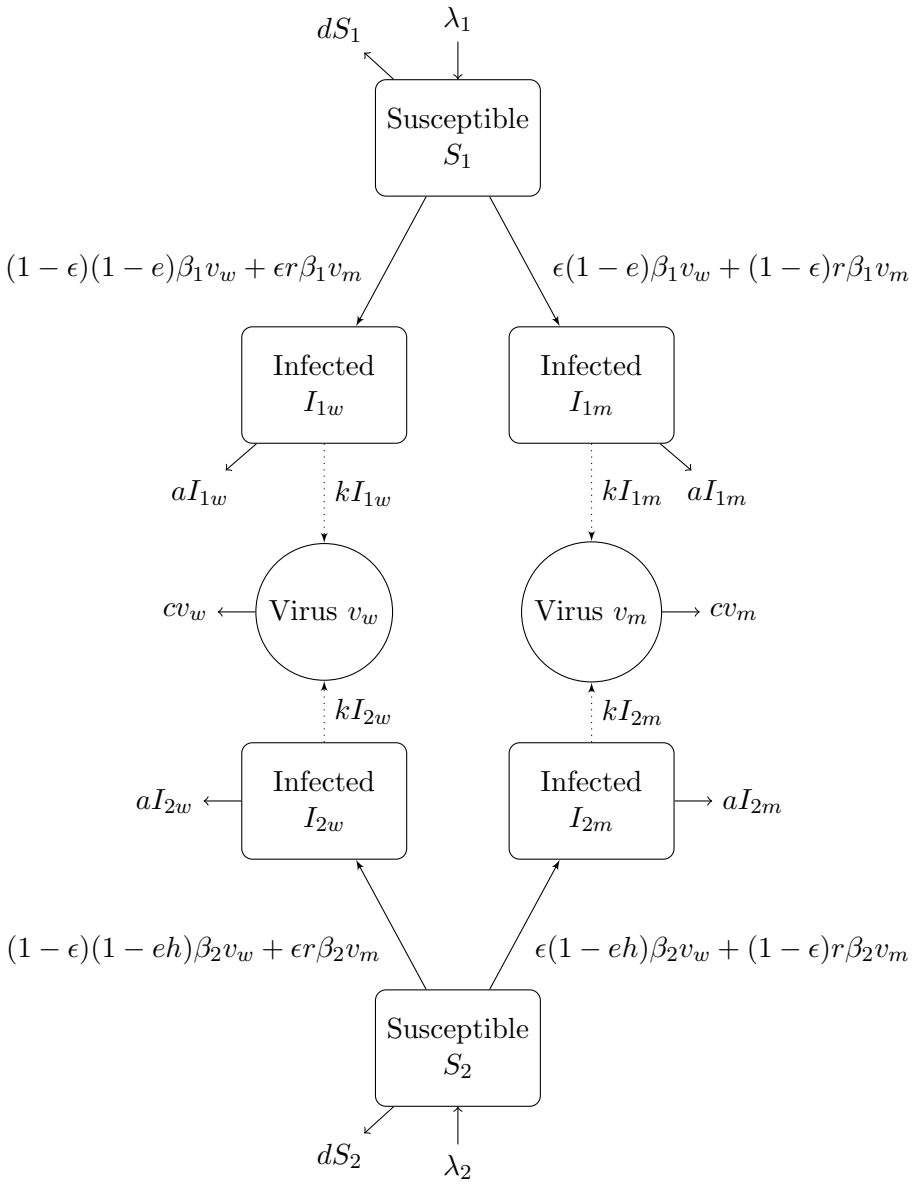

Figure 4-1: Schematic of two target cell two strain model. See text and Table 2.3 for futher details of parameters and variables.

and $R_{0w} = R_{01w} + R_{02w}$. The other variables are

$$\begin{aligned} S_1 =& \frac{\lambda_1}{d + (1-e)\beta_1 v_w} \\ I_{1w} =& \frac{(1-e)\beta_1 S_1 v_w}{a}, \\ S_2 =& \frac{\lambda_2}{d + (1-eh)\beta_2 v_w}, \\ I_{2w} =& \frac{(1-eh)\beta_2 S_2 v_w}{a}, \\ v_m =& L_m = I_{1m} = I_{2m} = O(\epsilon). \end{aligned}$$

All variables also have O(ϵ) terms.

When $R_{0w} > 1$ there is a single real positive root of the quadratic in v_w (5.5),leading to a biologically realistic wildtype dominant steady state.

3. The mutant dominant steady state depends on the roots of the quadratic:

$$\begin{aligned} & v_m^2 + y_1 v_m + y_0 = 0, \\ & y_1 = \frac{d}{r\beta_1}(1 - R_{01m}) + \frac{d}{r\beta_2}(1 - R_{02m}), \\ & y_0 = \frac{d^2}{r^2\beta_1\beta_2}(1 - R_{0m}), \end{aligned} \tag{4.3}$$

where $R_{01m} = \frac{\lambda_1 r\beta_1 k}{acd}$, $R_{02m} = \frac{\lambda_2 r\beta_2 k}{acd}$ and $R_{0m} = R_{01m} + R_{02m}$. The other variables are

$$\begin{aligned} S_1 =& \frac{\lambda_1}{d + r\beta_1 v_m} \\ I_{1m} =& \frac{r\beta_1 S_1 v_m}{a}, \\ S_2 =& \frac{\lambda_2}{d + r\beta_2 v_m}, \\ I_{2m} =& \frac{r\beta_2 S_2 v_m}{a}, \\ v_w =& L_w = I_{1w} = I_{2w} = O(\epsilon). \end{aligned}$$

Again all variables have O(ϵ) terms.

When $R_{0m} > 1$ there is a single real positive root of the quadratic in v_m (5.7), leading to a biologically realistic mutant dominant steady state.

4. The coexistence steady state only exists if $h \neq 1$ and is given by:

$$\begin{aligned}
S_1 =& \frac{ac((1-eh)-r)}{kr\beta_1((1-eh)-(1-e))},\\
S_2 =& \frac{ac(r-(1-e))}{k\beta_2((1-eh)-(1-e))},\\
v_w =& \frac{r\left(\beta_1 S_1\left(\lambda_2 - dS_2\right) - \beta_2 S_2\left(\lambda_1 - dS_1\right)\right)}{S_1 S_2 \beta_1 \beta_2((1-eh)-(1-e))},\\
v_m =& \frac{\beta_2(1-eh)S_2\left(\lambda_1 - dS_1\right) - \beta_1(1-e)S_1\left(\lambda_2 - dS_2\right)}{S_1 S_2 \beta_1 \beta_2((1-eh)-(1-e))},\\
I_{1w} =& \frac{S_1(1-e)\beta_1 v_w}{a},\\
I_{1m} =& \frac{S_1 r \beta_1 v_m}{a}\\
I_{2w} =& \frac{S_2(1-eh)\beta_2 v_w}{a},\\
I_{2m} =& \frac{S_2 r \beta_2 v_m}{a}.
\end{aligned}$$

All variables have additional terms of $\mathrm{O}(\epsilon)$.

The steady state expressions for S_1 and S_2 are both positive if $(1-e) < r < (1-eh)$. In addition providing v_w and v_m are positive the remaining variables are also positive. Therefore in order to ascertain whether the coexistence steady state is biologically realistic the constraints for $v_w > 0$ and $v_m > 0$ need to be investigated.

Local Stability Criteria

1. The Jacobian for the disease free steady state is

$$\begin{pmatrix}
-d & 0 & 0 & 0 & 0 & 0 & -\frac{(1-e)\beta_1\lambda_1}{d} & -\frac{r\beta_1\lambda_1}{d}\\
0 & -d & 0 & 0 & 0 & 0 & -\frac{(1-eh)\beta_2\lambda_2}{d} & -\frac{r\beta_2\lambda_2}{d}\\
0 & 0 & -a & 0 & 0 & 0 & \frac{(1-e)\beta_1\lambda_1}{d} & 0\\
0 & 0 & 0 & -a & 0 & 0 & 0 & \frac{r\beta_1\lambda_1}{d}\\
0 & 0 & 0 & 0 & -a & 0 & \frac{(1-eh)\beta_2\lambda_2}{d} & 0\\
0 & 0 & 0 & 0 & 0 & -a & 0 & \frac{r\beta_2\lambda_2}{d}\\
0 & 0 & k & 0 & k & 0 & -c & 0\\
0 & 0 & 0 & k & 0 & k & 0 & -c
\end{pmatrix}.$$

The characteristic equation for this matrix can be factorised into the following polynomials:

$$
\begin{aligned}
&(\Lambda + d)^2 = 0, \\
&\Lambda^3 + x_2\Lambda^2 + x_1\Lambda + x_0 = 0, \\
&\text{where} \\
&x_2 = 2a + c, \\
&x_1 = 2ac + a^2 - \frac{k}{d}((1-e)\beta_1\lambda_1 + (1-eh)\beta_2\lambda_2), \\
&x_0 = a\left(ac - \frac{k}{d}((1-e)\beta_1\lambda_1 + (1-eh)\beta_2\lambda_2)\right), \\
&\text{and} \\
&\Lambda^3 + y_2\Lambda^2 + y_1\Lambda + y_0 = 0, \\
&y_2 = 2a + c, \\
&y_1 = 2ac + a^2 - \frac{kr}{d}(\beta_1\lambda_1 + \beta_2\lambda_2), \\
&y_0 = a\left(ac - \frac{kr}{d}(\beta_1\lambda_1 + \beta_2\lambda_2)\right).
\end{aligned}
$$

All coefficients are positive and the disease free steady state is stable if and only if the basic reproductive ratio $\max(R_{0w}, R_{0m}) < 1$.

2. The characteristic polynomials for the wildtype only steady state can be factorised into the following polynomials:

$$(\Lambda + a)^2 = 0,$$

$$
\begin{aligned}
&\Lambda^4 + x_3\Lambda^3 + x_2\Lambda^2 + x_1\Lambda + x_0 = 0,\\
&\text{where}\\
&x_3 = c + a + (1-eh)\beta_2 + (1-e)\beta_1 + 2d,\\
&x_2 = ca - k(1-e)\beta_1 S_1 - k(1-eh)\beta_2 S_2\\
&\quad + d(2(a+c)+d) + (a+c+d)((1-e)\beta_1 + (1-eh)\beta_2)v_w\\
&\quad + (1-e)(1-eh)\beta_1\beta_2 v_w^2,\\
&x_1 = (a+c)(1-e)(1-eh)v_w^2\\
&\quad + ((ac+cd+ad)((1-e)\beta_1 + (1-eh)\beta_2) - k(1-e)(1-eh)\beta_1\beta_2(S_1+S_2))v_w\\
&\quad + d(ad+cd+2ac - 2k((1-e)\beta_1 S_1 + (1-eh)\beta_2 S_2)),\\
&x_0 = ac(1-e)(1-eh)\beta_1\beta_2 v_w^2\\
&\quad + (acd((1-e)\beta_1 + (1-eh)\beta_2) - dk(1-e)(1-eh)\beta_1\beta_2(S_1+S_2))v_w\\
&\quad + d^2(ac - k((1-e)\beta_1 S_1 + (1-eh)\beta_2 S_2)),
\end{aligned}
\tag{4.4}
$$

and

$$
\begin{aligned}
&\Lambda^2 + y_1\Lambda + y_0 = 0,\\
&\text{where}\\
&y_1 = a + c,\\
&y_0 = ac - kr\beta_1 S_1 - kr\beta_2 S_2.
\end{aligned}
\tag{4.5}
$$

The quartic polynomial (4.4) has positive coefficients when the intercept $x_0 > 0$. The intercept condition can be rearranged to give

$$
\begin{aligned}
&v_w^2 + z_1 v_w + z_0 > 0,\\
&z_1 = \frac{d}{(1-e)\beta_1}\left(1 - R_{01w}(S_1^w)\right) + \frac{d}{(1-eh)\beta_2}\left(1 - R_{02w}(S_2^w)\right),\\
&z_0 = \frac{d^2}{(1-e)\beta_1(1-eh)\beta_2}\left(1 - R_{0w}(S_1^w, S_2^w)\right),
\end{aligned}
\tag{4.6}
$$

where S_1^w and S_2^w denote the wildtype dominant steady state expressions for S_1 and S_2. This quadratic has the same form as the steady state expression for v_w (5.5), with $\frac{\lambda_i}{d}$ replaced with the wildtype dominant steady state expressions for S_i. At steady state, $R_{0w}(S_1^w, S_2^w) \equiv 1$, and therefore the coefficient $z_0 = 0$. Also as $R_{0w}(S_1^w, S_2^w) = R_{01w}(S_1^w) + R_{02w}(S_2^w) = 1$, the coefficient $z_1 > 0$. Therefore when $R_{0w} > 1$, meaning there is a real positive v_w, the intercept of the quartic polynomial (4.4) will also be positive.

The quadratic polynomial (4.5) has positive coefficients if

$$\frac{rk}{ac}(\beta_1 S_1^w + \beta_2 S_2^w) = R_{0m}(S_1^w, S_2^w) < 1,$$

where S_1^w and S_2^w denote the wildtype dominant steady state expressions for S_1 and S_2. When $h = 1$ this condition becomes $R_{0m} < R_{0w}$ or equivalently $r < (1 - e)$.

Therefore the wildtype dominant steady state is stable when $R_{0w} > 1$ and $R_{0m}(S_1^w, S_2^w) < 1$. The basic reproductive ratio, $R_{0w} > 1$, specifies when wildtype virus can invade a totally susceptible population. The expression $R_{0m}(S_1^w, S_2^w) < 1$ specifies that mutant virus cannot invade a susceptible population at the wildtype steady state level.

3. The mutant only steady state characteristic polynomial has the same form as that for the wildtype only steady state and is therefore stable when $R_{0m} > 1$ and $R_{0w}(S_1^m, S_2^m) < 1$, where S_1^m and S_2^m denote the steady state expressions of S_1 and S_2 at the mutant dominant steady state.

4. It is not possible to obtain a tractable characteristic polynomial for the coexistence steady state.

   Figure 4-2 shows when each of the steady states is stable as we vary the drug efficacy e. The coexistence steady state is only stable for a very small range of R_{0w} inbetween the two other endemic steady states being stable. It is only seen when drug penetrance $h < 1$ as in Figure 4-2. In Figure 4-2 $R_{0m} < R_{0w}$ when the mutant only endemic steady state becomes stable.

   However, we can infer the stability conditions from when the other steady states are unstable; when $R_{0w} > 1$, $R_{0m} > 1$, $R_{0w}(S_1^m, S_2^m) > 1$ and $R_{0m}(S_1^w, S_2^w) > 1$ the coexistence steady state is stable. This can be seen in Figure 4-3. Numerical testing showed that when the other steady states were unstable both strains of virus were present at the levels given by the coexistence steady state expressions.

   From Figures 4-2 and 4-3 we can see that coexistence can only occur for a very small range of parameter values and as such it is not likely to be biologically significant. In addition if we include mutation in the model all of the steady states show coexistence with one strain dominant over the other, as shown in Figure 4-4, however the point at when the switch in dominance occurs is the same.

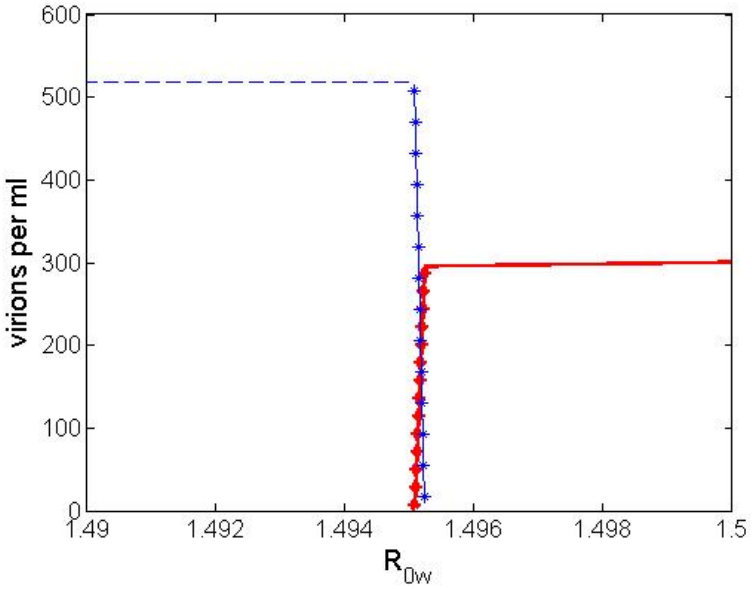

Figure 4-2: Figure showing when the three endemic steady states are stable. The wildtype strain v_w is denoted by the thick red line and the mutant strain v_m by the thin blue line. The dashed lines denote the mutant only endemic steady state, the solid lines the wildtype only endemic steady state and the asterisk marks denote the coexistence steady state. R_{0w} is varied by changing the value of the drug efficacy e, $r = 0.25$, $R_{0m} = 1.2825$; parameters are as given in Table 2.3.

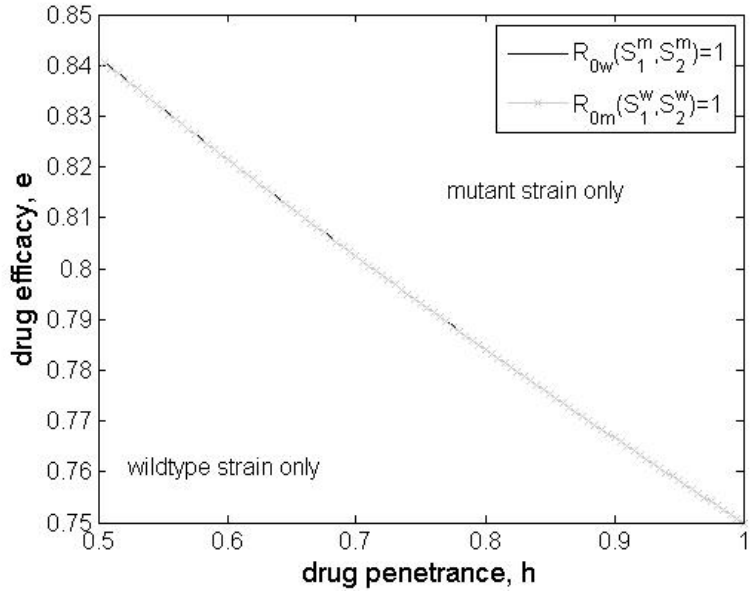

(a)

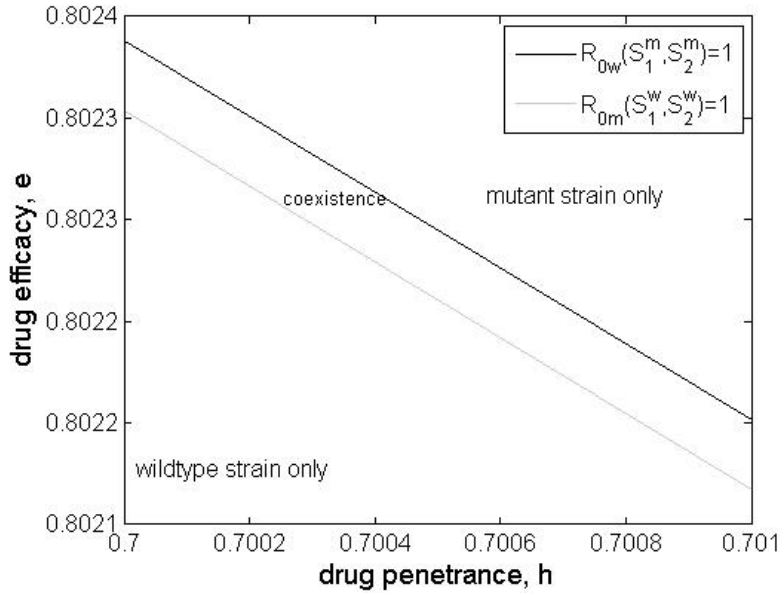

(b)

Figure 4-3: Graph showing the stability of the endemic steady states when $R_{0m} > 1$ ($r = 0.25$). a)drug penetrance h and drug efficacy e, varied, b)close up of region where $R_{0w} > 1$ to show that when $R_{0w}(S_1^m, S_2^m) > 1$ and $R_{0m}(S_1^w, S_2^w) > 1$ the coexistence steady state is stable. Other parameters as in Table 2.3.

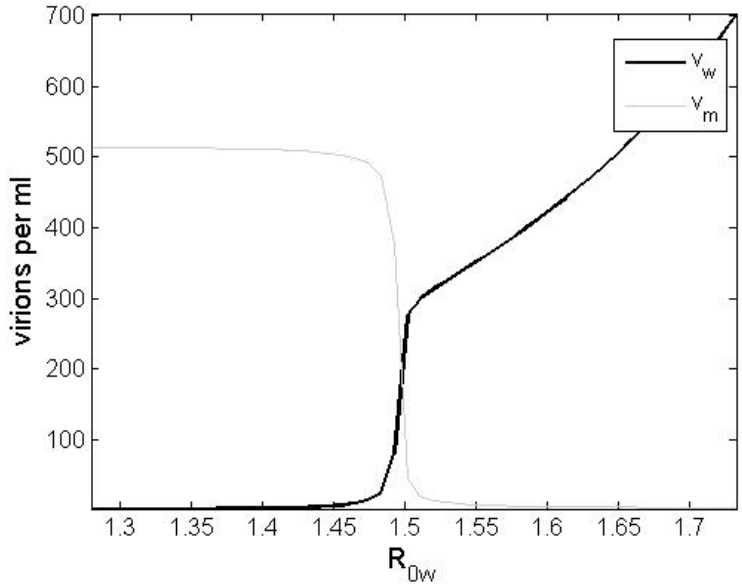

Figure 4-4: Figure showing the steady state viral loads in the target cell model with mutation. R_{0w} is varied by changing the value of the drug efficacy e, $r = 0.25$, $R_{0m} = 1.2825$, $\epsilon = 0.0005$; parameters are as given in Table 2.3.

The biologically interesting feature from the two target cell model (2.6): that it allowed low level viral loads at steady state with high levels of drug efficacy whether in the presence of a drug sanctuary (drug penetrance $h < 1$) or not ($h = 1$), can be found in the two strain version of the model (4.1) under certain circumstances. These being when $R_{0w} > 1 > R_{0m}$ and when $R_{0m} > R_{0w}$ with R_{0m} very close to 1 as shown in Figure 4-5a and Figure 4-5b respectively. Additionally when $h < 1$ we have that low level viral load is possible when $R_{0m} < R_{0w}$ for certain parameter values that allow the mutant virus to dominate.

4.3.3 Summary of Results

The two target cell two strain model is capable of showing coexistence in a competition version of the model. However, the range of parameters that allow coexistence to occur is so small that this steady state is unlikely to be seen *in vivo*. However, the presence of a drug sanctuary does cause some interesting behaviour. The switch over in stability from wildtype to mutant does not occur when the $R_{0w} = R_{0m}$ as in previous two strain models. The usual condition for disease free steady state stability holds, $R_{0i} < 1$, however the mutant can outcompete the wildtype even when $R_{0m} < R_{0w}$. Conditions for when the coexistence steady state is stable were found by analysing

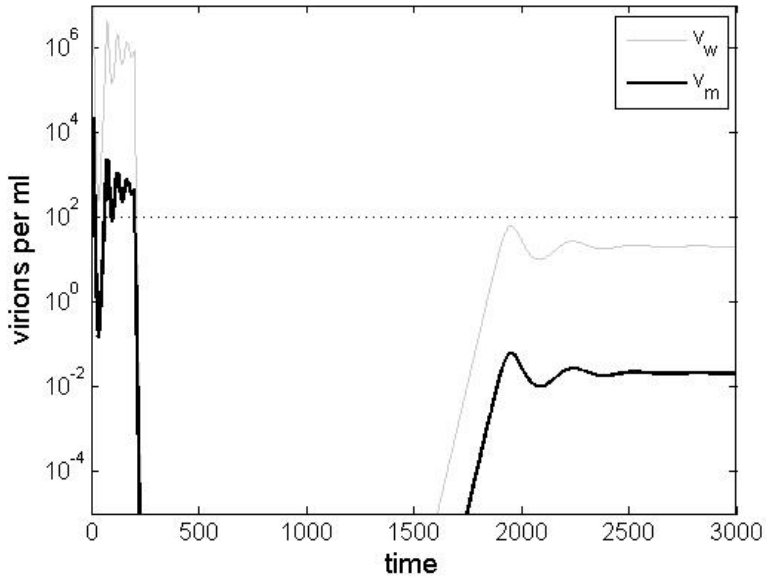

(a) $R_{0w} > 1 > R_{0m}$

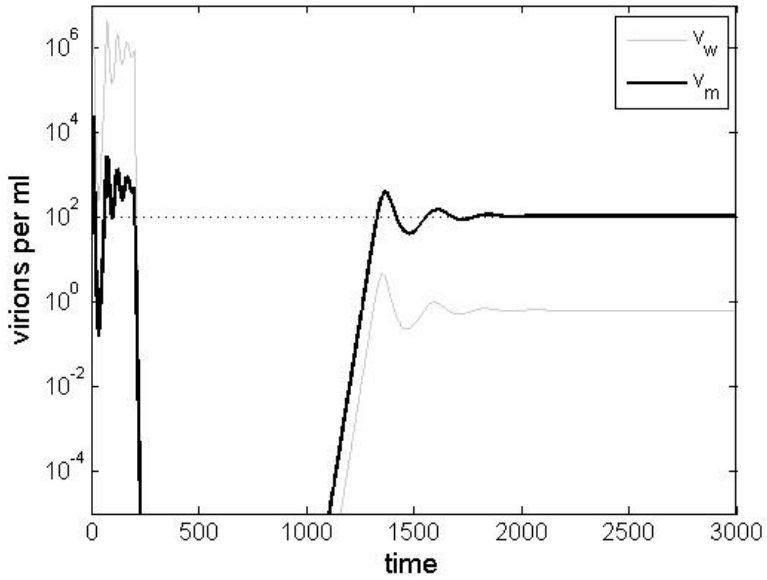

(b) $R_{0m} > R_{0w} > 1$

Figure 4-5: Graphs showing two target cell two strain model behaviour for two different parameter cases: a) $R_{0m} < 1, R_{0w} > 1$ ($r = 0.1$)and b) $R_{0m} > R_{0w}$ ($r = 0.21$). The dotted line is the detection threshold for viral load tests. Other parameter values as in Table 2.3. Drug treatment commenced at 200 days post infection.

the characteristic polynomials for the both the wildtype only and mutant only steady states and numerically checking that when the disease free, mutant only and wildtype only steady states are unstable the coexistence steady state is stable. The coexistence steady state is stable when invasion of one of the single strain only steady states is possible with the conditions $R_{0i}(S_1^{\hat{i}}, S_2^{\hat{i}}) > 1$, where $i = w, m$ and $\hat{i}$ is the other strain. These criteria for coexistence have previously been seen in Roberts [2007] in relation to a model of a fatal infection with two variants in a wild animal. The evolutionary version of the model shows the same behaviour as the competition model, i.e. the results are a perturbation of the competition model, as seen in the two strain evolutionary model analysed in Chapter 3.

The evolutionary version of the model still allows low level viral load to occur with the winning strain having the larger R_{0i} and this being close to but greater than 1. This model will be extended to include latently infected cells in Chapter 5.

4.4 Two Compartment Two Strain Model

We now explore the impact of a drug sanctuary and cell heterogeneity on drug resistance in a more complex setting: the two compartment model (2.3), from Chapter 2. As this model is more complicated we concentrate our analysis on the competition version of the model.

4.4.1 Model Equations

The model comprises of a system of non-linear ordinary differential equations and is based on that of Kepler and Perelson [1998]. It models the viral load in two body compartments: the blood and the male genital tract, taken to be compartment 1 and compartment 2 respectively. We assume that the volume of compartment 1 is greater than that of compartment 2 and with the inclusion of drug treatment, that compartment 2 may behave as a drug sanctuary with lower drug efficacy.

We consider two strains of virus in the model: a wild-type and a drug resistant strain taken to be strain w and strain m respectively. The concentration of susceptible cells, infected cells and free virions in each compartment are given by S_i, I_{ij}, and v_{ij} respectively, where $i = 1, 2$ indicates the compartment and $j = w, m$ denotes the viral strain. The virions are allowed to move between the blood and genital tract compartments. A schematic of the model is shown in Figure 4-6 for which we have the system of equations:

$$\begin{aligned}
\dot{S}_i =& \lambda_i - d_i S_i - \beta_{iw} S_i v_{iw} - \beta_{im} S_i v_{im}, \\
\dot{I}_{ij} =& \beta_{ij} S_i v_{ij} - a_i I_{ij}, \\
\dot{v}_{ij} =& k_{ij} I_{ij} - c_i v_{ij} + D_i (v_{\hat{i}j} - v_{ij}).
\end{aligned} \tag{4.7}$$

The symbol $\hat{i}$ means the other compartment. Modelling diffusion of viral particles between compartments using a discrete derivation of Fick's Law [Machouf et al., 2006] gives

$$D_1 = \frac{L}{1-u}, \qquad D_2 = \frac{L}{u},$$

where L is the transport coefficient and where the total volume is scaled to 1 and u is the volume of compartment 2. With this choice of diffusion coefficients, the system exhibits symmetry between compartments.

Drug treatment can be modelled implicitly by assuming that treatment directly reduces the corresponding viral parameter: β_{ij} for reverse transcriptase inhibitors and k_{ij} for protease inhibitors. Drug treatment is represented by scaling the relevant parameter (β_{ij} or k_{ij}) by a factor $(1-e)$, where e is the efficacy of the drug and ranges from 0

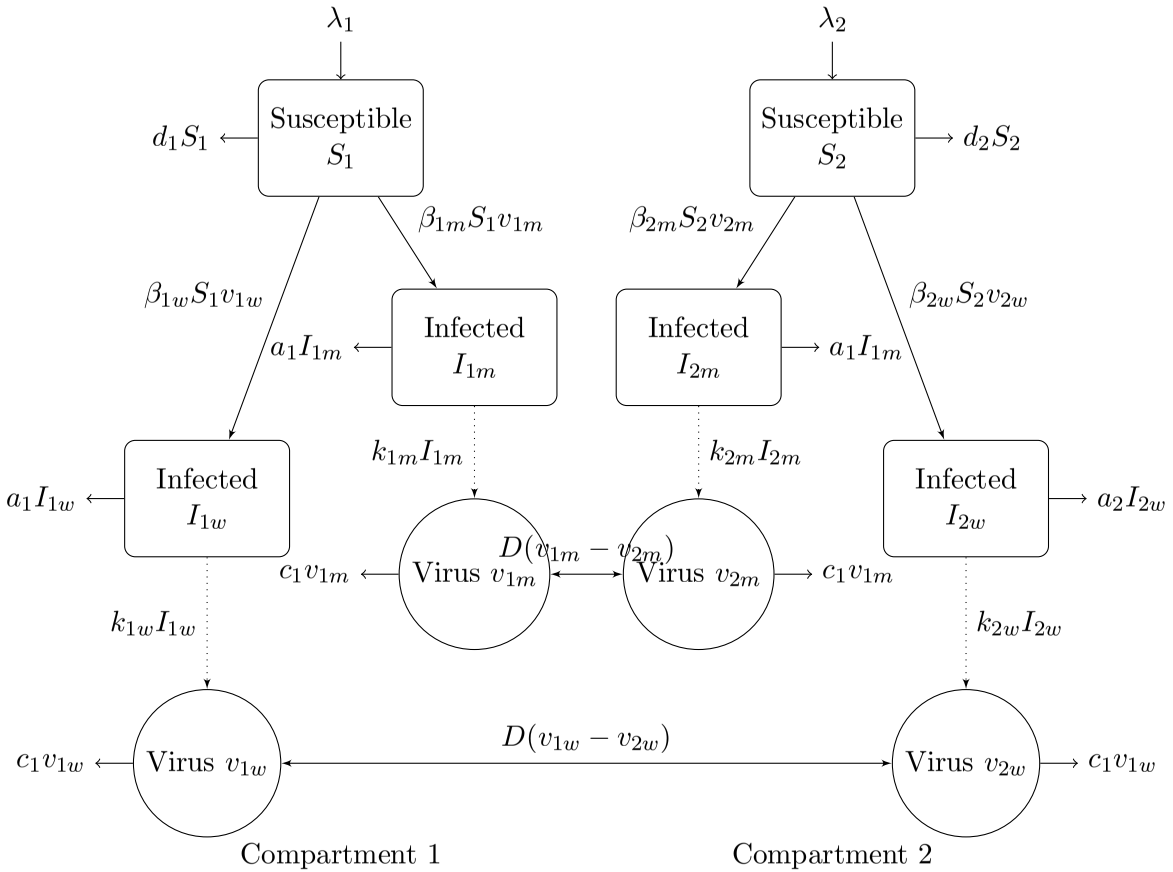

Figure 4-6: Schematic of the Two Compartment Two Strain Model (4.7) which allows virus diffusion between two separate body compartments. The diffusion is along a concentration gradient. In compartment 1 the diffusion term for wildtype virus is $\frac{L}{1-u}(v_{2w}-v_{1w})$ and in compartment 2 we have $\frac{L}{u}(v_{1w}-v_{2w})$, where L is the transport coefficient and u is the scaled size of compartment 2. The diffusion terms for drug resistant virus are modelled in the same way.

to 1. Drug penetrance in the second, smaller compartment is modelled by scaling drug efficacy e in compartment 2 by a factor h, where h is the drug penetrance ranging from 0 to 1. A summary of the parameters along with values used in numerical solutions can be seen in Table 4.1. The system (4.7) can be broken down into a number of simpler

Parameter	**Meaning**	**Value**
λ_i	birth rate of new cells	10^4 cells ml^{-1} day^{-1}
d_i	death rate of susceptible cells	0.01 cell^{-1} day^{-1}
β_{ij}	infection rate	2.4×10^{-8} virion^{-1} day^{-1}
a_i	death rate of infected cells	1 cell^{-1} day^{-1}
k_{ij}	number of new virions produced	3000 virions cell^{-1} day^{-1}
c_i	death rate of virions	23 day^{-1}
L	scaled transport coefficient	0.05 day^{-1}
u	scaled volume of small compartment	$0 - 0.5$
e	Drug efficacy in compartment 1	$0 - 1$
h	Drug penetrance in compartment 2	$0 - 1$
r	resistance factor	$0 - 1$

Table 4.1: Two compartment two strain model parameter descriptions and values.

systems to give insight into the behaviour of the full system. The full system (4.7) can be reduced to the basic model (1.1), of blood plasma dynamics with one strain of virus by setting $L = v_{1m} = I_{1m} = 0$. The blood plasma model with two strains of virus can be obtained by setting $L = 0$; analysis of this model can be found in Chapter 3. The main result from the two strain model is that the strain with the largest R_0 value outcompetes the other strain. The more interesting model of two compartments and one strain of virus, obtained by setting all of the mutant strain variables to zero, is analysed in Chapter 2. This model allows low level viral load at high drug efficacies with or without the presence of a drug sanctuary, due to the inclusion of cell heterogeneity to ensure the smaller compartment has a higher R_0 value under treatment. Cell heterogeneity also causes the viral load to differ between compartments which is more biologically realistic.

4.4.2 Steady State Analysis

Steady state analysis of the competition model is not possible when you allow all of the parameters to vary between compartments. However, if $u = 0.5$ (meaning the two compartments are the same size) and only the transmission parameters are allowed to vary, steady state expressions can be obtained. When $u = 0.5$, the diffusion coefficients $D_1 = D_2 = 2L$ so we will substitute $D_1 = D_2 = D$. There are 4 possible steady states: disease free, wildtype strain only, mutant strain only and coexistence.

1. The disease free steady state is

$$S_1 = \frac{\lambda}{d}, S_2 = \frac{\lambda}{d}, I_{1w} = I_{1m} = I_{2w} = I_{2m} = v_{1w} = v_{1m} = v_{2w} = v_{2m} = 0.$$

2. The wildtype strain only steady state is determined by the solution of a cubic equation in S_1:

$$x_3 S_1^3 + x_2 S_1^2 + x_1 S_1^2 + x_0 = 0,$$

where

$$\begin{aligned}
x_3 =& \beta_{1w}\beta_{2w}k^2 d(D+c),\\
x_2 =& (-(2D+c)\lambda\beta_{2w}k^2 + (D^2+Dc)adk)\beta_{1w}^2 - (2c^2+4Dc+D^2)ad\beta_{2w}k\beta_{1w},\\
x_1 =& ((2c^2+2D^2+5Dc)a\lambda\beta_{2w}k + (-Dc^2-2D^2c)a^2 d)\beta_{1w}\\
&+ (3Dc^2+2D^2c+c^3)a^2 d\beta_{2w},\\
x_0 =& -\lambda a^2\beta_{2w}c(2D^2+c^2+3Dc).
\end{aligned}$$

Other variables can be written in terms of S_1 and S_2 to give

$$\begin{aligned}
S_2 =& \frac{a(\beta_{1w}kS_1(c+D) - ac(c+2D))}{k\beta_{2w}(\beta_{1w}kS_1 - a(c+D))},\\
v_{1w} =& \frac{\lambda - dS_1}{\beta_{1w}S_1},\\
v_{2w} =& \frac{\lambda - dS_2}{\beta_{2w}S_2},\\
I_{1w} =& \frac{\beta_{1w}S_1 v_{1w}}{a},\\
I_{2w} =& \frac{\beta_{2w}S_2 v_{2w}}{a}.
\end{aligned}$$

Note that $x_3 > 0$ and $x_0 < 0$ meaning that there is always at least one positive real root. The condition for $S_2 > 0$ is $S_1 < \frac{ac}{\beta_{1w}k}\left(1 + \frac{D}{c+D}\right)$.

3. The mutant only steady state is determined by the solution of a cubic equation in S_1:

$$y_3 S_1^3 + y_2 S_1^2 + y_1 S_1^2 + y_0 = 0,$$

where

$$
\begin{aligned}
y_3 =&\beta_{1m}\beta_{2m}k^2d(D+c),\\
y_2 =&(-(2D+c)\lambda\beta_{2m}k^2+(D^2+Dc)adk)\beta_{1m}^2-(2c^2+4Dc+D^2)ad\beta_{2m}k\beta_{1m},\\
y_1 =&((2c^2+2D^2+5Dc)a\lambda\beta_{2m}k+(-Dc^2-2D^2c)a^2d)\beta_{1m}\\
&+(3Dc^2+2D^2c+c^3)a^2d\beta_{2m},\\
y_0 =&-\lambda a^2\beta_{2m}c(2D^2+c^2+3Dc).
\end{aligned}
$$

Other variables can be written in terms of S_1 and S_2 to give

$$
\begin{aligned}
S_2 =&\frac{a(\beta_{1m}kS_1(c+D)-ac(c+2D))}{k\beta_{2m}(\beta_{1m}kS_1-a(c+D))},\\
v_{1m} =&\frac{\lambda-dS_1}{\beta_{1m}S_1},\\
v_{2m} =&\frac{\lambda-dS_2}{\beta_{2m}S_2},\\
I_{1m} =&\frac{\beta_{1m}S_1v_{1m}}{a},\\
I_{2m} =&\frac{\beta_{2m}S_2v_{2m}}{a}.
\end{aligned}
$$

Note that $y_3 > 0$ and $y_0 < 0$ meaning that there is always at least one positive real root. The condition for $S_2 > 0$ is $S_1 < \frac{ac}{\beta_{1w}k}\left(1+\frac{D}{c+D}\right)$.

4. The coexistence steady state is determined by the solution to a quadratic containing S_1:

$$z_2(\frac{kS_1}{a})^2+z_1(\frac{kS_1}{a})+z_0=0,$$

where

$$
\begin{aligned}
z_2 =&\beta_{1w}\beta_{1m}(\beta_{2w}-\beta_2m)(c+D),\\
z_1 =&D^2(\beta_{1w}\beta_{2m}-\beta_{2w}\beta_{1m})+(c^2+2Dc)(\beta_{1w}+\beta_{1m})(\beta_{2m}-\beta_{2w}),\\
z_0 =&(\beta_{2w}-\beta_{2m})(3cD+2D+c^2).
\end{aligned}
$$

The expression for S_2 is the same as in the strain 1 only steady state, however

the expressions for the viral variables are considerably more complex:

$$
\begin{aligned}
v_{2w} =& \frac{\left((\lambda - dS_1) - \frac{\beta_{1m}S_1}{\beta_{2m}S_2D}(c - \frac{k\beta_{2m}S_2}{a} + D)(\lambda - dS_2)\right)}{\beta_{1w}S_1\left(\frac{D}{c - \frac{k\beta_{1w}S_1}{a} + D} - \frac{\beta_{2w}}{\beta_{1w}D}(c - \frac{k\beta_{2m}S_2}{a} + D)\right)}, \\
v_{1w} =& \frac{v_{2w}D}{c - \frac{k\beta_{1w}S_1}{a} + D}, \\
v_{2m} =& \frac{\lambda - dS_2 - \beta_{2w}S_2v_{2w}}{\beta_{2m}S_2}, \\
v_{1m} =& \frac{v_{2m}}{D}\left(c - \frac{k\beta_{2m}S_2}{a} + D\right), \\
I_{1w} =& \frac{\beta_{1w}S_1v_{1w}}{a}, \\
I_{2w} =& \frac{\beta_{2w}S_2v_{2w}}{a}, \\
I_{1m} =& \frac{\beta_{1m}S_1v_{1m}}{a}, \\
I_{2m} =& \frac{\beta_{2m}S_2v_{2m}}{a}.
\end{aligned}
$$

The sign of z_2 and z_0 depend on the same factor $(\beta_{2w} - \beta_{2m})$, meaning there are either no roots with positive real parts or 2 roots with positive real parts depending on the sign of z_1. If $\beta_{2w} > \beta_{2m}$ and $\frac{\beta_{2w}}{\beta_{2m}} > \frac{\beta_{1w}}{\beta_{1m}}$ then there are two roots to the quadratic with real parts. The condition implies that the wildtype strain has a greater advantage in compartment 2 than in compartment 1. Conversely, if $\beta_{2w} < \beta_{2m}$ and $\frac{\beta_{2m}}{\beta_{2w}} > \frac{\beta_{1m}}{\beta_{1w}}$ then the mutant strain has a greater advantage in compartment 2 than in compartment 1. With the usual assumptions regarding drug therapy and drug resistance we have two roots with positive real part if $(1 - eh) > r$ and $(1 - eh) > (1 - e)$. The other condition, $r > (1 - eh)$ and $(1 - e) > (1 - eh)$ is never satisfied as $0 < h < 1$. This means that in order for the quadratic in S_1 to have roots with positive real parts the wildtype strain must be fitter than the mutant strain in compartment 2 and there must be a drug sanctuary present, i.e. $h < 1$.

1. The Jacobian for the disease free steady state is

$$\begin{pmatrix}
-d & 0 & 0 & -\beta_{1w}\frac{\lambda}{d} & -\beta_{1m}\frac{\lambda}{d} & 0 & 0 & 0 & 0 & 0 \\
0 & -a & 0 & \beta_{1w}\frac{\lambda}{d} & 0 & 0 & 0 & 0 & 0 & 0 \\
0 & 0 & -a & 0 & \beta_{1m}\frac{\lambda}{d} & 0 & 0 & 0 & 0 & 0 \\
0 & k & 0 & -c-D & 0 & 0 & 0 & 0 & D & 0 \\
0 & 0 & k & 0 & -c-D & 0 & 0 & 0 & 0 & D \\
0 & 0 & 0 & 0 & 0 & -d & 0 & 0 & -\beta_{2w}\frac{\lambda}{d} & -\beta_{2m}\frac{\lambda}{d} \\
0 & 0 & 0 & 0 & 0 & 0 & -a & 0 & \beta_{2w}\frac{\lambda}{d} & 0 \\
0 & 0 & 0 & 0 & 0 & 0 & 0 & -a & 0 & \beta_{2m}\frac{\lambda}{d} \\
0 & 0 & 0 & D & 0 & 0 & k & 0 & -c-D & 0 \\
0 & 0 & 0 & 0 & D & 0 & 0 & k & 0 & -c-D
\end{pmatrix}.$$

The characteristic polynomial for the disease free steady state can be factorised into

$$(\Lambda+d)^2(\Lambda^4+x_3\Lambda^3+x_2\Lambda^2+x_1\Lambda+x_0)(\Lambda^4+y_3\Lambda^3+y_2\Lambda^2+y_1\Lambda+y_0)=0,$$

where

$$\begin{aligned}
x_0 =& a^2c^2\left(\left(1+\frac{D}{c}-R_{01w}\right)\left(1+\frac{D}{c}-R_{02w}\right)-\frac{D^2}{c^2}\right),\\
x_1 =& ac\left(\left(1+\frac{D}{c}-R_{01w}\right)(D+a+c)-\frac{D^2}{c}\right)+\\
&+ac\left(\left(1+\frac{D}{c}-R_{02w}\right)(D+a+c)-\frac{D^2}{c}\right),\\
x_2 =& ac\left(1+\frac{D}{c}-R_{01w}\right)+ac\left(1+\frac{D}{c}-R_{02w}\right)+\\
&+(a+c+D)^2-D^2,\\
x_3 =& a+c+D+a+c+D,\\
R_{0iw} =& \frac{\lambda\beta_{iw}k}{acd},
\end{aligned}$$

and

$$\begin{aligned}
y_0 =& a^2c^2\left(\left(1+\frac{D}{c}-R_{0m}\right)^2-\frac{D^2}{c^2}\right),\\
y_1 =& 2ac\left(\left(1+\frac{D}{c}-R_{0m}\right)(D+a+c)-\frac{D^2}{c}\right)\\
y_2 =& 2ac\left(1+\frac{D}{c}-R_{0m}\right)+(a+c+D)^2-D^2,\\
y_3 =& a+c+D+a+c+D,\\
R_{0m} =& \frac{\lambda\beta_m k}{acd}.
\end{aligned}$$

The disease free steady state is stable when all of the coefficients x_i and y_i are positive. This occurs when $R_{0m} < 1$ and $R_{0w} < 1$. It is possible to obtain R_{0w}, using the next generation method, as the positive root of the quadratic:

$$R_{0w}^2-\left(\frac{\lambda k(c+D)(\beta_{2w}+\beta_{1w})}{acd(c+2D)}\right)R_{0w}+\frac{\beta_{1w}\beta_{2w}\lambda^2k^2}{a^2cd^2(c+2D)}=0.$$

2. It is not possible to obtain stability criteria for the other steady states analytically, however numerical solutions showed that when the disease free steady state was unstable one of the three endemic steady states was stable as can be seen in Figure 4-7. The coexistence steady state is seen inbetween the wildtype and mutant only steady states as in the two target cell two strain model (4.1). Additionally the bifurcation points from wildtype to coexistence to mutant do not correspond to conditions on R_{0i} for $i = w, m$. The nature of the coexistence steady state is explored more in the next section where the full model is considered.

4.4.3 Numerical Analysis

The full system (4.7) was investigated numerically to see how the combined effects of drug heterogeneity (i.e. a drug sanctuary) and cell heterogeneity affect steady state solutions. This model has a disease free steady state and three possible disease steady states. The disease steady states are strain 1 only ($v_{1m} = v_{2m} = I_{1m} = I_{2m} = 0$), strain 2 only ($v_{1w} = v_{2w} = I_{1w} = I_{2w} = 0$) and coexistence, where all viral strain variables are non-zero.

We follow our previous work and assume the mutant strain (strain m) is not affected by drug treatment but that this comes at a cost so we set $\beta_{1m} = \beta_{2m} = \beta_m = r\beta_w$. Also, in the absence of drug we assume the wildtype has the same values in both

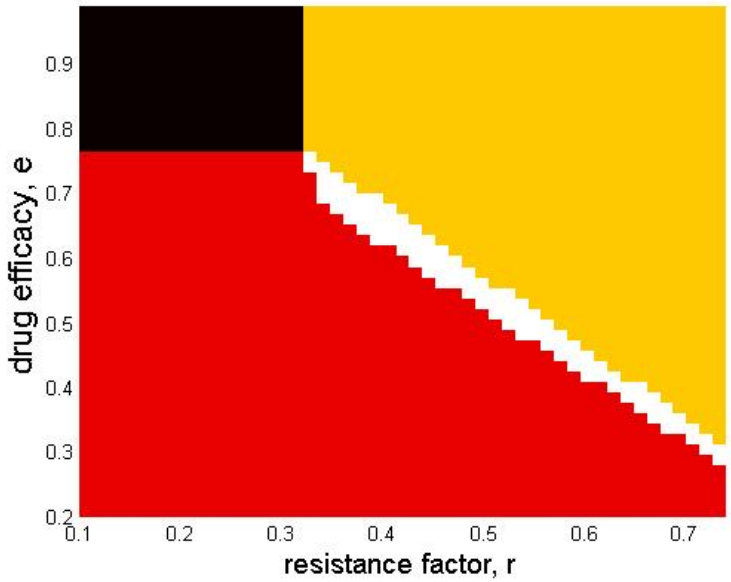

Figure 4-7: Graphs showing how the steady state stability changes with drug efficacy, e and resistance factor, r. The black region is the disease free steady state, the red (dark grey if greyscale) region is wildtype only, the yellow (light grey if greyscale) region is mutant only and the white region is coexistence. Parameter values were the same in each compartment with $u = 0.5$ and drug penetrance $h = 0.9$. Other parameter values as in Table 4.1.

compartments i.e. $\beta_{1w} = \beta_{2w} = \beta_w$. We assume that in that absence of drugs, strain w is fitter than strain m by setting $0 < r < 1$. This scenario leads to competitive exclusion in the full model such that the wildtype strain outcompetes the mutant strain. This result holds for all sizes of compartment 2 and values of the infected cell death rate in compartment 2 a_2, which we varied in the numerical analysis.

If there is no drug sanctuary in compartment 2 and the drug is above critical efficacy to give

$$(1 - e) < r$$

then the mutant strain m outcompetes the wildtype w, again regardless of the values of the other parameters in the model. This is because the other parameters affect both strains equally and without a drug sanctuary the drug also affects the wildtype strain the same in both compartments.

When a drug sanctuary is included in the model in the same way as in Chapter 2 i.e $\beta_{2w} = (1 - eh)\beta_w$, where $h < 1$, we see the most interesting results: both competitive exclusion and strain coexistence are possible depending on the values of the key model parameters r, u and a_2. When $r < 1 - e$ we again get competitive exclusion with the wildtype outcompeting the mutant strain, conversely when $r > 1 - eh$ the wildtype is outcompeted. However when

$$1 - e < r < 1 - eh$$

we can see competitive exclusion or strain coexistence depending on the other parameters in the model. This can be seen in Figure 4-8. When coexistence was seen further investigations were carried out to determine the dominant strain in each compartment. Given certain parameter conditions we see differential dominance between the two compartments. By this we mean that the mutant strain is dominant in compartment 1 and the wildtype is dominant in compartment 2. In Figure 4-8a the resistance factor is quite low ($r = 0.33$) meaning that the mutant cannot be dominant in both compartments or competitively exclude the wildtype. As the advantage to the wildtype increases with decreasing infected cell death rate in compartment 2 and increasing relative size of compartment 2, the wildtype can dominate the mutant in both compartments, or outcompete the mutant entirely.

In Figure 4-8b the resistance factor is high ($r = 0.7$) so the opposite occurs: the wildtype cannot outcompete the mutant. When the advantage to the wildtype decreases, a_2 increasing and u decreasing, the mutant can dominate in both compartments, or outcompete the wildtype. Figure 4-9 shows how the steady state stability is affected by the drug efficacy and resistance factor in more detail for varying cases of heterogeneity. Parameters were chosen so that all of the five steady state behaviours are

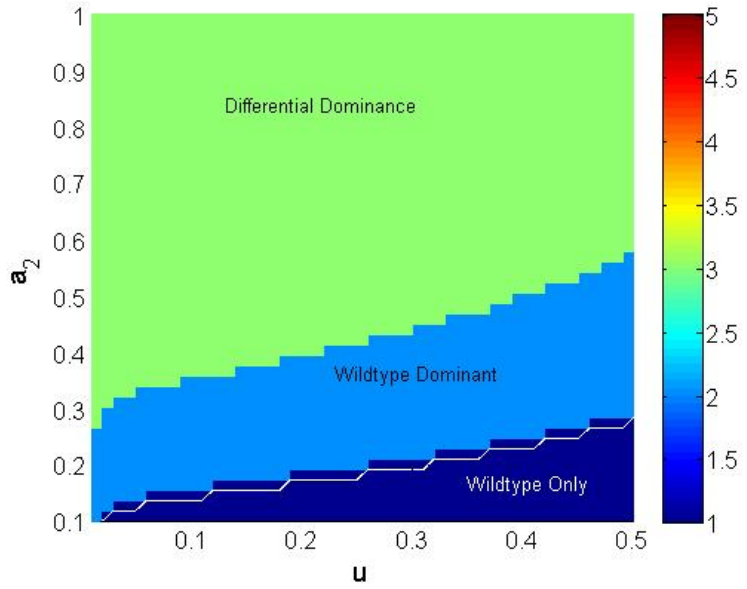

(a) $e = 0.75, r = 0.33$

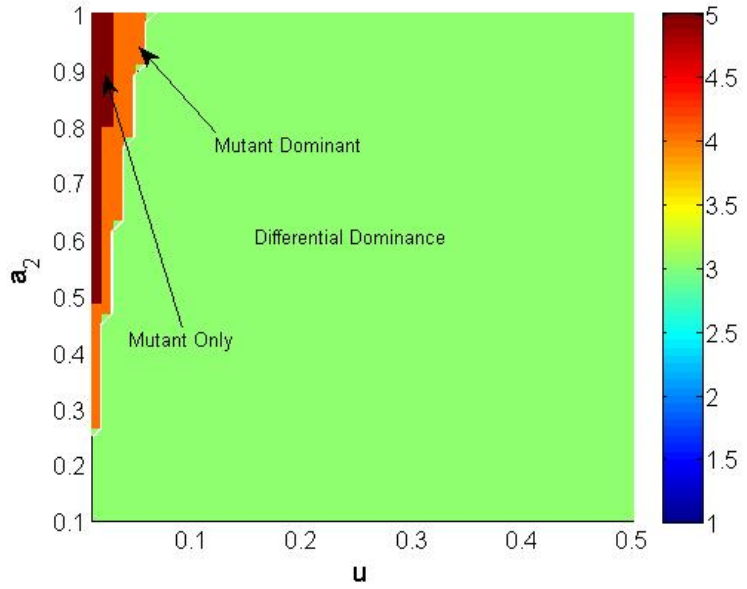

(b) $e = 0.5, r = 0.7$

Figure 4-8: Viral load steady state and dominance. Graphs showing the steady state behaviour and dominance of strains in the 2 compartment model for a range of values of u and a_2 : a) drug efficacy $e = 0.75$ and drug penetrance $h = 0.5$ and resistance factor $r = 0.33$ and b) drug efficacy $e = 0.5$, drug penetrance $h = 0.5$ and resistance factor $r = 0.7$. Key: 1 - wildtype only, 2 - wildtype dominant in both compartments, 3 - mutant dominant in compartment 1 and wildtype dominant in compartment 2, 4 - mutant dominant in both compartments, 5 - mutant only. Other parameter values as in Table 4.1.

possible. Figure 4-9a is the base case with both compartments the same size, with no cell heterogeneity ($a_1 = a_2$). As the resistance factor r is increased the fitness of the mutant increases, changing the stable steady state from wild type only, to wildtype dominant, differential dominance, mutant dominant and mutant only. For small values of $r < 1 - e$ the wildtype outcompetes the mutant. For larger values of r we see the same behaviour moving through the steady state behaviours as the drug efficacy decreases corresponding to less fit wildtype virus. When the second compartment is small in relation to the blood, as shown in Figure 4-9b the range of values of e and r for which we see coexistence decreases. This is because the wildtype has a much smaller advantage than before. In Figure 4-9c the infected cell death rate in compartment 2 is smaller than in compartment 1 ($a_2 = 0.5, a_1 = 1$) giving an extra advantage to the wildtype virus, widening the range of values of r for which coexistence is seen.

An interesting feature of the coexistence steady state is the magnitude of the viral loads in each compartment, as shown in Figures 4-10 and 4-11. From Figure 4-10 we can see that as the relative size of compartment 2 increases the concentration of the wildtype increases in both compartments whereas the concentration of mutant decreases. This is due to the advantage the wildtype gains when the second compartment, acting as a drug sanctuary, is larger. Figure 4-11 shows similar behaviour with the wildtype increasing as the second compartment becomes more advantageous for strain w, i.e. when the infected cell death rate a_2 decreases. A further interesting point is that each strain is found at a relatively high amount in both compartments. In the evolutionary models in Chapter 3 we showed that the minority strain is found at $O(\epsilon)$ relative to the dominant strain (in the two strain model). Here there is no mutation and we have coexistence with both strains present at above the threshold of detection (100 virions per ml).

4.4.4 Summary of Results

The two compartment two strain model is capable of showing coexistence under certain parameter conditions. Cell heterogeneity is not capable of allowing coexistence in isolation, this is because the cell heterogeneity affects both strains equally. When the second compartment is modelled as a drug sanctuary coexistence can occur. Increasing the relative size of the drug sanctuary, u, allows coexistence to occur for higher values of drug efficacy. When cell heterogeneity is also present, modelled here by allowing the infected cell death rate to vary between compartments, the parameter ranges for which coexistence is seen are also increased. The bigger the advantage that the wildtype strain has over the mutant strain in compartment 2, due either to the drug sanctuary being larger (u larger), the drug penetrance being lower (lower h) or the cell heterogeneity

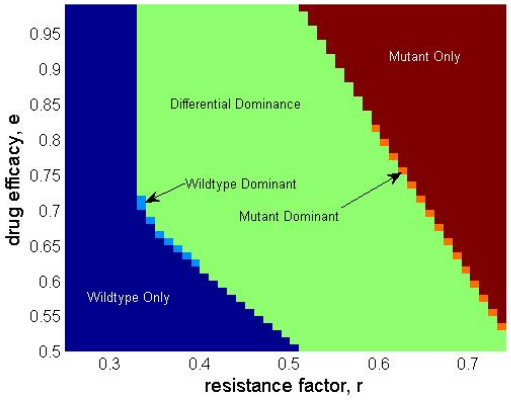

(a) $u = 0.5, a_2 = a_1$

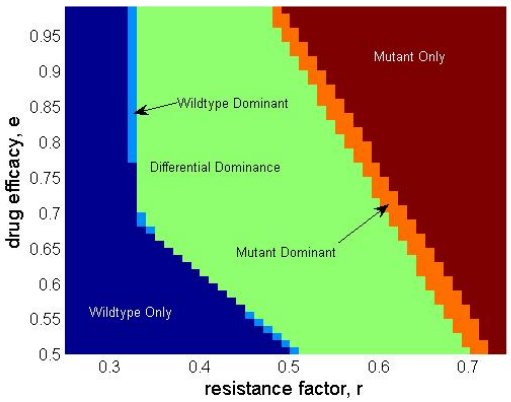

(b) $u = 0.05, a_2 = a_1$

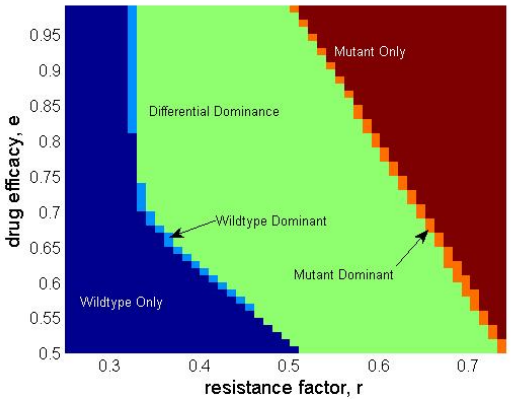

(c) $u = 0.05, a_2 = 0.5$

Figure 4-9: Graphs showing the steady state behaviour and dominance of strains when drug efficacy e, and resistance factor r are varied for different parameter sets: a)No cell heterogeneity and a drug sanctuary the same size as the blood compartment, b)No cell heterogeneity and a small drug sanctuary, c)Cell heterogeneity and a small drug sanctuary. Other parameter values as in Table 4.1 with $h = 0.5$.

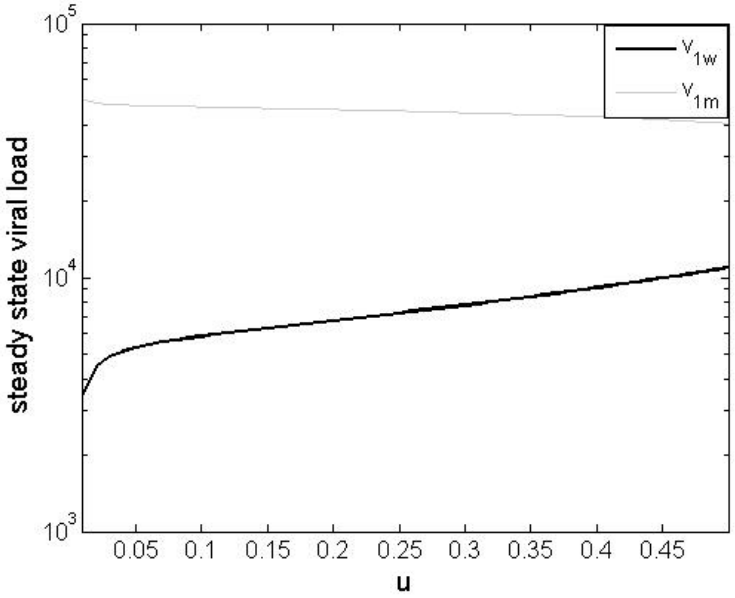

(a) compartment 1

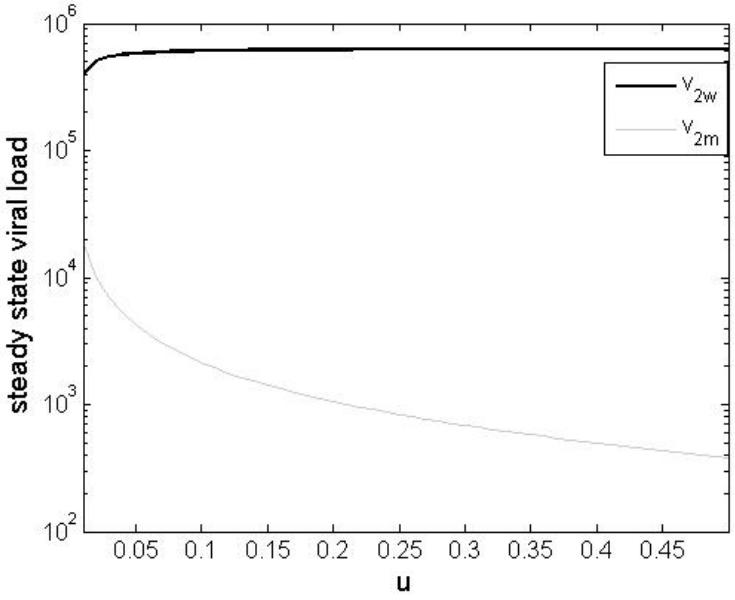

(b) compartment 2

Figure 4-10: Graphs show how the steady state viral load in the two compartments is affected by the relative size of the second compartment, u. $a_2 = a_1 = 1, h = 0.5, e = 0.75, r = 0.33$, other parameter values as in Table 4.1.

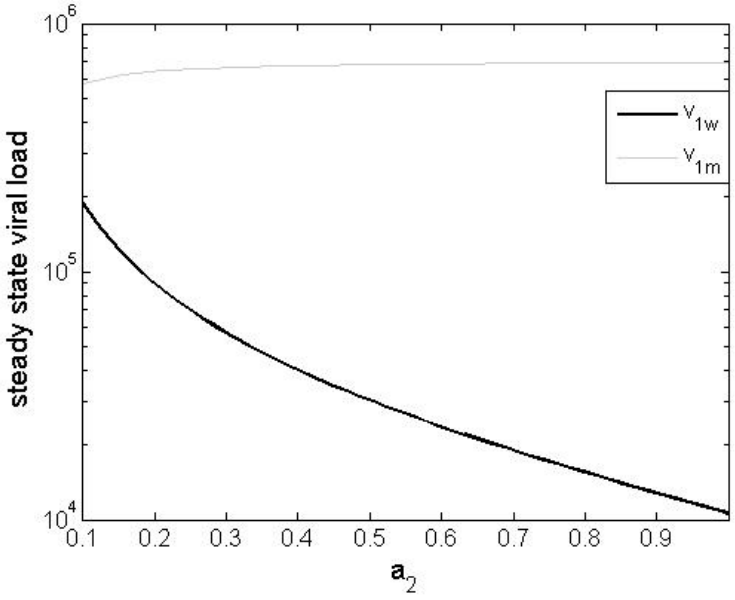

(a) compartment 1

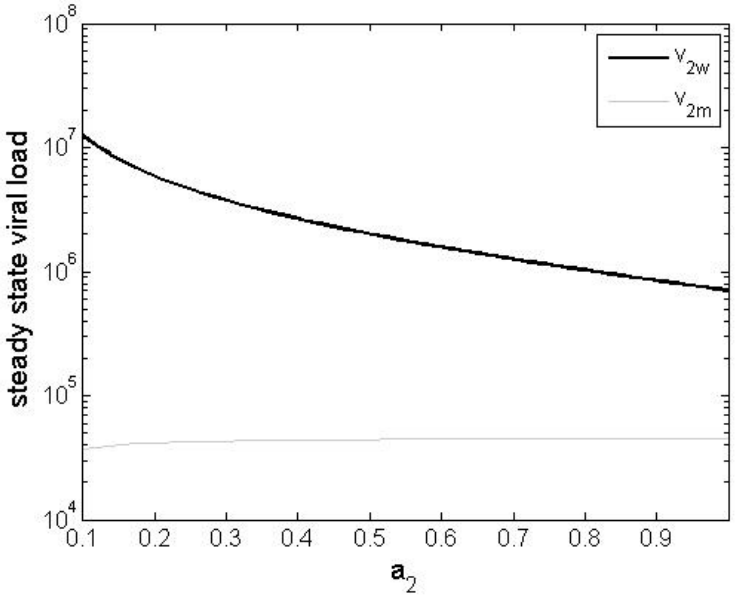

(b) compartment 2

Figure 4-11: Graphs showing how the steady state viral load in the two compartments is affected by the infected cell death rate in compartment 2, a_2. $u = 0.5, h = 0.5, e = 0.5, r = 0.7$, other parameter values as in Table 4.1.

being more prononounced (a_2 smaller than a_1) the larger the ranges of resistance factor r or drug efficacy e for which coexistence is seen.

The viral load of the minority strains in compartment 1 when coexistence occurs are larger than would be expected from a two strain evolutionary model, which are of the order of the mutation rate.

4.5 Conclusions

The two target cell two strain model is an extension of the model described in Callaway and Perelson [2002]. Although coexistence is possible in the model, the range of parameters for which it can be seen means that it is not likely to be biologically significant. However the presence of a drug sanctuary in this model allows the mutant strain to outcompete the wildtype strain even when the basic reproductive ratio is smaller than that of the wildtype. This is due to the mutant strain being able to invade the wildtype only steady state when $R_{0m}(S_1^w, S_2^w) > 1$. This is significant as it would mean that mutant strains will be seen *in vivo* at higher drug efficacies than their fitness derived from *in vitro* experiments would suggest as these use only one target cell type [Holland et al., 1991].

Inclusion of a drug sanctuary and cell heterogeneity in a two compartment model allows resistant and wildtype viral strains to coexist under certain circumstances (Figure 4-8). This novel result casts doubt on previous model assumptions [Kepler and Perelson, 1998] that the fitter drug resistant strain would competitively exclude the weaker, wildtype strain. However, it should be noted that this assumption would hold true for the very small sizes of compartment 2 and identical cell parameters used in the analysis by Kepler and Perelson [1998].

When coexistence occurs, differential dominance of strains in the two compartments can also be seen, meaning that different proportion of strains occurs in the blood and semen. This is also a new result which has implications for the transmission of drug resistant strains to other individuals. Given that only blood plasma viral strains are monitored on therapy, the clinician may not get a full picture of the population of viral strains likely to be transmitted. Interestingly the viral loads seen in compartment 1 (blood compartment) when coexistence occurs show the minority strain at a much higher concentration than in evolutionary models in one compartment such as the two strain model from Chapter 3. This suggests that the presence of a drug sanctuary could account for the higher prevalences of strains seen *in vivo*.

Further clinical study of blood and semen viral resistant strains could be carried out to check the validity of these mechanisms, of which the most pressing is to determine

the nature of target cells for HIV in the male genital tract.

This model could be extended to investigate the consequences of increased drug effectiveness in the male genital tract, for drugs such as zidovudine and lamuvidine [Cohen et al., 2007]. This could be accomplished by allowing $u > 0.5$ and relabelling the compartments so that the drug sanctuary compartment is the blood plasma compartment. Another extension could be to model the effects of triple drug therapies (where different drug types are used concurrently) on drug resistance patterns.

Chapter 5

Modelling Latently Infected Cells

5.1 Introduction

5.1.1 Chapter Outline

The previous chapter was concerned with modelling the effect of drug sanctuaries on drug resistance. In this chapter we turn our attention to a different biological phenomenon which produces an heterogeneous environment, latent infection of susceptible cells. This has been suggested as the cause of viral persistence on suppressive therapy [Chun et al., 1995, 1997a] and we shall present the relevant biological background here. The composition of the latently infected cell reservoir is also of interest. The wildtype viral strain can be found in the reservoir for years after commencement of therapy and drug resistant strains are typically only seen when treatment has been interrupted or there have been bouts of non-compliance resulting in high viral loads [Ruff et al., 2002].

The aim of this chapter is to explore the impact of latent cells on viral strain structure within the host. To this end we investigate the interaction between two viral strains and latently infected cells for different ways of modelling the activation and maintenance of the latently infected cell reservoir. As it is unclear what happens once cells are activated, in terms of cell replication, three scenerios are presented. The first is a model with constant activation and a constant death rate, i.e. no replication mechanism for latent cells. The second includes bystander proliferation. The final scenario describes asymmetric cell division upon activation whereby the daughter cells produced can be latently or actively infected cells. We also analyse the same mechanisms with the two target cell two strain model as the underlying system, to see whether a model with a more robust mechanism for obtaining low level viral load has an impact on our results. For each model steady states are found, the stability of these analysed where possible and numerical solutions determined for a range of interesting parameter sets.

We begin by reviewing recent work involving latent cells and HIV; we end by drawing biological conclusions from the model analysis.

5.1.2 Motivation and Background

One of the main reasons that HIV cannot be eradicated by antiretroviral therapy is the presence of a cellular reservoir consisting of infected memory CD4+ T cells [Chun et al., 1995, 1997a]. These cells have integrated HIV provirus but are not actively producing virions and are therefore called latently infected cells. The cells become activated through contact with antigens (particles or organisms foreign to the body) which they are specific for and start producing virus [Chun et al., 1997b, 1998]. A memory cell is created by proliferation of an active CD4+ T cell and its job is to allow the immune system to act quickly next time it encounters the same antigen. Only a few memory cells are produced when a T cell is activated and so the number of latently infected T cells is very small compared to that of actively infected T cells [Chun et al., 1995].

Once treatment is initiated three distinct viral decay phases are seen in patients [Ho et al., 1995, Perelson et al., 1995, Arnaout et al., 2000, Müller et al., 2002]. The first phase is proportional to the death rate of infected cells, whereas the second phase is proportional to the death rate of long-lived infected cells such as macrophages. The third phase of decay has been linked to the decline of the latent cell reservoir [Finzi and Siliciano, 1998]; this phase has a long half-life of 6-44 months [Zhang et al., 1999, Siliciano et al., 2003]. This reservoir may include infected cells which could generate infective virions in the future.

The latent cell reservoir may also play a role in the production of viral blips [Rong and Perelson, 2009a,b,c]. These are a phenomenon seen in patients on otherwise suppressive therapy [Di Mascio et al., 2003]. The viral load rises from below the threshold level for detection (50 copies per ml) for a short period of time, then falls again. A number of causes of viral blips have been suggested, including the activation of memory cells, either latently infected [Rong and Perelson, 2009a,b,c] or susceptible [Jones and Perelson, 2005, 2007], due to the presence of specific antigens. Both cases would result in an increase in the number of actively infected cells which would release more virus into the body.

In addition to the connection with viral blips the latent cell reservoir provides information on the viral strains that have circulated in an individual during infection [Ruff et al., 2002]. Ruff et al. [2002] examined the genetic characteristics of clones of HIV-1 from the latent cell reservoir. They showed that wild type virus was present in the latent reservoir despite many years on therapy and that resistance mutations seen

were generally those selected by non-suppressive therapy due to treatment interruptions and non-compliance. This suggests that the latent reservoir can act as an archive for strains of virus seen during infection.

In recent years there has been interest in using mathematical models to explain the impact of latent cells on the behaviour of viral loads on therapy [Müller et al., 2002, Kim and Perelson, 2006, Rong and Perelson, 2009a,b,c]. Of these, several mathematical models have been derived to offer explanations why the third stage of decay is so slow [Müller et al., 2002, Kim and Perelson, 2006]. Müller et al. [2002] found that the rate of decay was proportional to the latent cell death rate. The activation rate of latent cells was modelled as a distribution in order to take into account that antigens that are more common are likely to be encountered early on leaving latent cells specific for rarer antigens during the latter stages of infection. Their aim was to explain the deccelerating rate of viral decay seen in patients. Although the model assumed 100% effective treatment, it only considered reverse transcriptase inhibitors. Suppressive therapy usually consists of a protease inhibitor and two reverse transcriptase inhibitors. Completely effective protease inhibitors would mean that no new infectious virions would be produced from newly activated latently infected cells. This does not happen suggesting that treatment is less effective; this is borne out by evidence that circulating virions are capable of replication [Sahu et al., 2010] and that the third stage of decay of the virus is so slow.

Kim and Perelson [2006] concluded that when drug efficacy is greater than some critical efficacy the contribution of virus to the latent cell reservoir is insignificant, and that the latent cell reservoir can perservere in the long term if the activation rate is close in value to the net proliferation rate. Kim and Perelson [2006] modelled latent cell activation using a negative exponential term. This was to mimic the activation of latently infected cells specific to common antigens early in infection. They also allowed latent cells to undergo bystander proliferation whereby latent cells could replicate without being activated. The effect of reverse transcriptase inhibitors and protease inhibitors were reduced to a single parameter acting on the infection rate. The main results were that when drug efficacy is greater than the critical efficacy the contribution of virus to the latent cell reservoir is insignificant. If the minimum activation rate is zero and the drug is completely effective, viral and latent reservoir persistence could be obtained if the death rate of latent cells is slightly greater than the bystander proliferation rate. When the minimum activation rate is greater than zero and the drug is completely effective then both latent cells and virus can be maintained if the net proliferation rate is equal to the minimum activation rate. The results of this model when drug treatment is completely effective do not make sense biologically in that the infectious virus

population would decay quickly leaving only non-infectious virus.

Other models have been derived to investigate the role of latent cells in producing viral blips [Rong and Perelson, 2009a,b,c]. Rong and Perelson [2009b] analysed a latent cell model with activation modelled using a switch mechanism to imitate the patient encountering antigens. They also assumed that the latent cells divided upon activation and that the daughter cells could either be latent cells or actively infected cells with the proportion of each produced being modelled by a given parameter. This allowed the latent cell reservoir to be maintained and the switching mechanism for activation allowed viral blips to occur. The parameters affecting the switching mechanism and the proportion of new actively infected cells produced during activation could be altered to give varying half-lives of the latent cell population as seen in the literature. The authors used a density dependent death rate for infected cells to obtain low level viral loads on therapy. As discussed in a previous chapter this method of obtaining low level viral load can give unreasonable target cell levels depending on the degree of density dependence used. The value used in this paper was very high and gives unrealistically large numbers of target cells prior to therapy and very low numbers of infected cells throughout. The authors make no mention of this, however they assume the patient has reached the treatment steady state prior to using this model.

A second model using an alternative mechanism for latent cell reservoir maintenance, programmed expansion and contraction, has also been analysed by the same group [Rong and Perelson, 2009c]. An intermediate state upon activation between latent cells and activated cells was modelled from which cells can undergo proliferation, return to latency, die once the antigen is no longer present or become actively infected. This model also included the same switching mechanism and density dependent death rate of infected cells as Rong and Perelson [2009b]. Similar results were obtained also with viral blips created upon activation.

All of these models have different mechanisms for latent cell reservoir maintenance or persistence as the real one is unknown, but what seems clear is that the latent cell reservoir cannot be maintained simply by ongoing viral replication on therapy.

We now present models which include latent cells and multiple viral strains to consider the impact of latently infected cells on the viral strain structure within a host. We first consider a simple one target cell model to explore the links between strain variation, latent cell composition and time to strain switchover in the latent cell archive. We then consider the same latent cell mechanisms in the two target cell model which gives more realistic underlying HIV dynamics within the host.

5.2 Base Model with Latent Cells

We consider two strains of virus, wildtype and mutant, in the model in the same way as the two strain evolution model (3.3) from Chapter 3. We include latently infected cells in the model, produced when susceptible cells become infected. We analyse a general model whereby the latent cell dynamics are assumed to be given by generic parameters then carry out numerical experiments for each scenario: no proliferation, bystander proliferation and asymmetric cell division.

5.2.1 Model Equations

The concentration of latent cells is given by L_i where $i = w, m$ denotes the viral strain. The corresponding model equations are given as:

$$\begin{aligned}
\dot{S} =& \lambda - dS - \beta_w S v_w - \beta_m S v_m, \\
\dot{L}_i =& f((1-\epsilon)\beta_i S v_i + \epsilon \beta_{\hat{i}} S v_{\hat{i}}) - P L_i, \\
\dot{I}_i =& (1-f)((1-\epsilon)\beta_i S v_i + \epsilon \beta_{\hat{i}} S v_{\hat{i}}) + Q L_i - a I_i, \\
\dot{v}_i =& k I_i - c v_i,
\end{aligned} \tag{5.1}$$

where $i = w, m$ and $\hat{i}$ is the other one. A summary of the parameters is given in Table 5.1. A schematic of the model is shown in Figure 5-1. The proportion of new infections that become latent is given by f, the mutation rate is ϵ, the net loss of latent cells is given by P and the rate at which latent cells become actively infected is given by Q. The forms of the functions P and Q for each model scenario can be found in Table 5.2.

We wish to determine how the latent reservoir impacts on viral strain distribution within a host that is subject to a drug regime. To achieve this, we analyse a cascade of models derived from the full model (5.1), defined in terms of the functions P and Q as follows:

- Model 0: No latent cells. The null neutral model case, derived from (5.1) simply by setting to zero the proportion, f, of infected cells becoming latently infected. This is a two strain evolution model which we analysed in Chapter 3. The main results from this model were that the strain with the largest R_{0i} value was dominant, provided that $R_{0i} > 1$, and the losing strain is present at $O(\epsilon)$.

- Model 1: No latent cell proliferation; constant latent cell activation rate. In this case $P = \alpha + d_l$ where α is the constant per capita activation rate and d_l is the per capita death rate of latent cells. The corresponding per capita rate at which latent cells become active, $Q = \alpha$.

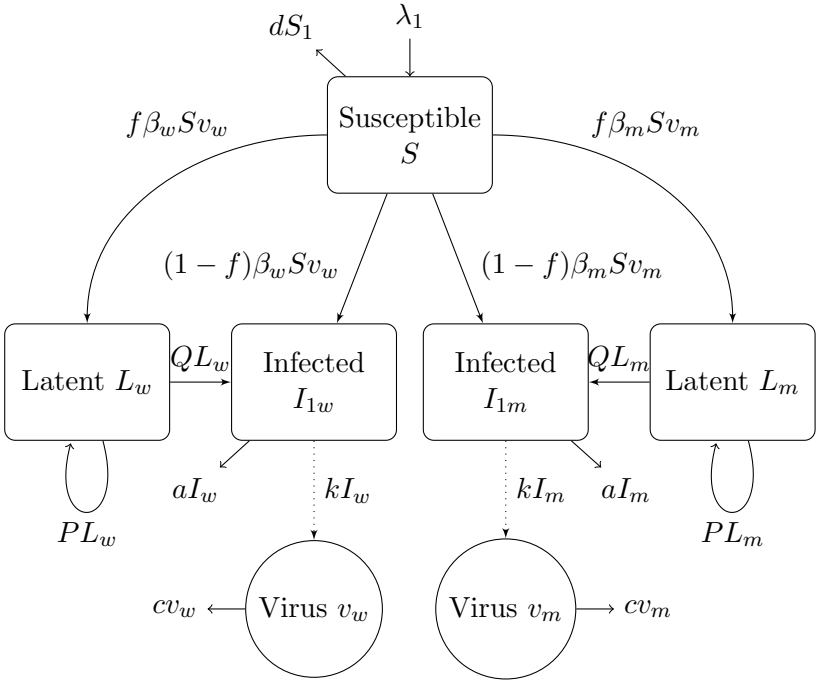

Figure 5-1: Schematic of the Basic Latent Cell model (5.1).

Parameter Description	**Value**
λ, Birth rate of new cells	10^4 cells ml^{-1} day^{-1}
β_w, Infection rate	2.4×10^{-8} virion^{-1} day^{-1}
β_m, Infection rate	$0.33 \times \beta_w$ virion^{-1} day^{-1}
ϵ, Proportion mutating	0.0005
d, Death rate of target cells	0.01 day^{-1}
a, Death rate of infected cells	1 day^{-1}
d_l, Death rate of latently infected cells	0.004 day^{-1}
c, Death rate of virions	23 day^{-1}
k, Production rate of virions	3000 virions cell^{-1} day^{-1}
e, Drug efficacy	0.8
r, Resistance factor	0.33
α, Activation rate	0.01 day^{-1}
f, Proportion becoming latent cells	0.0001
p, Proliferation rate of latent cells	0.012 day^{-1}
p_l, Probability that a daughter cell will be latent	0.48

Table 5.1: Base model with Latent cells parameter descriptions and values.

	Model 1	**Model 2**	**Model 3**
P	$\alpha + d_l$	$\alpha + d_l - p$	$\alpha(1-2p_l) + d_l$
Q	α	α	$2\alpha(1-p_l)$

Table 5.2: Table showing definitions of P and Q for different models. See model sections for more information.

- Model 2: Bystander proliferation; ongoing proliferation of latent cells. Here $P = \alpha + d_l - p$ where p is the per capita proliferation rate. The rate at which latent cells become actively infected remains the same as Model 1.
- Model 3: Asymmetric latent cell division; activation linked to cell division. This model includes a different process of cell proliferation based on the model of Rong and Perelson [2009b]. Proliferation is linked to activation resulting in $P = \alpha(1-2p_l)$ and $Q = 2\alpha(1-p_l)$, where p_l is the probability that a daughter cell is latently infected.

A steady state analysis is performed on the general model and numerical solutions are presented for each case.

5.2.2 Steady State Analysis

If $f \neq 0$ and $\epsilon = 0$, a competition model with 2 strains of virus and latently infected cells is obtained. There are three possible steady states of the general model, the disease free steady state and two endemic steady states.

1. The disease free steady state has all variables zero except $S = \lambda/d$.
2. There are two endemic steady states, one for each strain of virus w and m, which are

$$\begin{aligned} S =& \frac{Pac}{((1-f)P+Q)k\beta_i}, \\ v_i =& \frac{d}{\beta_i}(R_{0i}-1), \\ I_i =& \frac{c}{k}v_i, \\ L_i =& \frac{acf}{k((1-f)P+Q)}v_i, \end{aligned} \tag{5.2}$$

for $i = w, m$, where

$$R_{0i} = \frac{\lambda\beta_i k}{acd}\left((1-f) - \frac{fQ}{P}\right).$$

An important point to note is that the latent cell steady state is proportional to the viral load steady state.

The Jacobian matrix for this system is

$$\begin{pmatrix} -d-\beta_w v_w-\beta_m v_m & 0 & 0 & 0 & 0 & -\beta_w S & -\beta_m S \\ f\beta_w v_w & -P & 0 & 0 & 0 & f\beta_w S & 0 \\ f\beta_m v_m & 0 & -P & 0 & 0 & 0 & f\beta_w S \\ (1-f)\beta_w v_w & Q & 0 & -a & 0 & (1-f)\beta_w S & 0 \\ (1-f)\beta_m v_m & 0 & Q & 0 & -a & 0 & (1-f)\beta_m S \\ 0 & 0 & 0 & k & 0 & -c & 0 \\ 0 & 0 & 0 & 0 & k & 0 & -c \end{pmatrix}.$$

1. The characteristic polynomial in Λ for the disease free steady state can be factorised to give

$$\begin{aligned} &\Lambda + d = 0, \\ &\Lambda^3 + x_2\Lambda^2 + x_1\Lambda + x_0, \\ &\text{where} \\ &x_2 = a + d + P, \\ &x_1 = (a+c)P + ac - \frac{(1-f)\lambda\beta_w k}{d}, \\ &x_0 = acP - \frac{\lambda\beta_w k((1-f)P + fQ)}{d}, \\ &\text{and} \\ &\Lambda^3 + y_2\Lambda^2 + y_1\Lambda + y_0, \\ &\text{where} \\ &y_2 = a + d + P, \\ &y_1 = (a+c)P + ac - \frac{(1-f)\lambda\beta_m k}{d}, \\ &y_0 = acP - \frac{\lambda\beta_m k((1-f)P + fQ)}{d}. \end{aligned}$$

   The coefficients of each of the polynomials are positive, and the disease free steady state stable, if and only if $\max(R_{0w}, R_{0m}) < 1$.

2. The characteristic polynomial in Λ for each endemic steady state can be gener-

alised and factorised to give

$$\Lambda^4 + x_3\Lambda^3 + x_2\Lambda^2 + x_1\Lambda + x_0 = 0,$$

where

$$x_3 = P + a + c + R_{0i},$$

$$x_2 = R_{0i}(P + a + c) + P\left(a + c - \frac{(1-f)ac}{(1-f)P + fQ}\right) + a(a+c),$$

$$x_1 = R_{0i}(d(a+c)P + ac) - acP\frac{(1-f)d}{(1-f)P + fQ},$$

$$x_0 = acdP(R_{0i} - 1),$$

and

$$\Lambda^3 + y_2\Lambda^2 + y_1\Lambda + y_0 = 0$$

where

$$y_2 = P + a + c,$$

$$y_1 = (a+c)P + ac\left(1 - \frac{\beta_{\hat{i}}(1-f)P}{\beta_i((1-f)P + fQ)}\right),$$

$$y_0 = acP\left(1 - \frac{\beta_{\hat{i}}}{\beta_i}\right).$$

for $i = w, m$, where $\hat{i}$ is the other strain. The disease steady state i is stable if $R_{0i} > 1$ and $\beta_i > \beta_{\hat{i}}$. This model shows competitive exclusion.

If $f \neq 0$ and $\epsilon \neq 0$ the resulting model is a 2 strain mutation model with latently infected cells. As with the two strain evolution and competition models studied previously (Chapter 3) we expect that the endemic steady states will be perturbations of those found in the competition model ($\epsilon = 0$). The disease free steady state is again $S = \lambda/d$ and all other variables equal to zero. Again there are two endemic steady states, however both strains of virus are present in both steady states. The endemic steady state expressions can be found using perturbation analysis around the small

parameter ϵ. The steady state expressions to the order of ϵ are

$$\begin{aligned} S =& \frac{Pac}{((1-f)P+fQ)k\beta_i}(1+\epsilon), \\ v_i =& \frac{d}{\beta_i}(R_{0i}-1)\left(1+\epsilon\frac{\beta_i}{\beta_{\hat{i}}^2}(\beta_{\hat{i}}-\beta_i)\right)-\epsilon\frac{d}{\beta_i}, \\ v_{\hat{i}} =& \epsilon\left(\frac{d}{\beta_{\hat{i}}}(R_{0i}-1)-\frac{\beta_i}{\beta_{\hat{i}}}\right), \\ I_i =& \frac{c}{k}v_i, \\ L_i =& \frac{acf}{k((1-f)P+fQ)}v_i, \end{aligned} \tag{5.3}$$

for $i = w, m$. Note that as $v_{\hat{i}}$ is $O(\epsilon)$ both $I_{\hat{i}}$ and $L_{\hat{i}}$ are $O(\epsilon)$. These steady state expressions have the same R_{0i} expressions as the competition model. The real R_{0i} for this system is a perturbation by a factor of $1-\epsilon$ to $O(\epsilon)$.

5.2.3 Numerical Solutions

For all three models to be discussed we have modelled drug treatment and drug resistance as in previous chapters. Numerical solutions of the model were carried out using the parameter values given in Table 5.1.

The composition of the latent cell reservoir, i.e. which viral strain the latently infected cells have integrated into their genetic code, is affected by the viral population in the blood plasma. From the steady state expressions (5.3) it can be seen that the latent cell reservoir will be made up predominantly of cells infected with the dominant strain of virus. Therefore if any archiving of viral strains occurs it must be transient and the length of time the archive is present for will be determined by parameters in the model that affect both viral and latent cell dynamics. We measure archive length as the time between the dominance swapping over in the free virus and the latent cell reservoir (from wildtype to resistant strain dominant).

We chose values of drug efficacy, e, and the resistance factor, r, to give $R_{0m} > R_{0w}$ on treatment with R_{0m} greater than but close to 1 to obtain low level viral loads at steady state.

Model 1: No Proliferation

Figure 5-2 shows that there is a delay between the switchover of strains in the viral and latent cell reservoirs once treatment is commenced; there is a short-lived archive in the latent cell population. In this simple model with no proliferation there are only three

latent cell parameters: the rate at which latent cells are created through infection, f, the activation rate, α and the death rate, d_l. Figure 5-3 shows the effect that each parameter has on the length of time the archive is present once treatment commences and the resistant strain steady state becomes stable. Increasing the activation rate, α, decreases the time to switchover. This makes intuitive sense; activation results in a cell being lost from the latent cell reservoir to become an actively infected cell. Also the difference between an order of magnitude of α changes the switchover time from around 300 days ($\alpha = 0.01$) to less than 100 days ($\alpha = 0.1$). In contrast, the death rate of latent cells, d_l has a much smaller effect: from around 255 days ($d_l = 0.001$) to 215 days ($d_l = 0.01$). The largest value for the death rate in Figure 5-3b, $d_l = 0.01$, is the same as the death rate of susceptible cells. This would not be a sensible value for the death rate of latently infected cells as they are memory cells and should therefore have a longer lifespan than actively infected cells. An increase in the death rate of latently infected cells decreases the amount of time an archive is present for as does increasing the proportion of cells that become latently infected, f as shown in Figure 5-3c. Increasing f means that the ongoing viral replication has a bigger effect on latent cell dynamics, with the resistant strain taking less time to infiltrate the latent cell reservoir.

The activation rate α has the largest impact on the time to the loss of the archive out of the three latent cell parameters in this simple model. However a very small value of α would be needed to obtain an archive length in the region of years as has been shown *in vivo* [Ruff et al., 2002]. Thus we explore the potential of a maintenance mechanism to lengthen the time that the archive is present for.

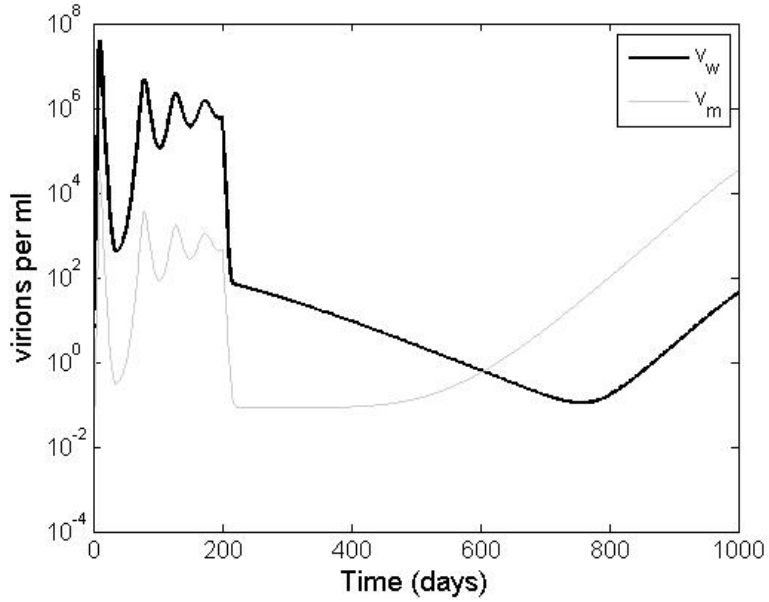

(a)

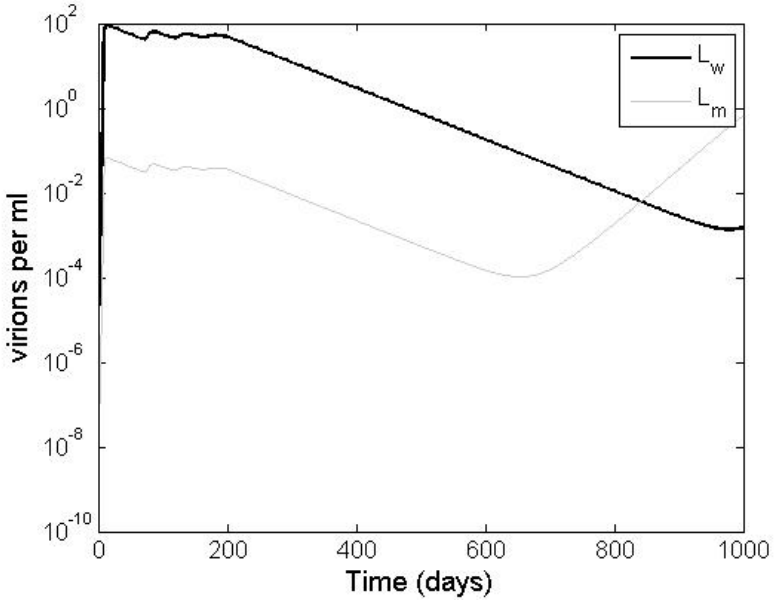

(b)

Figure 5-2: Model 1: Graphs showing a numerical solution where the mutant strain is dominant after treatment is initiated at 200 days; a) viral load, b) latent cell reservoir. Parameter values are as in Table 5.1.

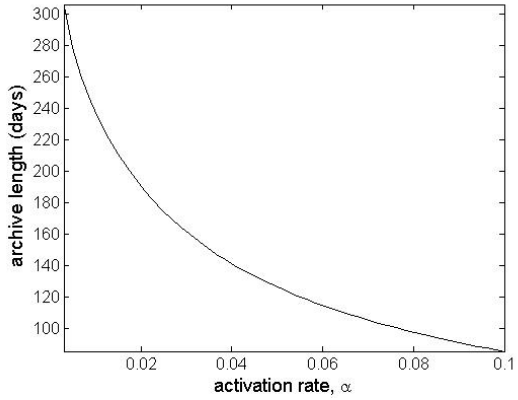

(a)

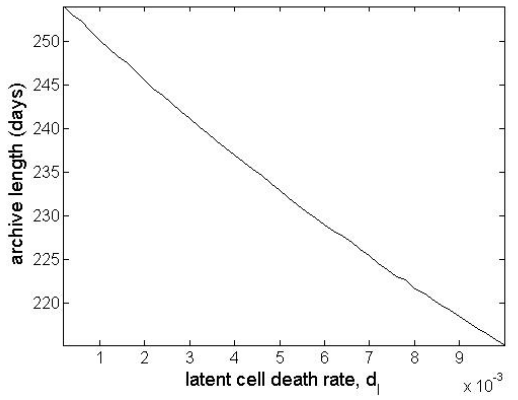

(b)

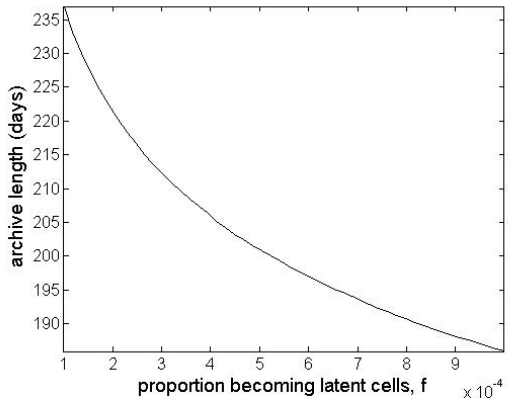

(c)

Figure 5-3: Model 1: Graphs showing how latent cell parameters affect the archive time: a) Varying the activation rate α, b) Varying the latent cell death rate d_l, c) Varying the proportion of cells that become latent, f. Parameter values used can be found in Table 5.1.

Model 2: Bystander Proliferation

We now consider a simple replication mechanism for latent cells, known as bystander proliferation, based on the one strain model by Kim and Perelson [2006]. This means that no outside stimuli such as the binding of antigens, are needed in order for proliferation to occur. We replace d_l with $d_l - p$. As we now have a negative part to the function P we must ensure that the proliferation rate $p < \alpha + d_l$ so that $P > 0$. This is so that the steady state expressions remain valid. If $P < 0$ then the ordinary differential equations for latent cells are entirely positive and only the disease free steady state is possible.

Numerical solutions of this model show that longer archive times are possible as shown in Figure 5-4. In Figure 5-4a the proliferation rate, $p = 0.012$ so that all the values of α allow endemic steady states to occur. As with Model 1, an increase in α corresponds to a decrease in archive duration. However in this case, for small values of α we have very long archive times of around 1000 days. This is because of the bystander proliferation of latent cells. In Figure 5-4b we see that as the proliferation rate increases up to $p = 0.012$ ($\alpha = 0.01$) the archive time also increases. There is a vertical asymptote at $p = 0.014$ due to the condition on P as mentioned above.

Also of note is that the archive time is affected by the fitness of the mutant strain as seen in Figure 5-5. As the resistance factor r increases, reflecting a rise in fitness, the archive time decreases. This is because there is more ongoing viral replication which then dominates the latent cell dynamics.

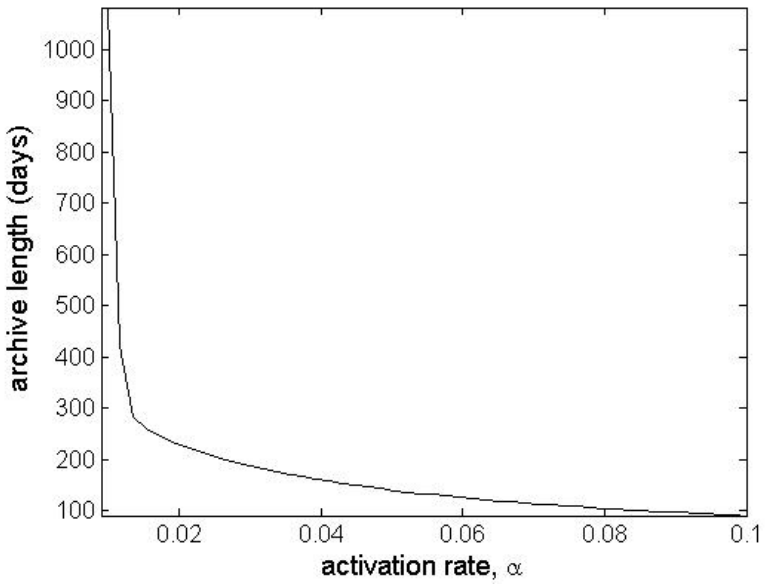

(a)

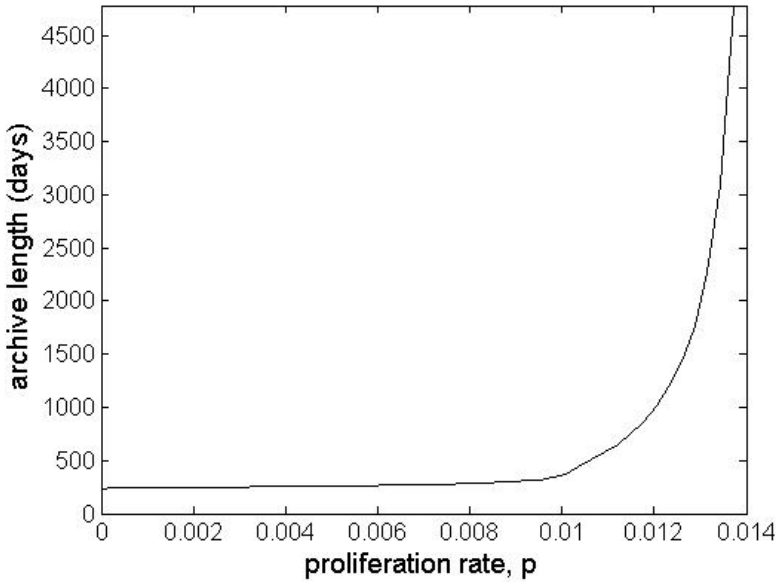

(b)

Figure 5-4: Model 2: Graphs showing how latent cell parameters affect the archive time: a) Varying the activation rate α, b) Varying the latent cell proliferation rate p. Parameter values used can be found in Table 5.1.

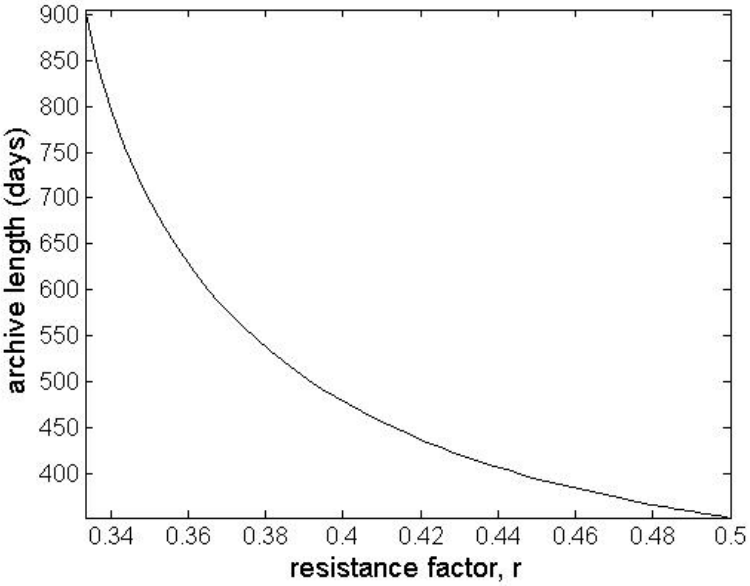

Figure 5-5: Model 2: Graph showing how the resistance factor r affects the archive time. Parameter values used can be found in Table 5.1.

Model 3: Asymmetric cell division upon activation

The final scenario that we will analyse is based on the one strain asymmetric cell division model proposed by Rong and Perelson [2009b] which assumes that upon activation by an antigen the latent cells divide to produce two daughter cells. We assume that the parent cell is lost when the daughter cells are created. The forms of P and Q can be derived as follows: if we take the probability of a daughter cell being latently infected to be p_l then the expected number of new latent cells upon activation is

$$\left(2 \times p_l^2 + 1 \times 2p_l(1-p_l) - 1\right) L_i = (2p_l - 1)L_i$$

and the expected number of active cells is

$$\left(2 \times (1-p_l)^2 + 1 \times 2p_l(1-p_l)\right) L_i = 2(1-p_l)L_i.$$

As these events only happen when the cells encounter antigen the expressions are multipied by a factor of α, therefore $P = \alpha(1-2p_l) + d_l$ and $Q = 2\alpha(1-p_l)$.

The model by Rong and Perelson [2009b] included a switching mechanism to imitate latent cells encountering antigen. This was to enable viral blips to be created upon activation of the latent cells. Figure 5-6 shows how using an average value for α compares with a switching version of the model; using an average value for α gives the mean solution of the switching version of the model. As we are not interested in modelling viral blips we will use an average value for α in our numerical solutions.

In Figure 5-7 we can see that the asymmetric division mechanism allows archiving of viral strains in the latent cell reservoir.

Figure 5-8 shows how the different model parameters affect the archive time. In Figure 5-8a we see that the value of p_l, the probability that a daughter cell will be latent, has different effects on the time to the loss of the archive: when $p_l < 0.5$, the value of P increases as the activation rate, α is increased, resulting in decreasing time to strain switchover in a similar manner to models 1 and 2. However, when $p_l > 0.5$, the value of P decreases as α is increased and the archive time increases once a threshold value of α is reached. It is unclear why there is this threshold behaviour.

As we saw previously in model 2, increasing the resistance factor, r, decreases the archive time as in Figure 5-8b. The longer archive times are very dependent on the value of the resistance factor. This is due to the nature of the dependence of the magnitude of viral load on r. The decrease in the archive time is not monotonic with increasing r. Again the reason for this is unclear.

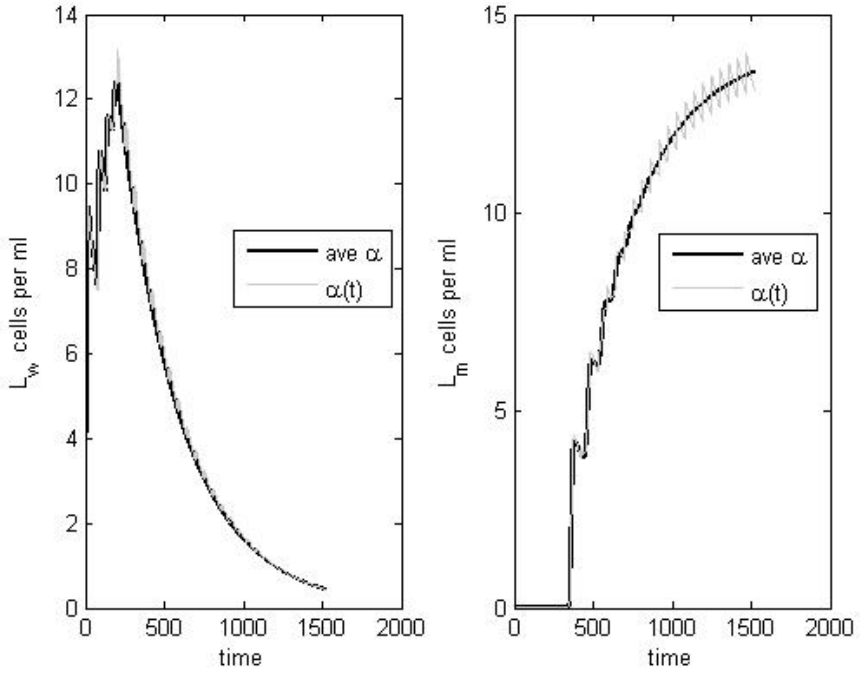

Figure 5-6: Model 3: Graph comparing the model with activation switching on and off (on for 5 days, off for 50 days) and the model with an average value for $\alpha = 1/11 \times 0.1$. Drug treatment commenced at 200 days. See Table 5.1 for other parameter values.

5.2.4 Summary

The latent cell model without a maintenance mechanism cannot support a long term archive of wildtype virus in the latent cell reservoir.

The bystander proliferation model is the simplest mechanism for latent cell proliferation and does allow longer term archiving of wildtype virus. The fitness of the mutant strain has a big effect on the length of time the archive is present for, with larger values of the resistance factor, r, decreasing the archive time.

The asymmetric cell division model also allows archiving of viral strains in latently infected cells. Interestingly, the behaviour of the model with regards to the activation rate depends on whether a daughter cell is more likely to be latently or actively infected, with a larger proportion of daughter latent cells upon division causing an increase in the archive time for higher activation rates.

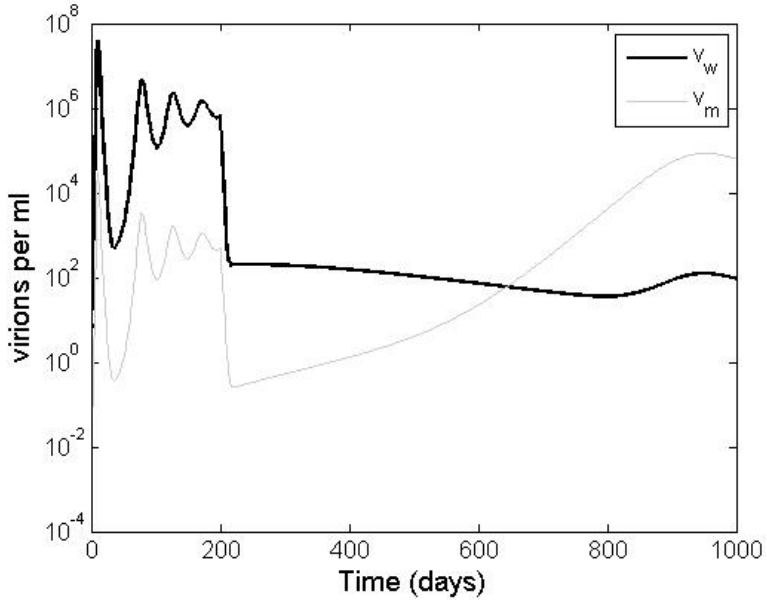

(a)

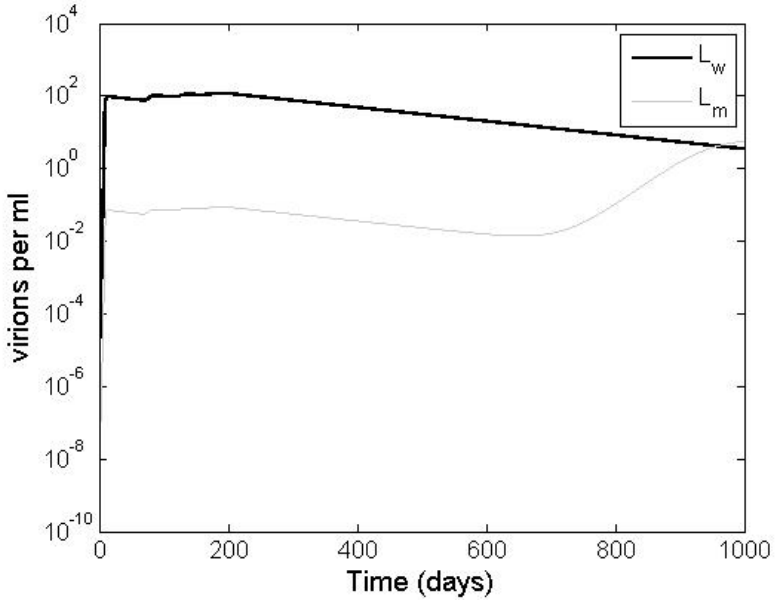

(b)

Figure 5-7: Model 3: Graphs showing a numerical solution where the mutant strain is dominant after treatment is initiated at 200 days; a) viral load, b) latent cell reservoir. Parameter values are as in Table 5.1.

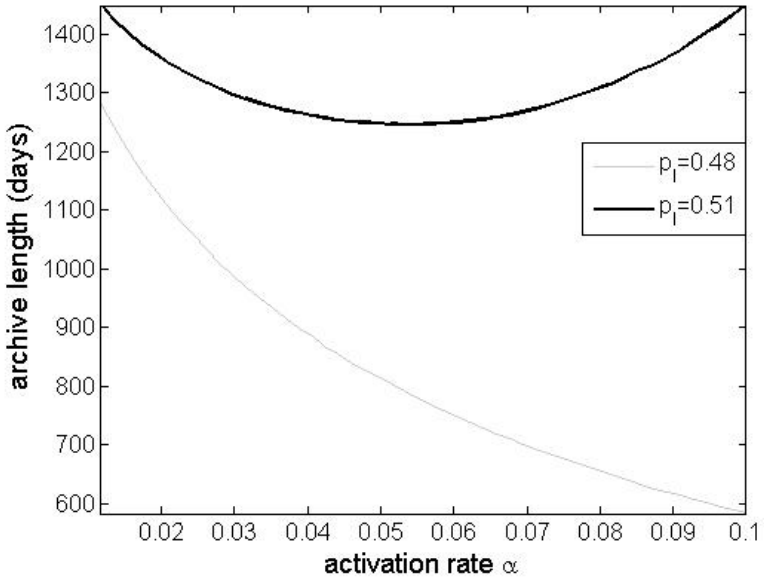

(a)

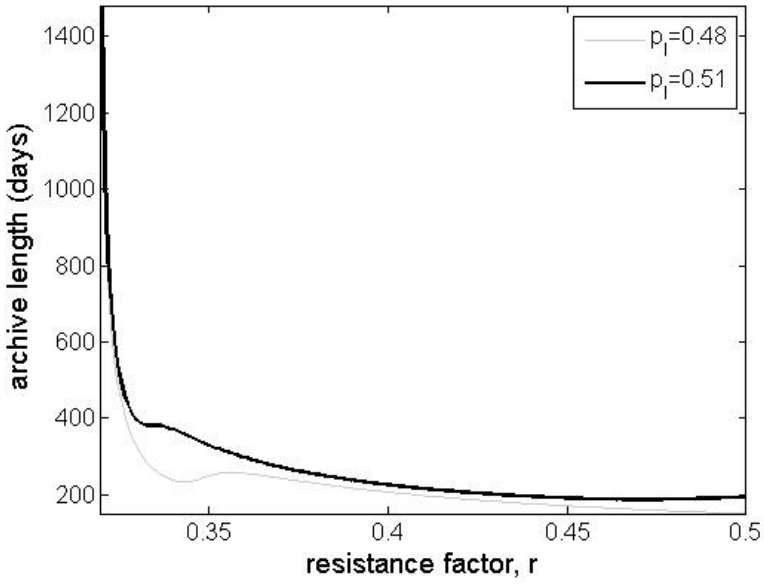

(b)

Figure 5-8: Model 3: Graphs showing how the archive time is affected by various model parameters: a) activation rate, α ($r = 0.32$) and b) resistance factor ($\alpha = 0.01$). Other parameter values are as given in Table 5.1.

5.3 Two target cell model with latent cells

5.3.1 Model Equations

Rong and Perelson [2009b] used a one strain model with a density dependent death rate for infected cells (which was discussed in Chapter 2) as their underlying model when incorporating asymmetric division. The qualitative behaviour of a density dependent death rate model depends on the degree of density dependence. The values used by Rong and Perelson [2009b] give unreasonable solutions before treatment is started. However, the initial conditions used were after therapy had been initiated. It would be better to use a more robust model to obtain low level viral load on therapy. We therefore adapt the two target cell model for each of the different latent cell scenarios to see how this affects our results.

We have extended the two target cell two strain model, analysed in Chapter 4, to include latent cells. The primary target cells are assumed to be the ones most commonly associated with HIV, CD4+ T cells. The secondary target cells are assumed to be macrophages which are found at lower concentrations in the blood compared with CD4+ T cells [Stevenson and Gendelman, 1994] and which do not require activation to become infected [Wodarz et al., 1999] thereby having a higher infection rate. There is evidence that macrophages can be latently infected [Embretson et al., 1993, Stevenson and Gendelman, 1994]. However we assume that only the primary CD4+ cells can be latently infected to make the model more tractable; our results therefore provide baseline behaviours which are likely to be enhanced by the inclusion of latently infected macrophages. The equations given here include drug treatment in order to show the presence of a drug sanctuary. A schematic for the model without mutation can be seen in Figure 5-9.

$$
\begin{aligned}
\dot{S}_1 =& \lambda_1 - dS_1 - S_1((1-e)\beta_1 v_w + r\beta_1 v_m),\\
\dot{S}_2 =& \lambda_2 - dS_2 - S_2((1-eh)\beta_2 v_w + r\beta_2 v_m),\\
\dot{L}_w =& fS_1((1-\epsilon)(1-e)\beta_1 v_w + \epsilon r\beta_1 v_m) - PL_w,\\
\dot{L}_m =& fS_1(\epsilon(1-e)\beta_1 v_w + (1-\epsilon)r\beta_1 v_m) - PL_m,\\
\dot{I}_{1w} =& (1-f)S_1((1-\epsilon)(1-e)\beta_1 v_w + \epsilon r\beta_1 v_m) + QL_w - aI_{1w},\\
\dot{I}_{1m} =& (1-f)S_1(\epsilon(1-e)\beta_1 v_w + (1-\epsilon)r\beta_1 v_m) + QL_m - aI_{1m},\\
\dot{I}_{2w} =& S_2((1-\epsilon)(1-eh)\beta_2 v_w + \epsilon r\beta_2 v_m) - aI_{2w},\\
\dot{I}_{2m} =& S_2(\epsilon(1-eh)\beta_2 v_w + (1-\epsilon)r\beta_2 v_m) - aI_{2m},\\
\dot{v}_w =& k(I_{1w} + I_{2w}) - cv_w,\\
\dot{v}_m =& k(I_{1m} + I_{2m}) - cv_m,
\end{aligned}
\tag{5.4}
$$

Parameter Description	**Value**
λ_1, Birth rate of primary target cells	10^4 cells ml^{-1} day^{-1}
λ_2, Birth rate of secondary target cells	1.533 cells ml^{-1} day^{-1}
β_1, Infection rate	2.4×10^{-8} virion^{-1} day^{-1}
β_2, Infection rate	10^{-4} virion^{-1} day^{-1}
r, Resistance factor	0.21
ϵ, Proportion mutating	0.0005
d, Death rate of target cells	0.01 day^{-1}
a, Death rate of infected cells	1 day^{-1}
d_l, Death rate of latently infected cells	0.004 day^{-1}
c, Death rate of virions	23 day^{-1}
k, Production rate of virions	3000 virions cell^{-1} day^{-1}
α, Activation rate	0.05 day^{-1}
f, Proportion becoming latent cells	0.00001
e, Drug efficacy	0.9
h, Drug penetrance	0.7
p, Proliferation rate	0.05 day^{-1}
p_l, Probability of a latent daughter cell	$0.48 - 0.51$

Table 5.3: Table showing parameter values used in numerical solutions.

where $0 < r < 1$ describing the cost of resistance to the drug and the expressions P and Q are as defined in Table 5.2. The other parameters are as described in previous models, a summary is given in Table 5.3. As with the base model with latent cells (5.1), we analyse three different scenarios: no latent cell proliferation, bystander proliferation and asymmetric cell division upon activation. For analysis of the model without latent cells ($f = 0$), see Chapter 4 and for the one strain two target cell model see Chapter 3. The steady state analysis is carried out on the general model and numerical solutions are obtained for each scenario.

5.3.2 Steady state analysis

From the differential equations for latently infected cells (5.4), it is clear that if $f > 0$ and P is negative there are no endemic steady states. This is because the left hand side of the differential equation would be positive meaning that the concentration of latent cells will always grow. The analysis below assumes that if $f > 0$ then $P > 0$.

It is not possible to obtain explicit expressions for steady states when $\epsilon > 0$. However we can find series solutions of the form $T = \sum_{i=0}^{\infty} \epsilon^i T_i$, where $T = S, I, v$ is a given state variable. Below we give the O(1) solutions which are equivalent to finding the steady states of the corresponding competition model ($\epsilon = 0$). Setting $\epsilon = 0$ and the left hand sides of the system of ordinary differential equations (5.4) to zero we obtain

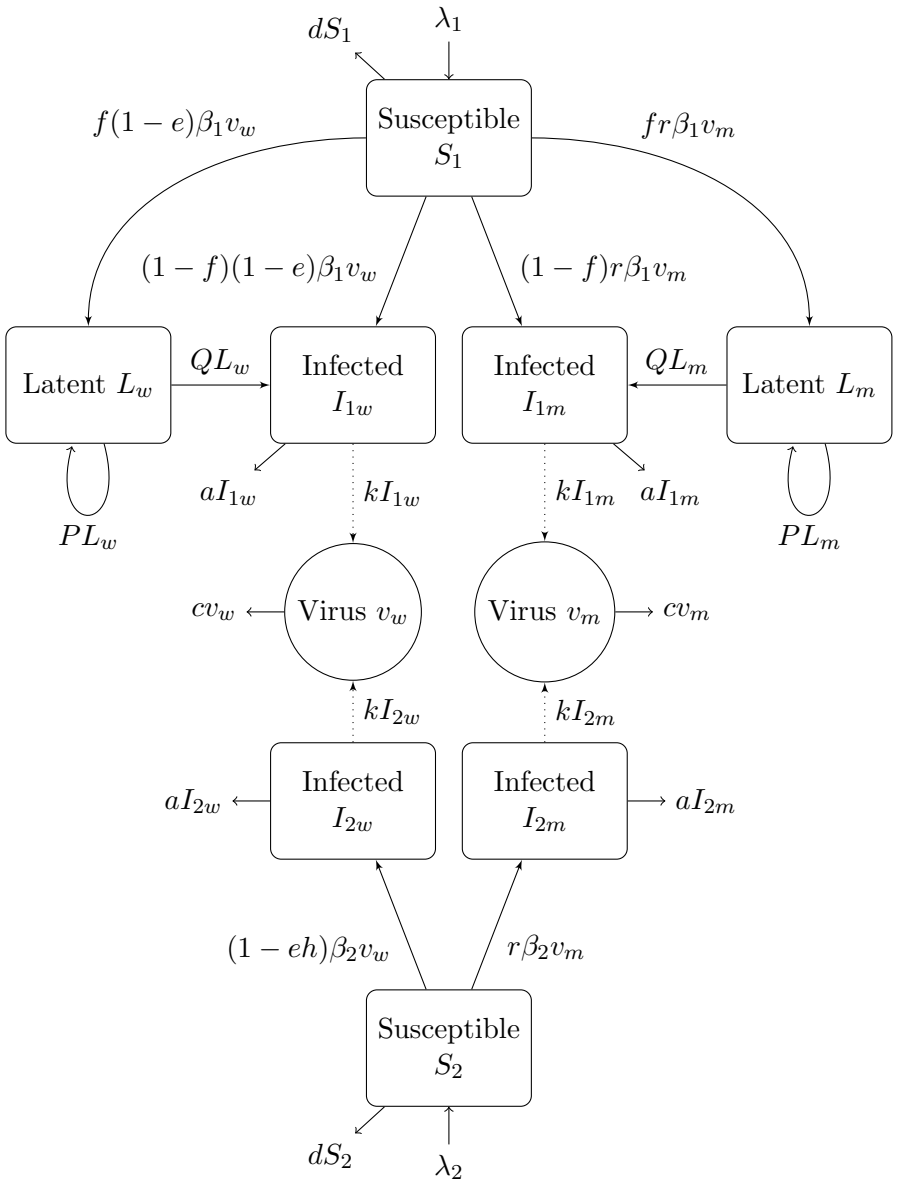

Figure 5-9: Schematic of two target cell two strain model with latent cells. See text and Table 5.3 for futher details of parameters and variables.

the following four steady states: disease free, dominant wild type, dominant resistant and 'coexistence'. The steady state and R_{0i} expressions for each model can be obtained by substituting in the relevant forms for P and Q.

1. The disease free steady state is $S_1 = \lambda_1/d, S_2 = \lambda_2/d$ with all other state variables equal to zero.

2. The dominant wild type steady state depends on the roots of the quadratic:

$$\begin{aligned} &v_w^2 + x_1 v_w + x_0 = 0, \\ &x_1 = \frac{d}{(1-e)\beta_1}(1 - R_{01w}) + \frac{d}{(1-eh)\beta_2}(1 - R_{02w}), \\ &x_0 = \frac{d^2}{(1-e)\beta_1(1-eh)\beta_2}(1 - R_{0w}), \end{aligned} \tag{5.5}$$

   where the basic reproductive ratios are $R_{01w} = \frac{\lambda_1(1-e)\beta_1 k}{acd}\left(1 - f + \frac{fQ}{P}\right)$, $R_{02w} = \frac{\lambda_2(1-eh)\beta_2 k}{acd}$ and $R_{0w} = R_{01w} + R_{02w}$. The other variables are

$$\begin{aligned} S_1 =& \frac{\lambda_1}{d + (1-e)\beta_1 v_w} \\ L_w =& \frac{f S_1 (1-e)\beta_1 v_w}{P}, \\ I_{1w} =& \frac{(1-e)\beta_1 S_1 v_w}{a}(1 - f + \frac{fQ}{P}), \\ S_2 =& \frac{\lambda_2}{d + (1-eh)\beta_2 v_w}, \\ I_{2w} =& \frac{(1-eh)\beta_2 S_2 v_w}{a}, \\ v_m =& L_m = I_{1m} = I_{2m} = 0. \end{aligned} \tag{5.6}$$

   All variables also have $\mathrm{O}(\epsilon)$ terms and are therefore non-zero. When $R_{0w} > 1$ the quadratic in v_w, (5.5), has one positive real root and the steady state is therefore biologically realistic.

3. The dominant mutant steady state depends on the roots of the quadratic:

$$\begin{aligned} &v_m^2 + y_1 v_m + y_0 = 0, \\ &y_1 = \frac{d}{r\beta_1}(1 - R_{01m}) + \frac{d}{r\beta_2}(1 - R_{02m}), \\ &y_0 = \frac{d^2}{r^2\beta_1\beta_2}(1 - R_{0m}), \end{aligned} \tag{5.7}$$

where $R_{01m} = \frac{\lambda_1 r\beta_1 k}{acd}\left(1 - f + \frac{fQ}{P}\right)$, $R_{02m} = \frac{\lambda_2 r\beta_2 k}{acd}$ and $R_{0m} = R_{01m} + R_{02m}$. The other variables are

$$\begin{aligned} S_1 =& \frac{\lambda_1}{d + r\beta_1 v_m} \\ L_m =& \frac{fS_1 r\beta_1 v_m}{P}, \\ I_{1m} =& \frac{r\beta_1 S_1 v_m}{a}(1 - f + \frac{fQ}{P}), \\ S_2 =& \frac{\lambda_2}{d + r\beta_2 v_m}, \\ I_{2m} =& \frac{r\beta_2 S_2 v_m}{a}, \\ v_w =& L_w = I_{1w} = I_{2w} = 0. \end{aligned} \tag{5.8}$$

Again all variables have O(ϵ) terms and are non-zero. When $R_{0m} > 1$ the quadratic in v_m, (5.7), has one positive real root and the steady state is therefore biologically realistic.

4. The coexistence steady state is given by:

$$\begin{aligned} S_1 =& \frac{Pac\beta_2((1 - eh) - r)}{((1 - f)P + fQ)kr\beta_1\beta_2((1 - eh) - (1 - e))}, \\ S_2 =& \frac{ac\beta_1(r - (1 - e))}{k\beta_1\beta_2((1 - eh) - (1 - e))}, \\ v_w =& \frac{r\left(\beta_1 S_1\left(\lambda_2 - dS_2\right) - \beta_2 S_2\left(\lambda_1 - dS_1\right)\right)}{S_1 S_2\beta_1\beta_2((1 - eh) - (1 - e))}, \\ v_m =& \frac{\beta_2(1 - eh)S_2\left(\lambda_1 - dS_1\right) - \beta_1(1 - e)S_1\left(\lambda_2 - dS_2\right)}{S_1 S_2\beta_1\beta_2((1 - eh) - (1 - e))}, \\ I_{1w} =& \frac{(1 - f)S_1(1 - e)\beta_1 v_w + QL_w}{a}, \\ I_{1m} =& \frac{(1 - f)S_1 r\beta_1 v_m + QL_m}{a} \\ I_{2w} =& \frac{S_2(1 - eh)\beta_2 v_w}{a}, \\ I_{2m} =& \frac{S_2 r\beta_2 v_m}{a}, \\ L_w =& \frac{fS_1(1 - e)\beta_1 v_w}{P}, \\ L_m =& \frac{fS_1 r\beta_1 v_m}{P}. \end{aligned} \tag{5.9}$$

All variables have additional terms of O(ϵ). The coexistence steady state only exists if $h \neq 1$. As the parameter values used give both P and Q positive the

steady state expressions for S_1 and S_2 are both positive if $(1-e) < r < (1-eh)$. In addition providing v_w and v_m are positive the remaining variables are also positive.

1. The Jacobian matrix for the disease free steady state is

$$\begin{pmatrix} -d & 0 & 0 & 0 & 0 & 0 & 0 & 0 & -(1-e)\beta_1 S1 & -r\beta_1 S1 \\ 0 & -d & 0 & 0 & 0 & 0 & 0 & 0 & -(1-eh)\beta_2 S2 & -r\beta_2 S2 \\ 0 & 0 & -P & 0 & 0 & 0 & 0 & 0 & f*(1-e)\beta_1 S1 & 0 \\ 0 & 0 & 0 & -P & 0 & 0 & 0 & 0 & 0 & fr\beta_1 S1 \\ 0 & 0 & Q & 0 & -a & 0 & 0 & 0 & (1-f)(1-e)\beta_1 S1 & 0 \\ 0 & 0 & 0 & Q & 0 & -a & 0 & 0 & 0 & (1-f)r\beta_1 S1 \\ 0 & 0 & 0 & 0 & 0 & 0 & -a & 0 & (1-eh)\beta_2 S2 & 0 \\ 0 & 0 & 0 & 0 & 0 & 0 & 0 & -a & 0 & r\beta_2 S2 \\ 0 & 0 & 0 & 0 & k & 0 & k & 0 & -c & 0 \\ 0 & 0 & 0 & 0 & 0 & k & 0 & k & 0 & -c \end{pmatrix}$$

The characteristic equation for this matrix can be factorised into the following polynomials in Λ:

$$(\Lambda + d)^2 = 0,$$
$$(\Lambda + a)^2 = 0,$$
$$\Lambda^3 + x_2\Lambda^2 + x_1\Lambda + x_0 = 0,$$
where
$$x_2 = P + a + c,$$
$$x_1 = ac + P(a+c) - \frac{k}{d}((1-f)(1-e)\beta_1\lambda_1 + (1-eh)\beta_2\lambda_2),$$
$$x_0 = P\left(ac - \frac{k}{d}((1-f+\frac{fQ}{P})(1-e)\beta_1\lambda_1 + (1-eh)\beta_2\lambda_2)\right),$$
and
$$\Lambda^3 + y_2\Lambda^2 + y_1\Lambda + y_0 = 0,$$
where
$$y_2 = P + a + c,$$
$$y_1 = ac + P(a+c) - \frac{kr}{d}((1-f)\beta_1\lambda_1 + \beta_2\lambda_2),$$
$$y_0 = P\left(ac - \frac{kr}{d}((1-f+\frac{fQ}{P})\beta_1\lambda_1 + \beta_2\lambda_2)\right),$$

All coefficients are positive and the disease free steady state is stable if and only

if the basic reproductive ratio $\max(R_{0w}, R_{0m}) < 1$.

2. The characteristic polynomial for the wildtype only steady state can be factorised into 2 linear factors, a cubic factor and a fifth order polynomial. The fifth order polynomial is not tractable so only the three smaller polynomial factors in Λ are shown here.

$$(\Lambda + a)^2 = 0$$
$$\Lambda^3 + x_2\Lambda^2 + x_1\Lambda + x_0,$$
where
$$x_2 = P + a + c,$$
$$x_1 = ac + P(a + c) - kr((1 - f)\beta_1 S_1 + beta_2 S_2),$$
$$x_0 = P\left(ac - kr\left(\left(1 - f + \frac{fQ}{P}\right)\beta_1 S_1 + \beta_2 S_2\right)\right).$$

   For the cubic factor to have roots that have negative real parts we require that $R_{0m}(S_1^w, S_2^w) < 1$, where S_1^w and S_2^w are the values of S_1 and S_2 respectively at the wildtype only steady state. This requirement is similar to that for the two target cell two strain model (4.1). When drug penetrance is equal in both compartments, $h = 1$, this condition becomes $(1 - e) > r$. The fifth order polynomial yields the condition that $R_{0w} > 1$ for this steady state to be stable.

3. The characteristic polynomial for the mutant only steady state is similar in form to the one for the wildtype only steady state. Therefore the mutant only steady state will be stable when $R_{0m} > 1$ and $R_{0w}(S_1^m, S_2^m) < 1$, where S_1^m and S_2^m are the mutant only steady state values of S_1 and S_2. When $h = 1$ we require $R_{0m} > 1$ and $r > 1 - e$ for stability.

4. The characteristic polynomial for the coexistence steady state is not tractable, it factorises to give two linear factors and an eighth order polynomial. It is sensible to assume that, as for the two target cell two strain model (4.1), the coexistence steady state is stable when $\min(R_{0w}, R_{0m}) > 1$, $R_{0m}(S_1^w, S_2^w) > 1$ and $R_{0w}(S_1^m, S_2^m) > 1$. When $h = 1$ the coexistence steady state no longer exists.

5.3.3 Numerical Solutions

As with the base model examples the values of the drug efficacy and resistance factor were chosen to give low level viral load on therapy with the mutant strain dominant. Due to the presence of the secondary target cells these values are not the same as the values from the base model.

Model 1: No proliferation

The composition of the latent cell reservoir, i.e. which viral strain the latently infected cells have integrated into their genetic code, is affected by the viral population in the blood plasma. The steady state expressions for the latent cell population show that the latent cell reservoir will consist mainly of cells infected with the dominant strain of virus with the weaker strain present at $O(\epsilon)$.

We can assume that under treatment the value of R_{0w} varies, whereas R_{0m} remains constant, reflecting resistance of the mutant strain to treatment. As the value of R_{0w} is decreased (meaning more effective treatment) the concentration of v_w decreases. When R_{0w} becomes less than R_{0m} dominance of the two strains reverses and the mutant strain v_m becomes dominant as shown in Figure 5-10. This change in strain dominance is also seen in the latently infected cell reservoir at steady state. However, before the steady state is reached, the viral strain that is dominant in the blood is different to that in the latent cell reservoir for a short period of time. Figure 5-11 shows how the activation rate of the latent cells affects the difference in the time taken for the strain switch over to occur in the blood and latent cell reservoir. The lower the activation rate the longer the time to strain switch over. One explanation for this is that the lower activation rate slows the rate at which latent cells become actively infected and feed into the cycle of new viral replications.

This model does not allow the archiving of viral strains in the latent cell reservoir for long periods of time. For the range of activation rates shown ($\alpha = 0.01 - 0.1$), the latent cell reservoir can archive wild type virus for short periods of around one year. The dominant strain in the plasma at steady state is also the dominant strain in the latent cell reservoir.

Model 2: Bystander proliferation

Figure 5-12a shows how the time to strain switch over in the latent cell population is affected by both the latent cell activation rate α (0.01-0.1), which reduces the size of the pool, and cell proliferation rate p, which increases it. Activation rates used here are the same as in Figure 5-11 but result in a much longer lived archive than for Model 1, even at very low prolifation rates, p. Figure 5-12b shows how the time to strain switch over is affected by the resistance factor r. As r increases, reflecting a fitter mutant virus, the time to strain switch over initially increases then decreases. The decreasing phase is thought to be due to the increase in ongoing viral replication; further work is needed explain the initial increase.

Numerical solutions were also obtained using different values of f, the proportion of

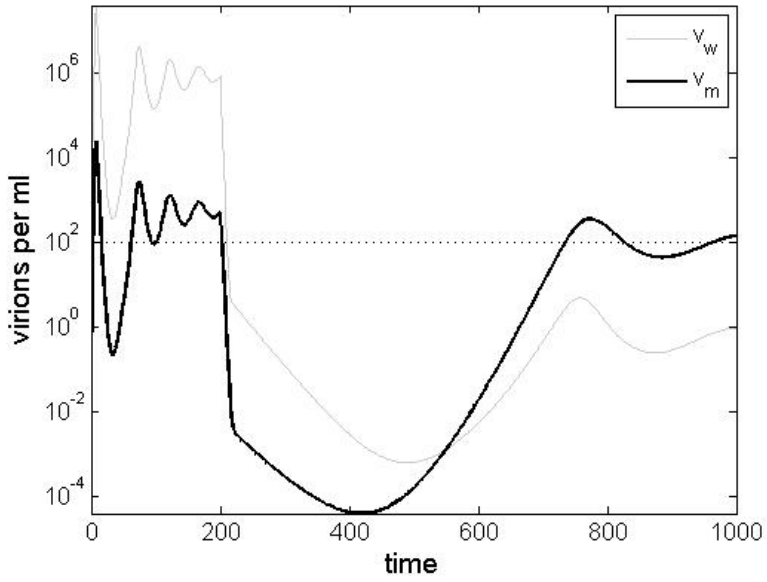

(a)

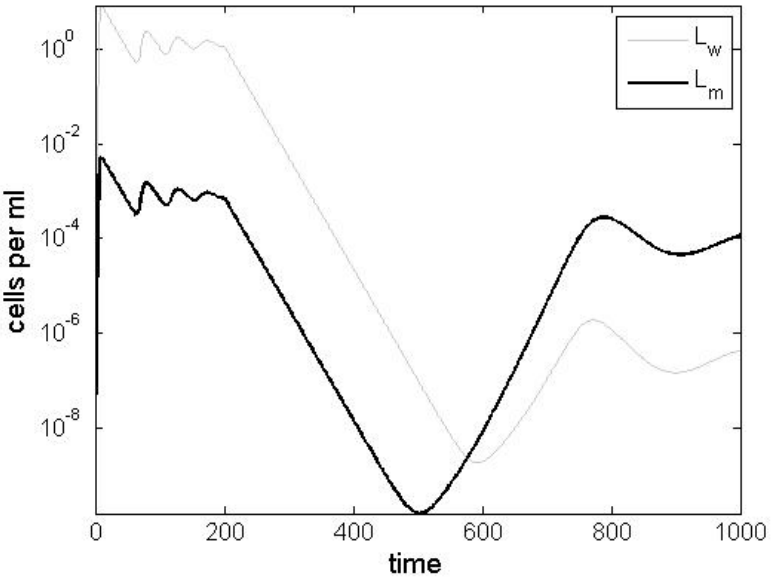

(b)

Figure 5-10: Model 1: Figure showing a numerical solution where the mutant strain is dominant after treatment is initiated at 200 days; a) viral load (dotted line is detection threshold), b) latent cell reservoir. Parameter values are as in Table 5.3.

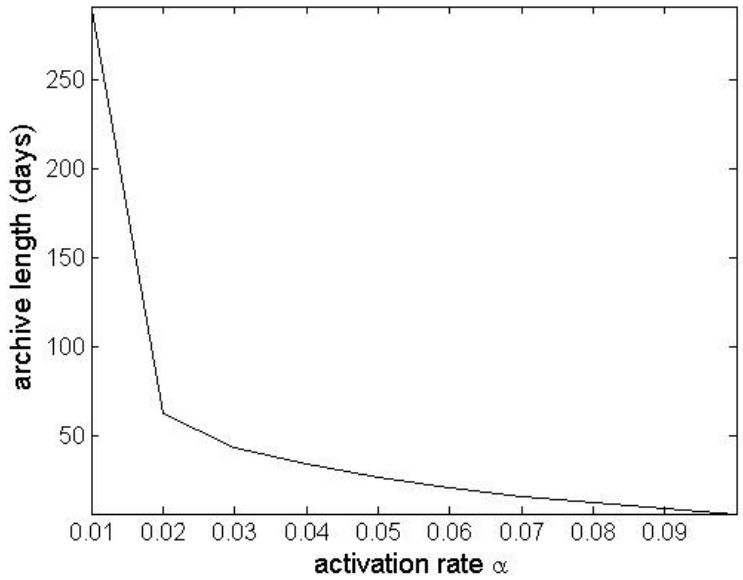

Figure 5-11: Model 1: Graph showing how the activation rate α affects the archive time in the latent cell reservoir. Parameter values are given in Table 5.3.

infected cells to become latent (not shown). As f increases the concentration of latent cells rises. However even large increases in f (eg 100 times the value used above) had little effect on the time to change in strain dominance; we suggest that this is because changes in f affect both types of latent cell equally.

Analysis of this model with its simple replication mechanism for latently infected cells indicates that archiving of wild type virus over a long time period even on therapy is possible.

Model 3: Asymmetric latent cell division upon activation

Numerical solutions for this model are shown in Figure 5-13. Time to strain switch over is greatly increased in this model compared with the previous models. This is due to the linkage between proliferation and activation.

The time it takes for the change in dominance within the latent cell population is affected by both the latent cell and the viral parameters. A number of numerical solutions were obtained for a range of the parameters α (activation rate), p_l (probability a daughter cell will be latent) and r (resistance factor). The results are shown in Figure 5-14. The behaviour of the model with respect to α changes depending on the value of p_l as shown in Figure 5-14a. When $p_l < 0.5$ (P increasing) the archive time decreases as α increases in a similar way to models 1 and 2. However if $p_l > 0.5$ (P decreasing)

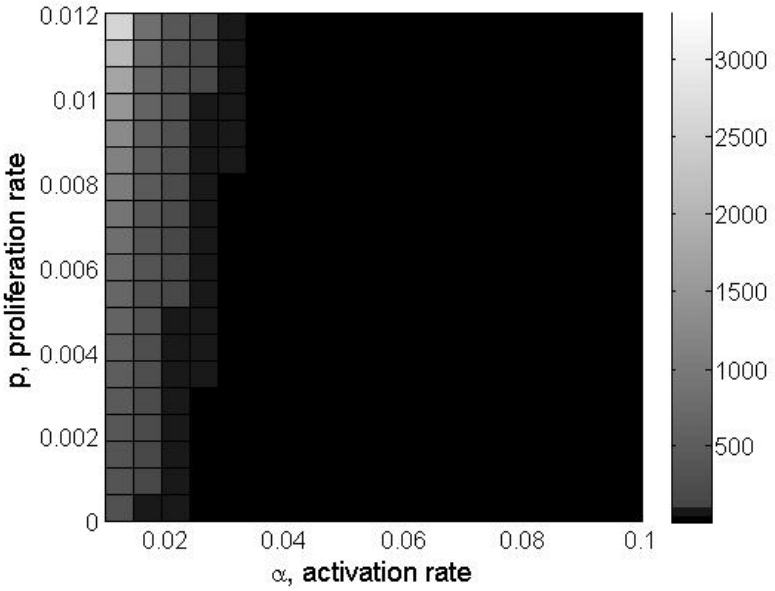

(a)

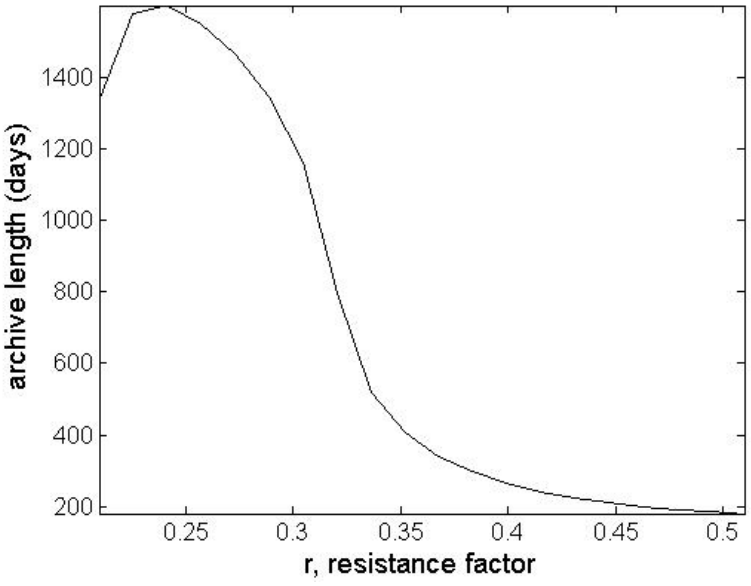

(b)

Figure 5-12: Model 2: Graphs showing how the archive time changes with different parameters: a)α and p are varied, b) r is varied ($p = 0.05$). Other parameters are given in Table 5.3.

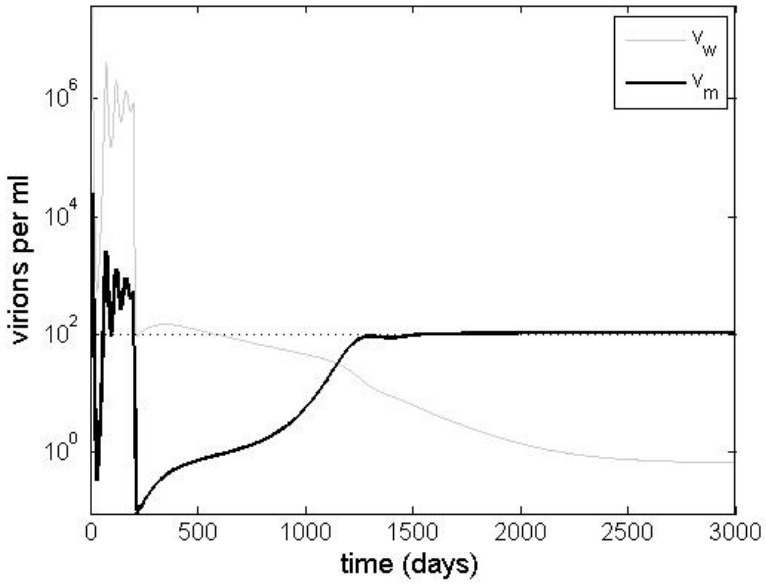

(a)

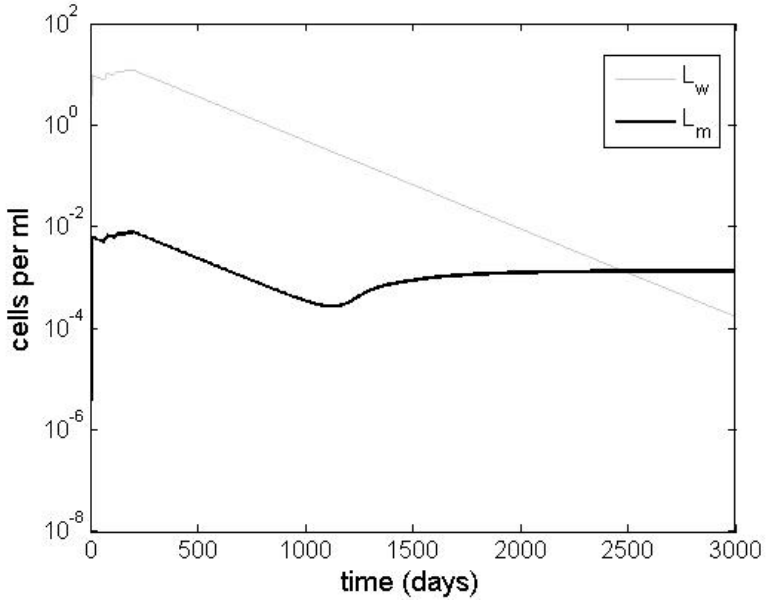

(b)

Figure 5-13: Model 3: Graph showing strain composition of the free virions and latent cell reservoirs before and after treatment; a) viral load (dotted line is detection threshold), b) latent cell reservoir. Treatment was commenced at 200 days. Parameter values used are from Table 5.3 with $p_l = 0.5$.

the archive time increases once a threshold level of α is reached. The reason for this threshold is unclear at present. In models 1 and 2 the value of P always increases as the activation rate α increases.

In Figure 5-14b we see that the time to change in dominance initially increases then decreases as the value of r increases, in a similar way to model 2. An increase in the resistance factor r means that the resistant virus can replicate more quickly once it is the fittest strain, in turn creating more L_m latently infected cells and decreasing the time until $L_m > L_w$. Initial investigation has not provided a clear explanation for the impact of increasing r, for small r on the time to switch over. It should be noted that if the resistance factor r is close to 1 and the mutant is only slightly less fit than the wild type strain in the absence of drugs, the switch over in dominance in the latent cell population will happen very quickly.

We have shown that the asymmetric division mechanism also allows archiving of wildtype virus.

5.3.4 Summary

We obtain the same qualitative results with the two target cell two strain model as the basic model. Namely that a maintenance mechanism is required for long term archiving of wildtype virus in the latent cell reservoir.

In order to obtain low level viral load with the two target cell two strain model we used a different parameter set to the basic model. This means that we cannot directly compare the two models. However we can see from comparing the archive times of the bystander proliferation mechanism for both models in Figures 5-5 and 5-12b that the two target cell two strain model allows longer archive times than the basic model for a wider range of values of r. The same behaviour can be seen for the asymmetric cell division mechanism in Figures 5-8b and 5-14b. This is most likely due underlying behaviour of the two target cell model which allows low level viral load for a wider range of values of drug efficacy and resistance factor.

5.4 Conclusions

We have demonstrated that a replication mechanism allows archiving of virus in the latent cell reservoir on treatment. This archiving is due to the fact that more latently infected cells are created by replication than by new infections. Other work has shown that the long life of the latent cell reservoir on treatment is unlikely to come from ongoing viral replication and is almost certainly due to replication of latently infected cells [Kim and Perelson, 2006, Müller et al., 2002]. It is not yet known whether this

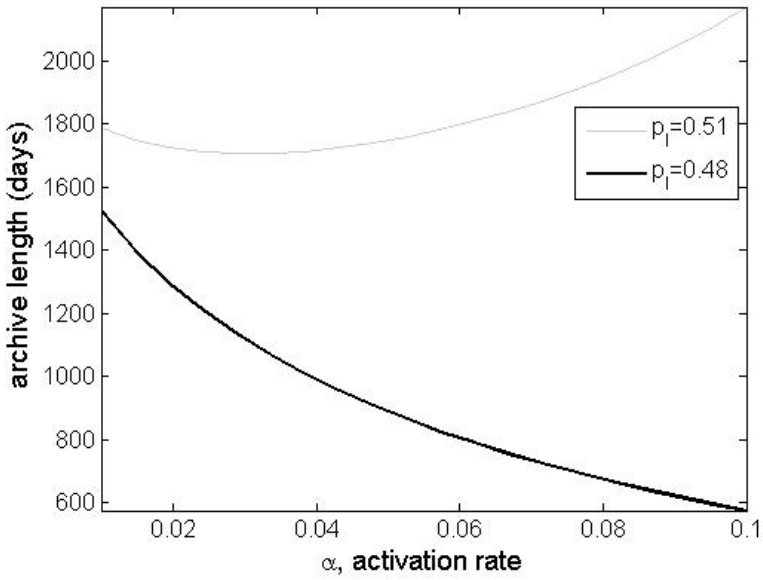

(a)

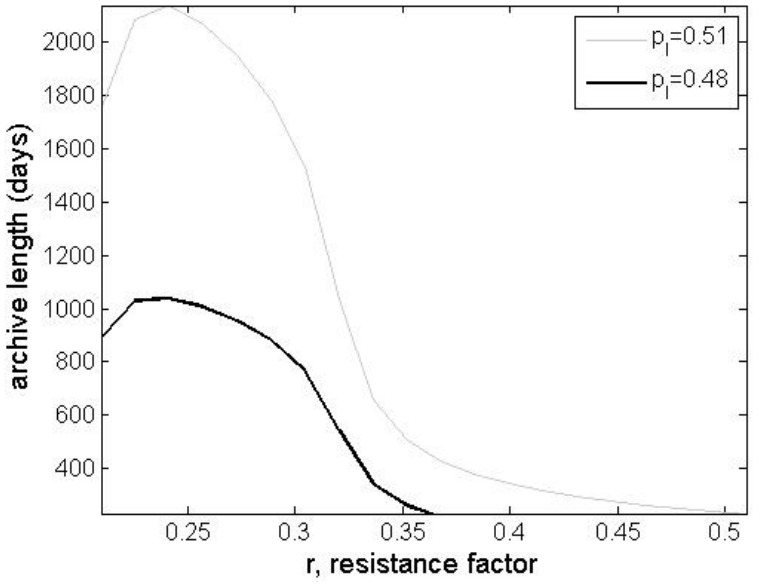

(b)

Figure 5-14: Model 3: Graphs showing time to latent cell strain switch over with varying a) α ($r = 0.21$) and b) r in Model 3. See Table 5.3 for the other parameter values.

self-renewal is upon activation of cells with their specific antigen or through bystander proliferation. We have shown that either mechanism allows archiving of virus. We have also seen that the replicative capacity of the dominant strain of virus has a role to play in the composition of the latent cell reservoir. The more fit the virus, the quicker the latent cell reservoir reflects the viral composition of the blood. This agrees with the observation that resistant virus is seen in the latent cell reservoir in patients on failing therapy where viral load is high [Ruff et al., 2002].

Unfortunately direct comparison of the two models containing a maintenance mechanism (when the underlying models are the same) is not possible due to the linking of proliferation and activation in model 3. However, for a certain set of parameters both models will give the same results. This is when $p = \alpha$ in model 2 and $p_l = 0.5$ in model 3 (with α and d_l the same in both models). In this case, proliferation and activation balance in both models with no net growth occuring, so that the density of latent cells will only increase if viral replication is ongoing at a high enough level.

There is some evidence that infected macrophages can evade the immune response, which implies that the death rate of an infected cell is similar to that of a healthy cell [Aquaro et al., 2002]. This would increase the replicative capacity of HIV in macrophage target cells. In addition, Weinberg et al. [1991] suggest that macrophages have a similar activation rate to CD4+ T cells which would decrease the replicative capacity. Both taken together would in effect cancel each other out to some degree, meaning our qualitative results would hold.

We have shown that it is possible to obtain the same qualitative results concerning an archive of viral strains with the basic model and two target cell models of HIV infection. What seems necessary in both models is ongoing viral replication at a very low level, which we can obtain with both models with a sufficiently small value of the resistance factor, r. Comparing the qualitative results from the two models suggests that the two target cell two strain model is more robust, giving longer archive times for a wider range of values of resistance factor.

One drawback to the models discussed here is that we only consider one drug and a single strain of virus resistant to that drug. As modern treatment practice is with HAART - typically three different drugs acting on two drug targets - we are unable to capture all of the relevant behaviour. The systems we have analysed are adequate for when someone is maintaining low level viral load, albeit with a mutant strain dominant, however they are not sufficient for a two drug target regimen. Obtaining low level viral loads with our models, when the resistant virus is dominant, is very sensitive to the value of the resistance cost factor, r. Expanding our models to include a second drug target, the protease enzyme, and a strain of virus resistant to the drug used could

facilitate a more robust mechanism for obtaining low level viral load. We anticipate that qualitatively similar results would be obtained for strain archiving in this more complicated setting.

Once the mechanism for latent cell proliferation has been discovered, parameter estimates for the growth rate as well as the activation rate of latently infected cells, would allow us to exploit our results in order to quantify viral strain archiving in the latent reservoir of HIV infection.

Chapter 6

Conclusions

The aim of this thesis is to investigate how, despite treatment, cell heterogeneity and drug resistance can cause long term persistence of HIV. We consider how cell heterogeneities, either through differing target cell behaviours or secondary target cell types, affect the long term behaviour of HIV infection. We examine models of multiple viral strains to assess the effect of drug resistance on viral persistence and extend our cell heterogeneity models to include multiple strains. Baseline model behaviours are studied throughout to correctly assign the cause of interesting results.

In Chapter 2 we study three different models. The first is a simple model of HIV infection with a constant input/output of virions, to assess the impact of another body compartment producing virions. The second is a two body compartment model which is analysed for different cases of cell heterogeneity. We find that when there are no differences between cells in each compartment, viral loads at steady state are equal and therefore this is not a biologically realistic scenario. The presence of a drug sanctuary in one of the compartments shows that protease inhibitors are more effective than reverse transcriptase inhibitors but that both drug types allow low level viral load at steady state for a large range of drug efficacies. Distinct target cell parameters between the two compartments give different viral load between compartments both prior to, and after commencing treatment. Cell heterogeneities also allow low level viral load without the presence of a drug sanctuary, which is important as some drugs are equally effective in both compartments. The inclusion of a drug sanctuary when cell heterogeneities are present widens the range of drug efficacies which enable viral persistence. The final model considered in Chapter 2 includes a secondary target cell with different birth process characteristics which can also facilitate viral persistence on treatment without the presence of a drug sanctuary. This is interesting as it gives viral persistence in the absence of external stimuli. The inclusion of a drug sanctuary

in the secondary target cell population increases the range of drug efficacies for which low level viral load can be seen.

In Chapter 3 we analyse competition and evolutionary models of multiple strains of virus where the additional strains are drug resistant mutants. We show that the competition models exhibit competitive exclusion with the fittest viral strain given by the largest basic reproductive ratio, R_0 outcompeting other strains. The behaviour of evolutionary models can be considered a perturbation of competition models with the losing strain/s present at the order of the level of mutation or less depending on the type of mutation model considered. If a mutant is more than two mutations away from the dominant strain it is not likely to be seen in the viral quasispecies due to the population size. Two different models of mutation were considered for three strain systems. The time to emergence is calculated for evolutionary models of two and three strains of virus. We find that the time to emergence is increased when the winning strain requires more than one mutation from the wildtype. Increasing the fitness of intermediate mutants only had a small affect on the time to emergence. These simple models of multiple strains cannot explain the relatively high prevalence of minority mutants in patients samples. As both the jump and serial three strain systems considered are not biologically realistic and a more sensible four strain model is much more complicated, models with two strains are utilised in Chapters 4 and 5.

Chapter 4 extends the two target cell model and two compartment models from Chapter 2 to include two competing strains of virus: wildtype and a drug resistant mutant. For both models inclusion of a drug sanctuary allows coexistence of viral strains in a competition model. Steady state analysis is possible for the two target cell model. The usual threshold behaviour for the disease free steady state to be stable, that is $R_0 < 1$, is seen. The endemic steady states are seen when $R_0 > 1$, however unlike the competition models from Chapter 3, coexistence can be seen when either strain could invade the other strain steady state. We find that this means that the mutant strain can be seen when it would be considered less fit than the wildtype in the usual one target cell model. When there is no drug sanctuary present threshold behaviours revert to the fittest strain wins, with the fittest strain determined by the R_0 values. The parameter ranges which allow coexistence in the two target cell model are very small and it is therefore not likely to be biologically significant. However the two compartment model shows coexistence when a drug sanctuary is present for large ranges of parameter values. In this case it is possible to obtain viral loads much higher than the order of mutation for the minority strain suggesting that drug sanctuaries are a possible source of this phenomenon. It is also possible to see differential strain dominance between the two body compartments with one strain dominant in the blood and the other in the small

compartment. This has consequences for clinicians and treatment options as only the blood viral complement is tested in clinical practice. Genotyping viral strains in the blood and male genital tract for different drug therapies, as well as determining the nature of target cells in the male genital tract would help us to validate our results.

In Chapter 5 we consider another form of cell heterogeneity, the formation of latent infected cells. We assess whether a replication mechanism for latently infected cells is necessary for viral archiving in the latent cell reservoir to occur. We find that longer term archiving is due to replication of latent cells rather than new rounds of infection. Two methods of replication are studied: bystander proliferation and asymmetric cell division, both causing a long term archive. The replicative capacity of the mutant or dominant strain has a large role to play in the persistence of the archive, with high R_0 values resulting in shorter term archives due to higher levels of ongoing viral replication. It is possible to show these results using two different underlying models: the basic model and the two target cell model, providing the mutant virus is dominant but has an R_0 very close to 1. This ensures low level viral load on treatment.

Clinical investigation into the replication mechanism of latently infected cells could help us to parameterise our models, enabling us to more accurately predict archiving of viral strains, as would finding a sensible value for the activation rate.

There are many avenues for further work which are suggested by the results of this thesis. It would be beneficial to develop more biologically realistic models which incorporate the triple drug therapies currently prescribed to patients. One drawback of ODE models is that if a mutant is the fittest strain on therapy it will become dominant, regardless of the pre-treatment level. This suggests the need to use stochastic models.

The way in which we have modelled drug resistance is very simplistic. Most resistant strains are in fact sensitive by some degree to drug treatment. All of the models described in this work could be adapted to investigate the consequences of relaxing the assumption of complete resistance. It would seem likely that this would decrease the fitness of the mutant strains and allow the wildtype strains to persevere for wider ranges of drug efficacy.

Not all drugs are less effective in the male genital tract and indeed there are some that are more effective. This could be investigated by assuming that the drug sanctuary is in the large compartment and the normal level of drug efficacy in the small compartment. It would be interesting to see whether coexistence would be seen in this scenario.

The effect of differential dominance in the two compartment model on HIV infection at population level could be explored using a nested approach similar to that of Coombs et al. [2007]. This would result in a PDE model of infection, with the strain transmitted

between partners dependent on the age of infection and treatment regime.

We have shown that cell heterogeneity has a role to play in the persistence of HIV on treatment, whether it be the presence of a drug sanctuary or through different target cells. The presence of drug sanctuaries can explain the levels of minority mutants in patients and also the differences in viral quasispecies seen in the blood and male genital tract. We have also shown that the maintenance of the latent cell population, when there is little ongoing viral replication, allows the persistence of a viral archive in the latent cell reservoir for many years. When viral replication is increased, due to a fitter mutant or non-suppressive therapy, our model predicts that the viral archive will be short lived. All of our results suggest avenues for further clinical research: namely genotyping of viral strains concurrently in the blood and genital tract, analysing the proportion of different strains in the blood on treatment and investigating the replication mechanism of latently infected cells. With this information we could validate and better parameterise our models to the benefit of HIV clinical practice.

Bibliography

S. Aquaro, R. Caliņ, J. Balzarini, M.C. Bellocchi, E. Garaci, and C.F. Perno. Macrophages and HIV infection: therapeutical approaches toward this strategic virus reservoir. *Antiviral Research*, 55(2):209–225, 2002.

R.A. Arnaout, A. Martin, et al. HIV-1 dynamics revisited: biphasic decay by cytotoxic t lymphocyte killing? *Proceedings of the Royal Society of London. Series B: Biological Sciences*, 267(1450):1347–1354, 2000.

C. L Ball, M. A. Gilchrist, and D. Coombs. Modeling within-host evolution of HIV: mutation, competition and strain replacement. *Bulletin of Mathematical Biology*, 69: 2361–2385, 2007.

S. Bonhoeffer, R. M. May, G. M. Shaw, and M. A. Nowak. Virus dynamics and drug therapy. *Proceedings of the National Academy of Science USA*, 1997.

B. G. Brenner, J-P. Routy, M. Pertrella, D. Moisi, M. Oliveira, M. Detorio, B. Spira, V. Essabag, B. Conway, R. Lalonde, R-P. Sekaly, and M. A. Wainberg. Persistence and fitness of multidrug-resistant Human Immunodeficiency Virus Type 1 acquired in primary infection. *Journal of Virology*, 76:1753–1761, 2002.

N. F. Britton. *Essential Mathematical Biology*, chapter 6. Springer, 2002.

T.D. Brock. *Biology of Microorganisms*, chapter 23. Prentice Hall International Editions, 8th edition, 1997.

R. A. Byrn, D. Zhang, R. Eyre, K McGowan, and A. A. Kiessling. HIV-1 in semen: an isolated virus reservoir. *The Lancet*, 350:1141, 1997.

D. S. Callaway and A. S. Perelson. HIV-1 infection and low steady state viral loads. *Bulletin of Mathematical Biology*, 64:29–64, 2002.

T.W. Chun, D. Finzi, J. Margolick, K. Chadwick, D. Schwartz, and R.F. Siliciano. In vivo fate of HIV-1-infected T cells: quantitative analysis of the transition to stable latency. *Nature Medicine*, 1(12):1284–1290, 1995. ISSN 1078-8956.

T.W. Chun, L. Carruth, D. Finzi, X. Shen, J.A. DiGiuseppe, H. Taylor, M. Hermankova, K. Chadwick, J. Margolick, T.C. Quinn, et al. Quantification of latent tissue reservoirs and total body viral load in HIV-1 infection. *Nature*, 387(6629): 183–188, 1997a.

T.W. Chun, L. Stuyver, S.B. Mizell, L.A. Ehler, J.A.M. Mican, M. Baseler, A.L. Lloyd, M.A. Nowak, and A.S. Fauci. Presence of an inducible HIV-1 latent reservoir during highly active antiretroviral therapy. *Proceedings of the National Academy of Sciences of the United States of America*, 94(24):13193, 1997b.

T.W. Chun, D. Engel, S.B. Mizell, L.A. Ehler, and A.S. Fauci. Induction of HIV-1 replication in latently infected CD4+ T cells using a combination of cytokines. *The Journal of Experimental Medicine*, 188(1):83, 1998. ISSN 0022-1007.

M. S. Cohen, C. Gay, A. D. M. Kashuba, S. Blower, and L Paxton. Narrative review: antiretroviral therapy to prevent the sexual transmission of HIV-1. *Annals of Internal Medicine*, 146:591–601, 2007.

D. Coombs, M. A. Gilchrist, and C. L. Ball. Evaluating the importance of within- and between-host selection pressures on the evolution of chronic pathogens. *Theoretical Population Biology*, 72:576–591, 2007.

J. K. Craigo and P. Gupta. HIV-1 in genital compartments: vexing viral reservoirs. *Current Opinion in HIV and AIDS*, 1:97–102, 2006.

J. K. Craigo, B. K Patterson, S. Paranjpe, K. Kulka, M. Ding, J. Mellors, R. C. Montelaro, and P. Gupta. Persistent HIV type 1 infection in semen and blood compartments in patients after long-term potent antiretroviral therapy. *AIDS Research and Human Retroviruses*, 20:1196–1209, 2004.

M. Di Mascio, M. Markowitz, M. Louie, C. Hogan, A. Hurley, C. Chung, D.D. Ho, and A.S. Perelson. Viral blip dynamics during highly active antiretroviral therapy. *Journal of Virology*, 77(22):12165, 2003.

L. Edelstein-Keshet. *Mathematical models in biology*. McGraw-Hill Companies, 1988.

J. Embretson, M. Zupancic, J.L. Ribas, A. Burke, P. Racz, K. Tenner-Racz, and A.T. Haase. Massive covert infection of helper t lymphocytes and macrophages by HIV during the incubation period of aids. *Nature*, 362(6418):359–362, 1993.

D. Finzi and R.F. Siliciano. Viral dynamics in HIV-1 infection. *Cell*, 93(5):665–671, 1998.

S.D.W. Frost and A.R. McLean. Quasispecies dynamics and the emergence of drug resistance during zidovudine therapy of HIV infection. *AIDS*, 8(3):323, 1994.

M.R. Furtado, D.S. Callaway, J.P. Phair, K.J. Kunstman, J.L. Stanton, C.A. Macken, A.S. Perelson, and S.M. Wolinsky. Persistence of HIV-1 transcription in peripheral-blood mononuclear cells in patients receiving potent antiretroviral therapy. *New England Journal of Medicine*, 340(21):1614–1622, 1999.

R. T. Gandhi, A. Wurcel, E. S. Rosenberg, M. N. Johnston, N. Helmann, M. Bates, M. S. Hirsch, and B. D. Walker. Progressive reversion of Human Immunodeficiency Virus Type 1 resistance mutations in vivo after transmission of a multiply drug-resistant virus. *Clinical Infectious Diseases*, 37:1693–1698, 2003.

B. Gazzard. British HIV Association (BHIVA) guidelines for the treatment of HIV-infected adults with antiretroviral therapy (2006). *HIV Medicine*, 7(8):487–503, 2006.

R. M. Grant, F. M. Hecht, M. Warmerdam, L. Liu, T. Lieglar, C. J. Petropoulos, N. S. Hellmann, M. Chesney, M. P. Busch, and J. O. Kahn. Time trends in primary HIV-1 drug resistance among recently infected persons. *Journal of the American Medical Association*, 288:181–188, 2002.

I. Gudelj, R. E. Beardmore, S. S. Arkin, and R. C. Maclean. Constraints on microbial metabolism drive evolutionary diversification in homogeneous environments. *Journal of Evolutionary Biology*, 20:1882–1889, 2007.

J. M. Heffernan, R. J. Smith, and L. M. Wahl. Perspectives on the basic reproductive ratio. *Journal of the Royal Society Interface*, 2:281–293, 2005.

D.D. Ho, A.U. Neumann, A.S. Perelson, W. Chen, J.M. Leonard, M. Markowitz, et al. Rapid turnover of plasma virions and cd4 lymphocytes in HIV-1 infection. *Nature*, 373(6510):123–126, 1995.

R.D. Hockett, J. Michael Kilby, C.A. Derdeyn, M.S. Saag, M. Sillers, K. Squires, S. Chiz, M.A. Nowak, G.M. Shaw, and R.P. Bucy. Constant mean viral copy number per infected cell in tissues regardless of high, low, or undetectable plasma HIV RNA. *The Journal of Experimental Medicine*, 189(10):1545, 1999. ISSN 0022-1007.

J.J. Holland, J.C. de la Torre, DK Clarke, and E. Duarte. Quantitation of relative fitness and great adaptability of clonal populations of RNA viruses. *Journal of Virology*, 65(6):2960, 1991.

L. E. Jones and A. S. Perelson. Opportunistic infection as a cause of transient viremia in chronically infected HIV patients under treatment with HAART. *Bulletin of Mathematical Biology*, 67:1227–1251, 2005.

L.E. Jones and A.S. Perelson. Transient viremia, plasma viral load, and reservoir replenishment in HIV-infected patients on antiretroviral therapy. *Journal of Acquired Immune Deficiency Syndromes*, 45(5):483, 2007.

S. C. Kalichman, G. Di Berto, and L. Eaton. Human Immunodeficiency Virus viral load in blood plasma and semen: review and implications of empirical findings. *Sexually Transmitted Diseases*, 35:55–60, 2008.

T. B. Kepler and A. S. Perelson. Drug concentration heterogeneity facilitates the evolution of drug resistance. *Proc. Natl. Acad. Sci. USA*, 95:11514–11519, 1998.

H. Kim and A. S. Perelson. Viral and latent reservoir persistence in HIV-1-infected patients on therapy. *PloS Computational Biology*, 2:1232–1247, 2006.

R.B. Kim, M.F. Fromm, C. Wandel, B. Leake, AJ Wood, D.M. Roden, and G.R. Wilkinson. The drug transporter p-glycoprotein limits oral absorption and brain entry of HIV-1 protease inhibitors. *Journal of Clinical Investigation*, 101(2):289, 1998.

B.A. Larder, G. Darby, and D.D. Richman. HIV with reduced sensitivity to zidovudine (azt) isolated during prolonged therapy. *Science*, 243(4899):1731, 1989.

A. M. Lever, editor. *The Molecular Biology of HIV/AIDS*. Molecular Medical Science Series. John Wiley & Sons, 1996.

J. A. Levy. *HIV and the Pathogenesis of AIDS*. ASM Press, 1995.

M. Lipsitch, C. Colijn, T. Cohen, W.P. Hanage, and C. Fraser. No coexistence for free: neutral null models for multistrain pathogens. *Epidemics*, 1(1):2–13, 2009.

S. J. Little, S. Holte, J-P. Routy, E. S. Daar, M. Markowitz, A. C. Collier, R. A. Koup, J. W. Mellors, E. Connick, B. Conway, M. Kilby, L. Wang, J. M. Whitcom, N. S. Hellman, and D. D. Richman. Antiretroviral drug resistance among patients recently infected with HIV. *The New England Journal of Medicine*, 347:385–394, 2002.

G. Liuzzi, A. Chirianni, M. Zaccarelli, D. Zinzi, V. Esposito, V. Guadagnino, A. Antinori, and M. Piazza. Differences between semen and plasma of nucleoside reverse transcriptase resistance mutations in HIV-infected patients, using a rapid assay. *In Vivo*, 2004:509–512, 2004.

S. H. Lowe, S. U. C. Sankatsing, S. Repping, F. van der Veen, P. Reiss, J. M. A. Lange, and J. M. Prins. Is the male genital tract really a sanctuary site for HIV? Arguments that it is not. *AIDS*, 18:1353–1362, 2004.

P. Macheras and A. Iliadis. *Modeling in Biopharmaceutics, Pharmacokinetics and Pharmacodynamics: Homogeneous and Heterogeneous Approaches (Interdisciplinary Applied Mathematics)*, chapter 8. Springer, 2006.

N. Machouf, R. Thomas, V. K. Nguyen, B. Trottier, M. R. Boulassel, M. A. Wainberg, and J. P. Routy. Effects of drug resistance on viral load in patients failing antiretrviral therapy. *Journal of Medical Virology*, 78:608–613, 2006.

L. M. Mansky. HIV mutagenesis and the evolution of antiretrolviral drug resistance. *Drug Resistance Updates*, 5:219–223, 2002.

M. Markowitz, M. Louie, A. Hurley, E. Sun, M. Di Mascio, A.S. Perelson, and D.D. Ho. A novel antiviral intervention results in more accurate assessment of Human Immunodeficiency Virus Type 1 replication dynamics and T-cell decay in vivo. *Journal of Virology*, 77(8):5037, 2003.

A. R. McLean and M. A. Nowak. Competition between zidovudine-senstive and zidovudine-resistant strains of HIV. *AIDS*, 6:71–79, 1992.

A. R. McLean, V. C. Emery, A. Webster, and P. D. Griffiths. Population dynamics of HIV within an individual after treatment with zidovudine. *AIDS*, 5:485–489, 1991.

AR McLean and SDW Frost. Zidovudine and HIV: Mathematical models of within-host population dynamics. *Reviews in Medical Virology*, 5(3):141–147, 1995.

V. Miller, A. Phillips, C. Rottmann, S. Staszewski, R. Pauwels, K. Hertogs, M.P. de Béthune, S.D. Kemp, S. Bloor, P.R. Harrigan, et al. Dual resistance to zidovudine and lamivudine in patients treated with zidovudine-lamivudine combination therapy: association with therapy failure. *Journal of Infectious Diseases*, 177(6):1521, 1998.

H. Mohri, S. Bonhoeffer, S. Monard, A.S. Perelson, and D.D. Ho. Rapid turnover of T lymphocytes in SIV-infected rhesus macaques. *Science*, 279(5354):1223, 1998. ISSN 0036-8075.

V. Müller, J. V. Vigueras-Gòmez, and S. Bonhoeffer. Decelerating decay of latently infected cells during prolonged therapy for Human Immunodeficiency Virus Type 1 infection. *Journal of Virology*, 76:8963–8965, 2002.

M. A. Nowak and R. M. May. *Virus dynamics: mathematical principles of immunology and virology*. Oxford University Press, 2000.

M. A. Nowak, R. M. Anderson, A. R. McLean, T. F. W. Wolf, J. Goudsmit, and R. M. May. Antigenic diversity thresholds and the development of AIDS. *Science*, 254: 963–969, 1991.

M.A. Nowak, S. Bonhoeffer, G.M. Shaw, and R.M. May. Anti-viral drug treatment: dynamics of resistance in free virus and infected cell populations. *Journal of Theoretical Biology*, 184(2):203–217, 1997.

S. Palmer, M. Kearney, F. Maldarelli, E.K. Halvas, C.J. Bixby, H. Bazmi, D. Rock, J. Falloon, R.T. Davey Jr, R.L. Dewar, et al. Multiple, linked Human Immunodeficiency Virus Type 1 drug resistance mutations in treatment-experienced patients are missed by standard genotype analysis. *Journal of Clinical Microbiology*, 43(1): 406, 2005.

S. Palmer, V. Boltz, N. Matinson, F. Maldarelli, G. Gray, J. McIntyre, J. Mellors, L. Morris, and J. Coffin. Persistance of nevirapine-resistant HIV-1 in women after single-dose nevirapine therapy for prevention of maternal-to-fetal HIV-1 transmission. *Proceedings of the National Academy of Sciences of the United States of America*, 103:7094–7099, 2006.

A. S. Perelson, A. U. Neumann, M. Markowitz, J. M. Leonard, and D. D. Ho. HIV-1 dynamics in vivo: Virion clearance rate, infected cell life span and viral generation time. *Science*, 271:1582–1586, 1996.

A.S. Perelson, D.E. Kirschner, and R. De Boer. Dynamics of HIV infection of CD4+ T cells. *Mathematical Biosciences*, 114(1):81–125, 1993. ISSN 0025-5564.

A.S. Perelson, P. Essunger, Y. Cao, M. Vesaneir, A. Hurley, K. Sakselat, M. Markowitz, and D.D. Ho. Decay characteristics of HIV-1-infected compartments during combination therapy. *Nature*, 267:483–489, 1995.

C.F. Perno, F.M. Newcomb, D.A. Davis, S. Aquaro, R.W. Humphrey, R. Calio, and R. Yarchoan. Relative potency of protease inhibitors in monocytes/macrophages acutely and chronically infected with Human Immunodeficiency Virus. *The Journal of Infectious Diseases*, 178(2):413–422, 1998. ISSN 0022-1899.

D. Pillay, S. Taylor, and D. D Richman. Incidence and impact of resistance against approved antiretroviral drugs. *Reviews in Medical Virology*, 10:231–253, 2000.

P. Puddu, S. Fais, F. Luciani, G. Gherardi, ML Dupuis, G. Romagnoli, C. Ramoni, M. Cianfriglia, and S. Gessani. Interferon-γ up-regulates expression and activity of p-glycoprotein in human peripheral blood monocyte-derived macrophages. *Laboratory Investigation*, 79(10):1299–1309, 1999.

B. Ramratnam, S. Bonhoeffer, J. Binley, A. Hurley, L. Zhang, J.E. Mittler, M. Markowitz, J.P. Moore, A.S. Perelson, and D.D. Ho. Rapid production and clearance of HIV-1 and hepatitis C virus assessed by large volume plasma apheresis. *The Lancet*, 354(9192):1782–1785, 1999.

J. D. Reeves and A. J. Pifer. Emergind drug targets for antiretroviral therapy. *Drugs*, 65(13):1747–1766, 2005.

UK Collaborative Group HIV Drug Resistance, UK CHIC Steering Committee, and UK Register HIV Seroconverters Site. Evidence of a decline in transmitted HIV-1 drug resistance in the United Kingdom. *AIDS*, 21:1035–1039, 2007.

R.M. Ribeiro, S. Bonhoeffer, and M.A. Nowak. The frequency of resistant mutant virus before antiviral therapy. *AIDS*, 12(5):461, 1998.

MG Roberts. The pluses and minuses of 0. *Journal of the Royal Society Interface*, 4 (16):949–961, 2007.

L. Rong and A. S. Perelson. Modeling HIV persistence, the latent reservoir, and viral blips. *Journal of Theoretical Biology*, 260:308–331, 2009a.

L. Rong and A. S. Perelson. Asymmetric division of activated latently infected cells may explain the decay kinetics of the HIV-1 latent reservoir and intermittent viral blips. *Mathematical Biosciences*, 217:77–87, 2009b.

L. Rong and A. S. Perelson. Modeling latently infected cell activation: viral and latent reservoir persistence, and viral blips in HIV-infected patients on potent therapy. *PLoS Computational Biology*, 5(10):e1000533, 2009c.

L. Rong, Z. Feng, and A. S. Perelson. Emergence of HIV-1 drug resistance during antiretroviral treatment. *Bulletin of Mathematical Biology*, 69:2027–2060, 2007a.

L. Rong, M. A. Gilchrist, Z Feng, and A. S. Perelson. Modelling within-host HIV-1 dynamics and the evolution of drug resistance: trade-offs between viral enzyme function and drug susceptibility. *Journal of Theoretical Biology*, 247:804–818, 2007b.

C. T. Ruff, S. C. Ray, P. Kwon, R. Zinn, A. Pendelton, N. Hutton, R. Ashworth, S Gange, T. C. Quinn, R. F. Siliciano, and D. Persaud. Persistence of wild-type virus

and lack of temporal structure in the latent reservoir for Human Immunodeficiency Virus Type 1 in pediatric patients with extensive antiretroviral exposure. *Journal of Virology*, 76:9481–9492, 2002.

Gautam K. Sahu, Juan C. Sarria, and Miles W. Cloyd. Recovery of Replication-Competent Residual HIV-1 from Plasma of a Patient Receiving Prolonged, Suppressive Highly Active Antiretroviral Therapy. *J. Virol.*, 84(16):8348–8352, 2010. doi: 10.1128/JVI.00362-10. URL http://jvi.asm.org/cgi/content/abstract/84/16/8348.

J.D. Siliciano, J. Kajdas, D. Finzi, T.C. Quinn, K. Chadwick, J.B. Margolick, C. Kovacs, S.J. Gange, and R.F. Siliciano. Long-term follow-up studies confirm the stability of the latent reservoir for HIV-1 in resting CD4+ T cells. *Nature medicine*, 9 (6):727–728, 2003.

R. J. Smith. Adherence to antiretroviral HIV drugs: how many doses can you miss before resistance emerges? *Proc. R. Soc. B*, 273:617–624, 2006.

R. J. Smith and L. M. Wahl. Drug resistance in an immunological model of HIV-1 infection with impulsive drug effects. *Bulletin of Mathematical Biology*, 67:783–813, 2005.

M. Stevenson and H.E. Gendelman. Cellular and viral determinants that regulate HIV-1 infection in macrophages. *Journal of Leukocyte Biology*, 56(3):278, 1994.

J. W. Tang and D. Pillay. Transmission of HIV-1 drug resistance. *Journal of Clinical Virology*, 30:1–10, 2004.

G. Tirado, G. Jove, R. Kumar, R. J. Noel, E. Reyes, G. Sepulveda, Y. Yamamura, and Anil Kumar. Differential virus evolution in blood and genital tract of HIV-infected females: evidence for the involvement of drug and non-drug resistance-associated mutations. *Virology*, 324:577–586, 2004.

A. UNAIDS. AIDS epidemic update: special report on hiv. *AIDS: December*, 2006, 2006.

Z. D. Ward, K. A. J. White, and G. A. K. van Voorn. Exploring the impact of target cell heterogeneity on HIV loads in a within-host model. *Epidemics*, 1:168–174, 2009.

JB Weinberg, TJ Matthews, BR Cullen, and MH Malim. Productive Human Immunodeficiency Virus Type 1 (HIV-1) infection of nonproliferating human monocytes. *The Journal of Experimental Medicine*, 174(6):1477, 1991.

H. S. Weinstock, I. Zaidi, W. Heneine, D. Bennet, J. G. Garcia-Lerma, Jr J. M. Douglas, M. LaLota, G. Dickinson, S. Schwarcz, L. Torian, D. Wendell, S. Paul, G. A. Goza, J. Ruiz, B. Boyett, and J. E. Kaplan. The epidemiology of antiretroviral drug resistance among drug-naive HIV-1 infected persons in 10 us cities. *Journal of Infectious Diseases*, 189:2174–2180, 2004.

D. Wodarz, A.L. Lloyd, V.A.A. Jansen, and M.A. Nowak. Dynamics of macrophage and t cell infection by HIV. *Journal of Theoretical Biology*, 196(1):101–113, 1999.

J.K. Wong, M. Hezareh, H.F. Günthard, D.V. Havlir, C.C. Ignacio, C.A. Spina, and D.D. Richman. Recovery of replication-competent HIV despite prolonged suppression of plasma viremia. *Science*, 278(5341):1291, 1997.

H. Zhang, G. Dornadula, M. Beumont, Jr. L. Livornese, B. Van Uitert, K. Henning, and R. J. Pomerantz. Human Immunodeficiency Virus type 1 in the semen of men receiving highly active antiretroviral therapy. *The New England Journal of Medicine*, 339:1803–1809, 1998.

L. Zhang, B. Ramratnam, K. Tenner-Racz, Y. He, M. Vesanen, S. Lewin, A. Talal, P. Racz, A.S. Perelson, B.T. Korber, et al. Quantifying residual HIV-1 replication in patients receiving combination antiretroviral therapy. *The New England journal of medicine*, 340(21):1605, 1999.

T. Zhu, N. Wang, A. Carr, D.S. Nam, R. Moor-Jankowski, D.A. Cooper, and D.D. Ho. Genetic characterization of Human Immunodeficiency Virus Type 1 in blood and genital secretions: evidence for viral compartmentalization and selection during sexual transmission. *Journal of Virology*, 70(5):3098, 1996.

Next Generation Method of Calculating R_0

The next generation method is described in detail in a number of articles including Heffernan et al. [2005] from which this summary is derived.

In the next generation method, R_0 is defined as the largest eigenvalue of the next generation operator. This operator can be obtained from a system of ordinary differential equations that describe a biological system. Two compartments, infected and non-infected, need to be determined from the model. Here the method is illustrated using the basic model of HIV (1.1).

$$\begin{aligned}\dot{S} &= \lambda - dS - \beta Sv,\\ \dot{I} &= \beta Sv - aI,\\ \dot{v} &= kI - cv.\end{aligned}$$

In this model there are 3 compartments, 2 of which are considered to be infected, the I and v compartments. We define a vector $\bar{x} = x_i$ for $i = 1..3$, where x_i denotes the concentration of cells or virions in that compartment. Then we define two matrices, $F_i(\bar{x})$ and $V_i(\bar{x})$. Let $F_i(\bar{x})$ be the rate of appearance of new infections in compartment i and let $V_i(\bar{x}) = V_i^i(\bar{x}) - V_i^+(\bar{x})$, wher V_i^+ is the rate of transfer of cells into compartment i by all other means and V_i^- is the rate of transfer out of compartment i. The next generation matrix operator FV^{-1} is formed from the matrices of partial derivatives of F_i and V_i with respect to x_i, evaluated at the disease free equilibrium.

For the basic model of HIV

$$F_i(\bar{x}) = \begin{pmatrix} \beta Sv \\ 0 \end{pmatrix},$$

$$V_i(\bar{x}) = \begin{pmatrix} aI \\ cV \end{pmatrix} - \begin{pmatrix} 0 \\ kI \end{pmatrix},$$

therefore

$$F = \begin{pmatrix} 0 & \frac{\beta\lambda}{d} \\ 0 & 0 \end{pmatrix},$$

$$V = \begin{pmatrix} a & 0 \\ -k & c \end{pmatrix}.$$

This gives the next generation matrix to be

$$FV^{-1} = \begin{pmatrix} \frac{\lambda\beta k}{acd} & \frac{\lambda\beta k}{acd} \\ 0 & 0 \end{pmatrix}.$$

The largest eigenvalue of this matrix is $R_0 = \frac{\lambda\beta k}{acd}$.

This is a useful method to use when the system under investigation is more complicated and it gives a more general expression for R_0 than the one given by finding the threshold criteria for disease free steady state stability. The expression for R_0 obtained from the next generation matrix method will give the same threshold criteria but is often in a more useable form for later analysis.